APPENDIX 1

Magnetic Modelling of Targets in the Arunta Part 2: Central Arunta Tenements (CSIRO Draft)

MINERAL RESOURCES FLAGSHIP
www.csiro.au

Magnetic Modelling of Targets in the Arunta

Part II: Central Arunta Tenements

Dr J.R. Austin

Report number EP156358
17th July 2015

Client: Core Exploration
Client contact: Colin Skidmore

Commercial-in-confidence

Australian Government
Department of Industry and Science
Business
business.gov.au
13 28 46
Delivered by AusIndustry
CORE

[Insert ISBN or ISSN and cataloguing-in-publication (CiP) information if required]

Mineral Resources Flagship

Citation

Austin, J.R. (2015) Magnetic Modelling of Targets in the Arunta - Part II: Central Arunta Tenements.

Copyright

Important disclaimer

Contents

Figures

Acknowledgments

This project was funded as part of a Research in Business (RiB) agreement between Research Connect, CSIRO and Core Exploration.

Executive summary

The Purpose of this report is to evaluate potential targets in Core Exploration's tenement package in the central Arunta Province referred to as the "Western Tenements", mainly based on evaluation of magnetic data.

The targets were selected blind, based on the magnetic signature, and/or geological context, in order to maintain some objectivity. Prior exploration work, where available/relevant was only consulted after initial evaluation of the target, in order to asses evaluations and/or provide some context to the modelling results. Unfortunately, there is not a great deal of easily accessible information that is also useful, so I mainly utilised mineral occurrence data, mapped geology, drilling data.

One of the unfortunate aspects of the reliance on publicly available data for this project is that there are no survey altitude data available for most NT aeromagnetic datasets. This creates two problems: 1. we cannot be sure of the exact vertical location of modelled bodies, and 2. we cannot accurately account for variability in the ground clearance due to topography. In addition, much of the data is flown at 400m line spacing, and of the better resolution data, much of it is oriented NE-SW, which is good for mapping NW-oriented magnetic fabrics, but is sub-optimal for modelling bodies using the line data. So the data imposes serious limitations on interpretability, and there are very few additional constraints, so the models presented here should be considered as approximations in terms of their location, properties and architecture.

While there is little data that can be used to really constrain the interpretations made in this report, and while the accuracy of the results are in some cases questionable, I am still excited by a number of these anomalies. In particular, those which have a favourable structural context (fault intersections and jogs), favourable host lithology and magnetic properties (e.g., Carbonate lithology and strong remanence), which are also proximal to known Cu occurrences. There are indeed several such targets, across a number of different tenements. There are also a number of anomalies that occupy favourable structural positions (fault intersections, jogs) that are proximal to known Au, Cu, REEs and or U, and that have significant magnetisation (and by inference magnetite present). These are prospective for IOCG mineralisation. In relation to potential for Magmatic Ni-Cu-PGE mineralisation, the bodies need to be fairly large, show signs of fractionation (e.g., petrophysical zonation) and be near surface to have any chance of being economic. Hence, it is my feeling that only two targets are worthy of follow up at this stage. Both are relatively large, and display evidence of zoning (which is inferred to reflect fractionation).

I have ranked the best of the targets empirically, based on their size, proximity to known mineral occurrences and their structural style as shown in the table in the conclusions.

1 Introduction

The Purpose of this report is to evaluate potential targets in Core Exploration's tenement package in the central Arunta Province (shown as "Western Tenements" in Fig 1), mainly based on evaluation of magnetic data. An Evaluation of the Jervois area was completed separately, was presented in May 2015, and has been provided in Part 1 as a PowerPoint slideshow (and word document). Clive Foss is also completing a separate study on the Mordor Pound area, in which magnetic modelling is underpinned by palaeomagnetic sampling, as provided in Part 3.

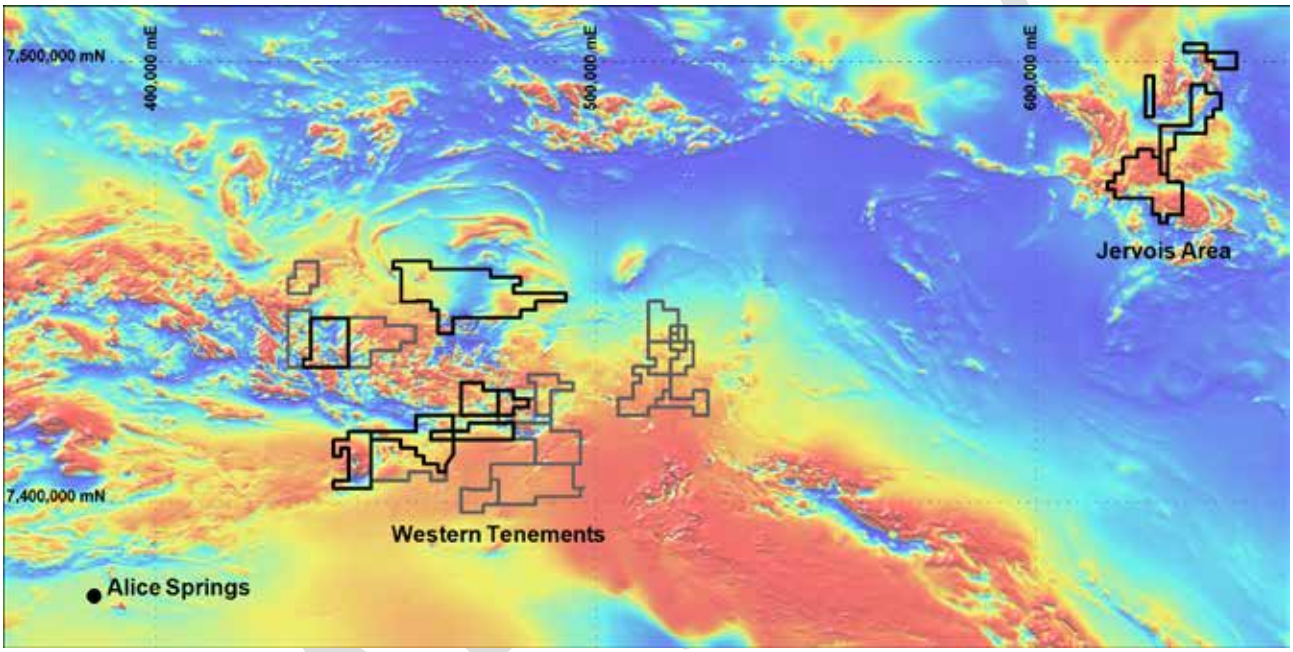

Figure 1: TMI data over the Arunta province NE of Alice Springs, and the location of Core Exploration tenements in black, and JV tenements in grey.

In this, Part II, of the reporting for this RIB project, I selected targets blind, based on the magnetic signature, and/or geological context, in order to maintain some objectivity. I consulted prior exploration work, where available/relevant after initial evaluation of the target, in order to asses my evaluations and/or provide some context to the modelling results. Unfortunately, there is not a great deal easily accessible information that is also useful, so I mainly utilised Mineral Occurrence data, mapped geology, drilling data.

One of the unfortunate aspects of the reliance on publicly available data for this project is that there is no survey altitude data available for most NT aeromagnetic datasets. Why I do not know. But it does create a problem in that we cannot be sure of the exact vertical location of modelled bodies. And furthermore, we cannot accurately account for variability in the ground clearance due to topography. So in essence, the data is not really suitable for generation of detailed magnetic models that accurately model the actual geology. Hence, the models presented here should be considered as approximations in terms of their location, properties and architecture. I have

endeavoured to focus on the anomalies that I feel are the most likely to be mineralised, vs. just geological, and as such have not completed an equal amount of work on all of the tenements.

There are no petrophysical data other than for the Mordor Pound area (which will be reported on separately by Clive Foss) and confidential data generated for other projects. So the petrophysical properties of the models (in particular the remanence directions) are either unconstrained, or at best are educated guesses, based on knowledge of the main directions present in the Arunta.

The interpretations are presented by tenement number. A systematic approach was not used throughout, mostly because the data quality, supporting data, and style of mineralisation sought differ dramatically from target to target. In general however, there has been some attempt to evaluate each target based on:

1. Probable style of mineralisation
2. Proximity to major (e.g., mantle tapping) structures
3. Proximity to known mineral occurrences
4. Structural Context and or structural controls
5. Size and or volume of potential ore body
6. Depth below surface

These criteria were used to make a shortlist of the better targets across the entire area.

2 Target Evaluation by tenement

2.1 EL 29689

2.1.1 South of tenement

Two interesting magnetic targets are located within EL 29689. One is a relatively sharp negative anomaly which sits in the west of the tenement (Fig 2). The other consists of a number of negative magnetic anomalies that appear to have a snake-like architecture (Fig 2). These snake-like negative anomalies appear to emanate from a negative anomaly just south of the tenement (marked by a red star). Both these negative anomalies sit along a NW-striking lineament along which several similar negative anomalies also occur (Fig 2). Several of these are mapped as Proterozoic mafic intrusions thought to be temporally related to the Giles/ Warakurna event (although that has not been confirmed by geochronology). However, these have been have been sampled as part of another (yet to be published) study in the Arunta completed by the author, and the results are consistent with such an inference. The interpretation that these anomalies all sit along a lineament suggests that a deep-seated structure is responsible for their localisation, and if correct this could act as a pathway for magma and /or fluids to be expelled from the mantle and into the mid to upper crust (i.e., a first order pathway for mineralisation).

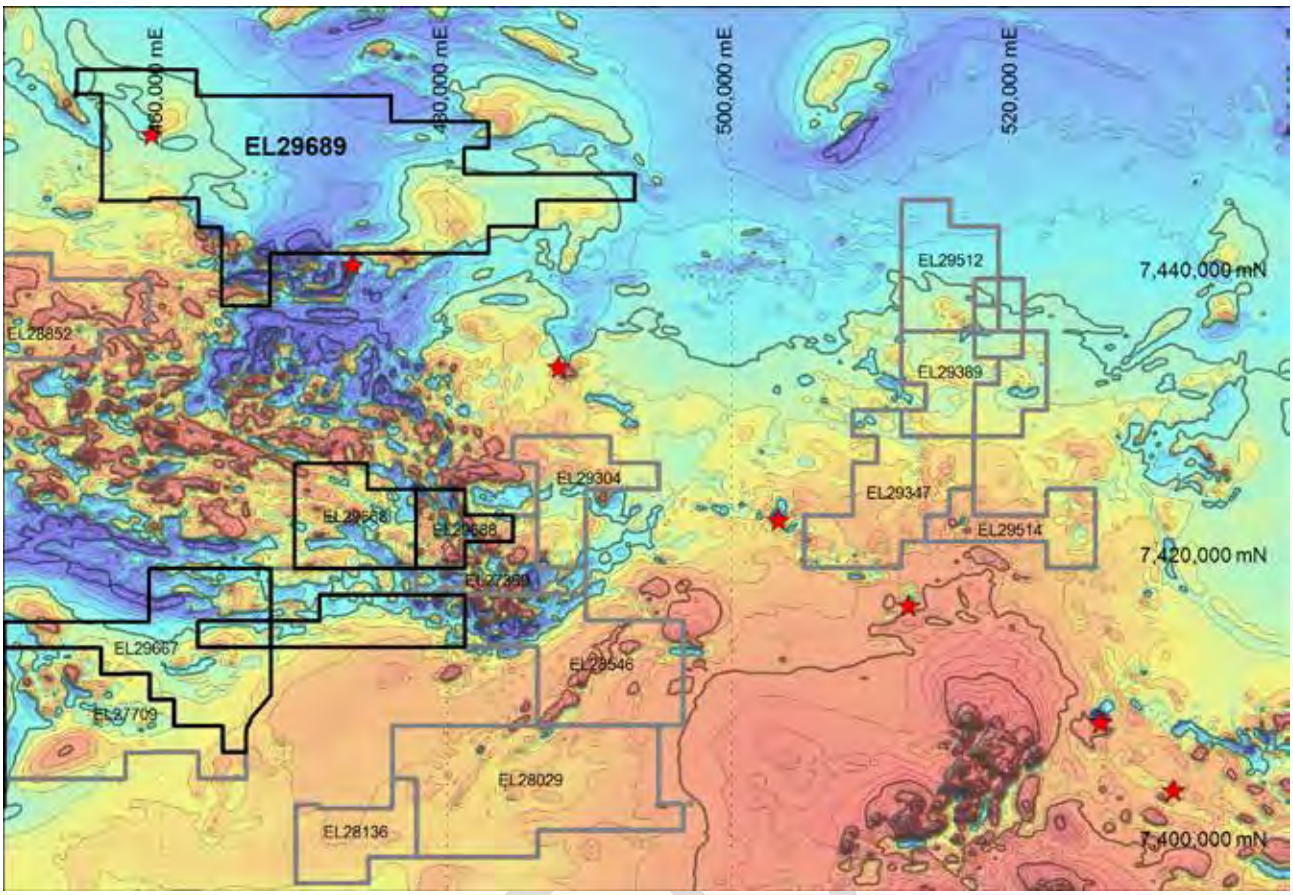

Figure 2: TMI data over the Western Tenements, detailing the position of a number of negative magnetic anomalies (marked by red stars) sitting along a NW-oriented lineament.

The negative snake-like anomalies that sit in the south of the tenement appear to emanate from a possible Giles aged feeder, which sits on a crustal-scale fluid pathway, and the snake like architecture suggests that these anomalies may in fact be chonoliths. Hence, these anomalies may be prospective for Ni-Cu-PGE mineralisation, similar to that observed at Nebo-Babel (e.g., Seat et al., 2007).

The snake-like anomalies are of interest because they have distinct remanent magnetisation that is clearly very strong (relative to their induced component), and that is known from several other sites in the Arunta to be present in Mafic-Ultramafic rocks in particular. For the most part these have steep- moderate downward directed magnetisations that are oriented toward the SSW. However, there are a number of discrete magnetisations, all associated with different stages of metamorphism and/or crustal unroofing during the Petermann and Alice Springs orogenies (i.e., most are related to metamorphic events between *ca* 430 and 300 Ma).

The proposed source and the majority of the snake-like anomalies sit outside the tenement to the south, but a portion extend into the southern extension of the tenement, as shown in Fig 3. A transformation of the TMI data was used which is termed an "ASO RTP" which transforms the magnetic data such that anomalies with the late Alice Spring Orogeny magnetisation (steep down to the SSW) should have positive symmetrical anomalies (Fig 4). Although both anomalies appear to be strong negatives, in fact they have quite different morphology. The southern two anomalies appear to have a steep downward magnetisation, as evidenced by their more-or-less symmetrical

negative anomalies in the TMI grid, and their associated symmetrical positive anomalies in the ASO_RTP grid. Conversely, the main northern anomaly has a dipole set in both grids, with the high in the SW and the low in the NE for the TMI, and opposite for the ASO transformation. This indicates a magnetisation direction with a SW declination and a shallow upward inclination. Their magnetisation directions (as modelled) are also consistent with measured metamorphic events at *ca 310-290 Ma* for the southern two, and *ca* 360 Ma for the northern anomaly.

The models generated for each anomaly (shown in green on Figs 3 and 4) are all fairly narrow, have very limited depth extent, and are somewhat sinuous, which is consistent with them being chonoliths. However, the mapped geology of this area suggests that they may not in fact be. The geology here is mapped as a calc-silicate member of the Strangeways Metamorphic Complex, probably the Cadney Metamorphics. Although, there does not appear to be a consistent surface expression of the modelled bodies within the tenement. There is a clear spatial correlation between the ASO_RTP magnetic anomaly of a section south of the tenement (Fig 5), and a pale-white coloured unit observed in an enhanced GoogleEarth imagery over the same area (Fig 6). This probably does suggest that the remanent anomaly is caused by the mapped pale unit, probably some type of calc-silicate, and it is probably also fair to infer that it could be some kind of skarn, given that skarns are well known to display remanent magnetisation.

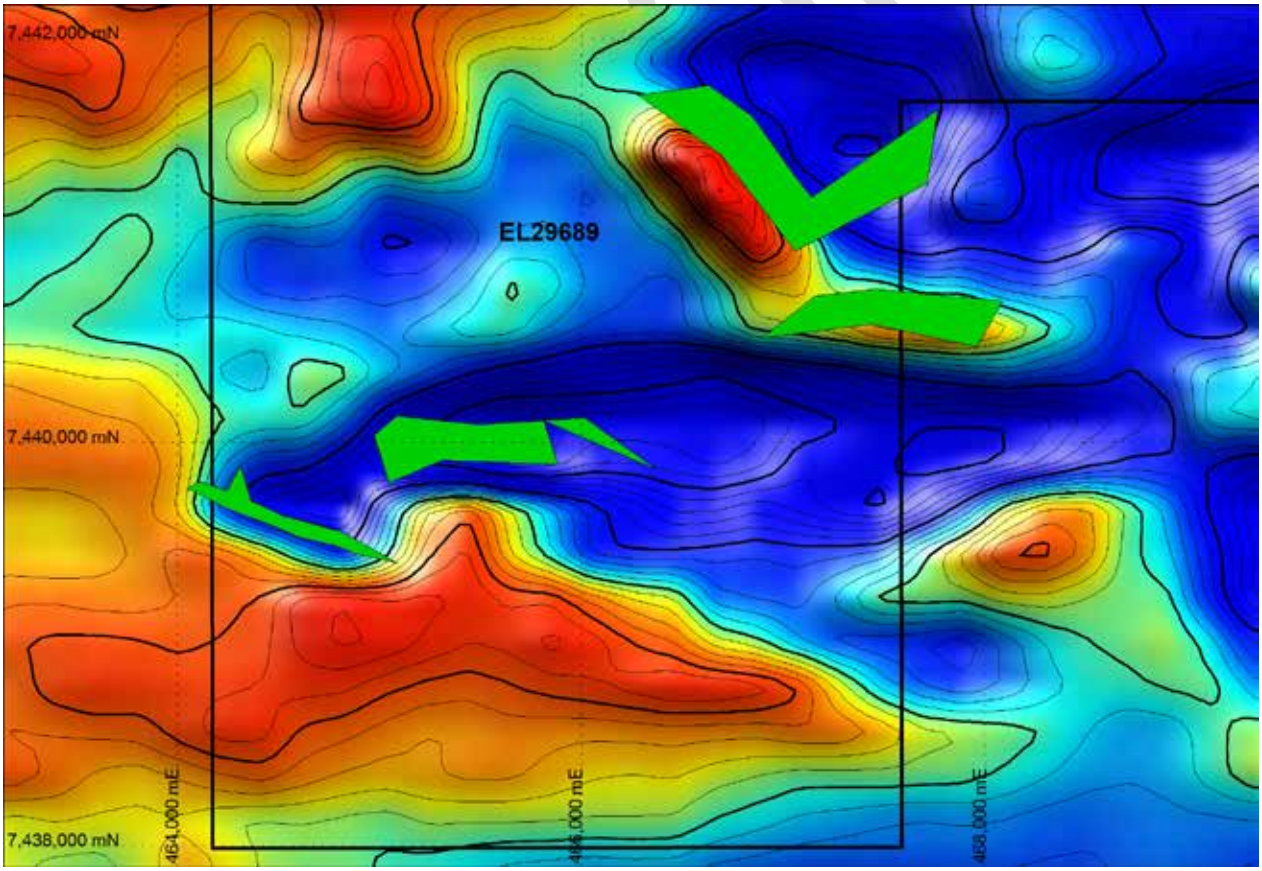

Figure 3: TMI data over the southern portion of EL 29689 displays a strong negative anomaly.

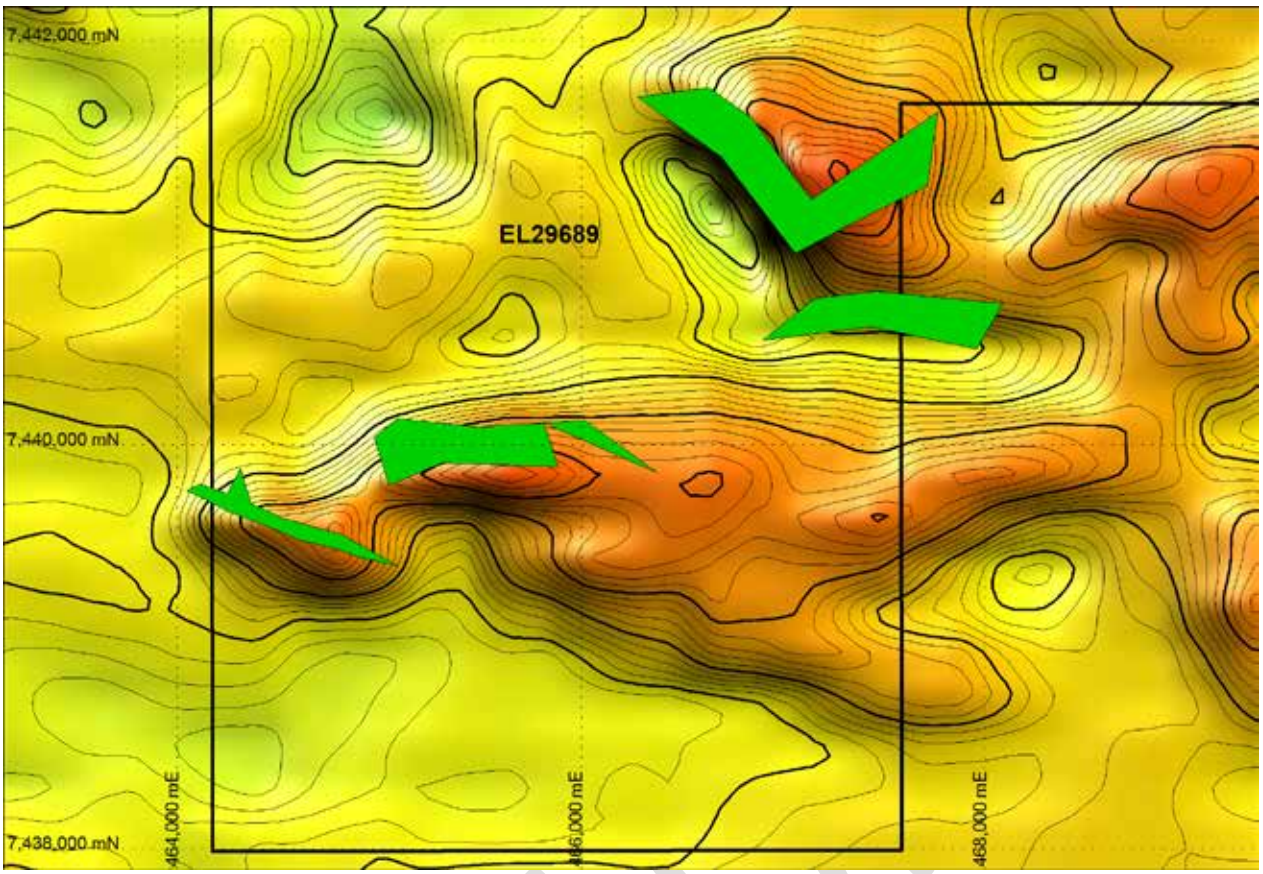

Figure 4: The ASO_RTP transformation of the TMI data is used to highlight magnetisation consistent with a *ca* 300 Ma metamorphic event during the Alice Spring Orogeny. Modelled bodies are shown in green.

Figure 5: The ASO_RTP transformation of the TMI highlights a "U-shaped" anomaly just south of the tenement.

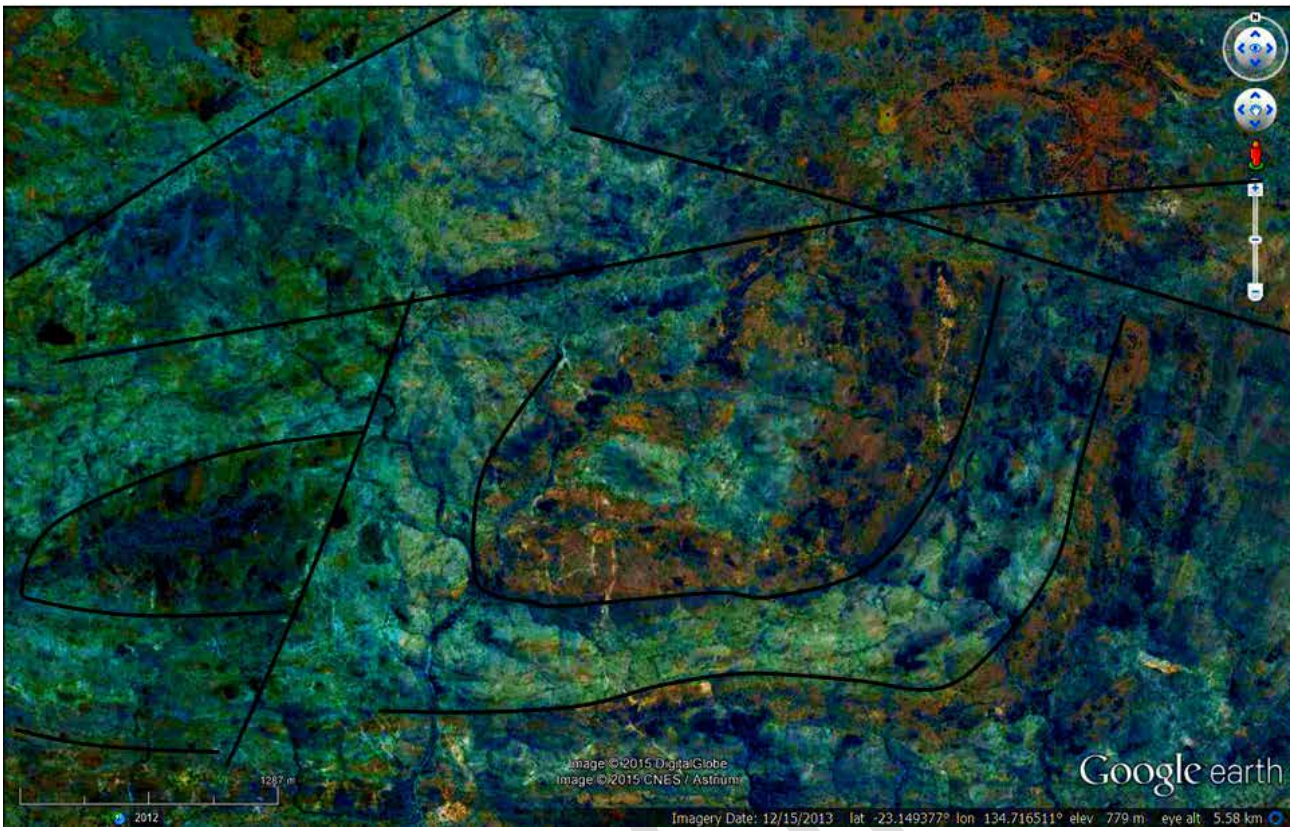

Figure 6: An enhancement of GoogleEarth™ imagery over the same area shown in Fig 5 illustrates a spatial coincidence between the u-shaped anomaly and a stratiform unit with a pale/white/blue surface expression.

We cannot from assessment of the magnetics data alone make any inference as to whether the interpreted skarn may have been formed via interaction with magmas or magmatic fluids, and so cannot determine its prospectivity beyond the interpretation that it could be a skarn. There is, however, an old copper working located nearby (Copper Queen; as shown on the Alice Spring 1:250k topographic map), which sits on the edge of the negative anomaly, possibly within a fault/ structural displacement (Fig 7). I would suggest a sensible follow up would be to examine these workings on the ground, in order to assess potential for skarn mineralisation. The deep crustal lineament could be a potential fluid source for such a skarn system.

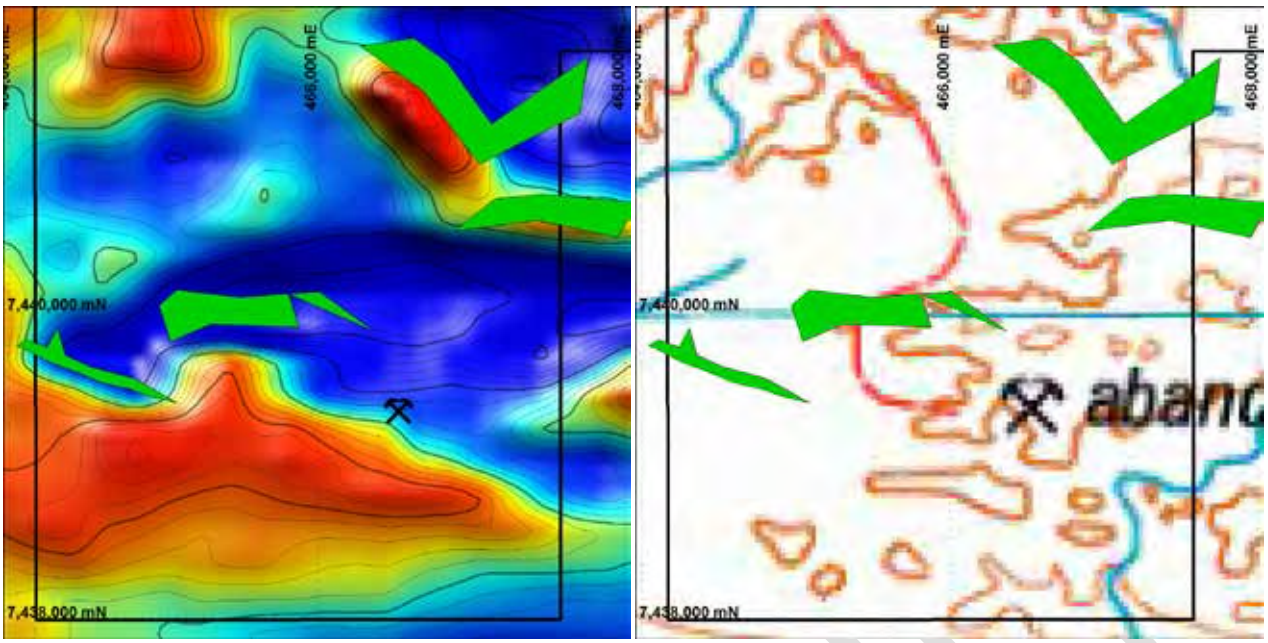

Figure 7: Highlights the location of a small copper prospect on the edge of the negative anomaly discussed above.

Prior work by Tanami Exploration

Tanami Exploration did carry out considerable exploration over this ground prior to 2004 and the results of their work provide some interesting insights into the source of these anomalies, and their potential for mineralisation. Tanami Exploration identified IOCG (Selwyn Style Cu-Au) and Coronation Hill-style Au-PGE (e.g., Needham & Stuart-Smith, 1987) mineralisation as their main targets. I would suggest that there is minimal, if any, difference between an IOCG and a skarn, and also add that there is also potential for Magmatic Ni-Cu-PGE deposits in this area.

The work completed by Tanami Gold was focussed on surface and shallow RAB geochemistry. The geochemical targets generated were then drilled to a greater (but still relatively shallow) depth, again using RAB (Potter, 2003). I only mention this because, I think their work, although significant in terms of spatial coverage, leaves a lot of potential untested at depth.

Interestingly, there is no mention of magnetics or any geophysical methods in the rather extensive report by Potter (2003). This is not necessarily surprising given Tanami Gold specialises in presumably non-magnetic Au-systems, but it is a key point, because we can reasonably assume that their targets are based on geochemistry alone. The report suggests the highest Au-Cu grades obtained from assay of the RAB holes appear to be associated with Magnetite-Garnet lithologies. Although I did not see mention of skarn in Potter (2003), this style of alteration is typical of skarn and in fact at least one of the prospects in this area (the one to the west of Copper Queen) is referred to as a skarn. So perhaps Core Exploration should be targeting magnetite skarns in this area. It is reasonably clear that a simple TMI map will not assist definition of the magnetite skarn, because the magnetisation is clearly remanent. However, when I compared drill-hole patterns to the location of peak magnetic anomalies in the ASO_RTP magnetic transformation (which corrects the magnetic field to the Alice Springs Orogeny remanence direction), I found that the drill holes almost test everything other that the peak of the ASO_RTP magnetic anomalies (Fig 8).

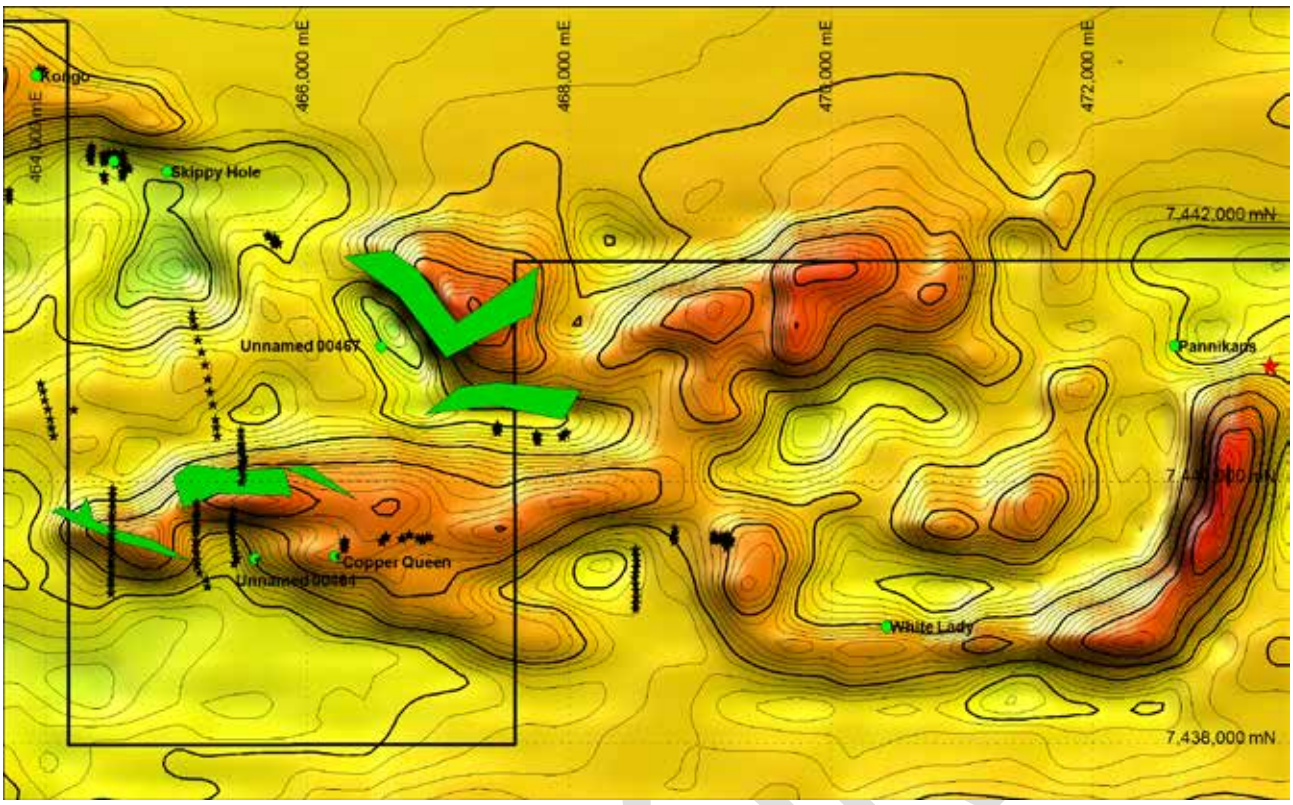

Figure 8: Shows the ASO-RTP transformation of magnetic data, and the location of RA drilling completed by Tanami Exploration (Potter, 2003). NB. In the majority of cases, the peak of the anomalies and/or the location occupies by the modelled magnetic bodies have not been tested by the drilling.

In summary: there are known Cu shows in the area; the highest Cu-Au grades are associated with Mt-alteration; but the peaks of the magnetisation (as opposed to the TMI peaks) are largely untested; and the terrain as a whole is largely open at depth. As such, I believe that these targets still offer excellent potential for a mineral discovery in this area.

In terms of exploration strategy for this area, I have three main concepts that would be worth testing further.

1. It could be that there is some kind of zonation within this system, such as is observed in many deposit styles (e.g., VHMS, BHT, SedEx) but most importantly IOCGs (e.g., Austin et al., 2013a, b) and skarn (e.g., Chang & Meinert, 2008). So we might expect there to be a progression from reduced to oxidised mineralogy with increasing distance from the fluid source (e.g., Pyrrhotite -> Magnetite-> Hematite). Mineralisation would commonly sit within one of these phases preferentially, generally at the more reduced end. So it is possible that the parts of this system that have been tested thus far are too far distal from the fluid source, and hence only sub-economic grades of mineralisation have been intersected. So Core Exploration may wish to focus future exploration closer to the fluid source (marked by a red star), which in this case I suspect is the major SE-trending lineament discussed previously. Untested targets with potential for skarn mineralisation are marked by a purple dotted line (Fig 9), e.g., along strike to the ENE of Copper Queen.

2. It could be that the mineralisation that has been intersected is a distal part of the system in a vertical sense. So we might expect that sub-economic (Supergene) mineralisation is commonly preserved in the near surface, but that more massive economic skarn mineralisation could be preserved deeper in the system. There are some clues in Tanami's exploration results (Potter,

2003) that may support this notion. I have plotted a red dot for drill holes where Cu grades above 1000ppm were intersected as a proxy for more intensively mineralised zones (Fig 9). Although hardly conclusive, the data do suggest that perhaps the mineralisation intersected is controlled by some linear features (e.g., brittle faults). If this is the case, the mineralisation observed could be secondary remobilisation/ supergene enrichment that is only a distal indicator or a more significant metal source. The observations of some of the mineral prospects in the area are consistent with this hypothesis, (e.g., minor malachite in micaceous schist, secondary uranium mineralisation). Obviously the only way to truly test this is with some deeper holes.

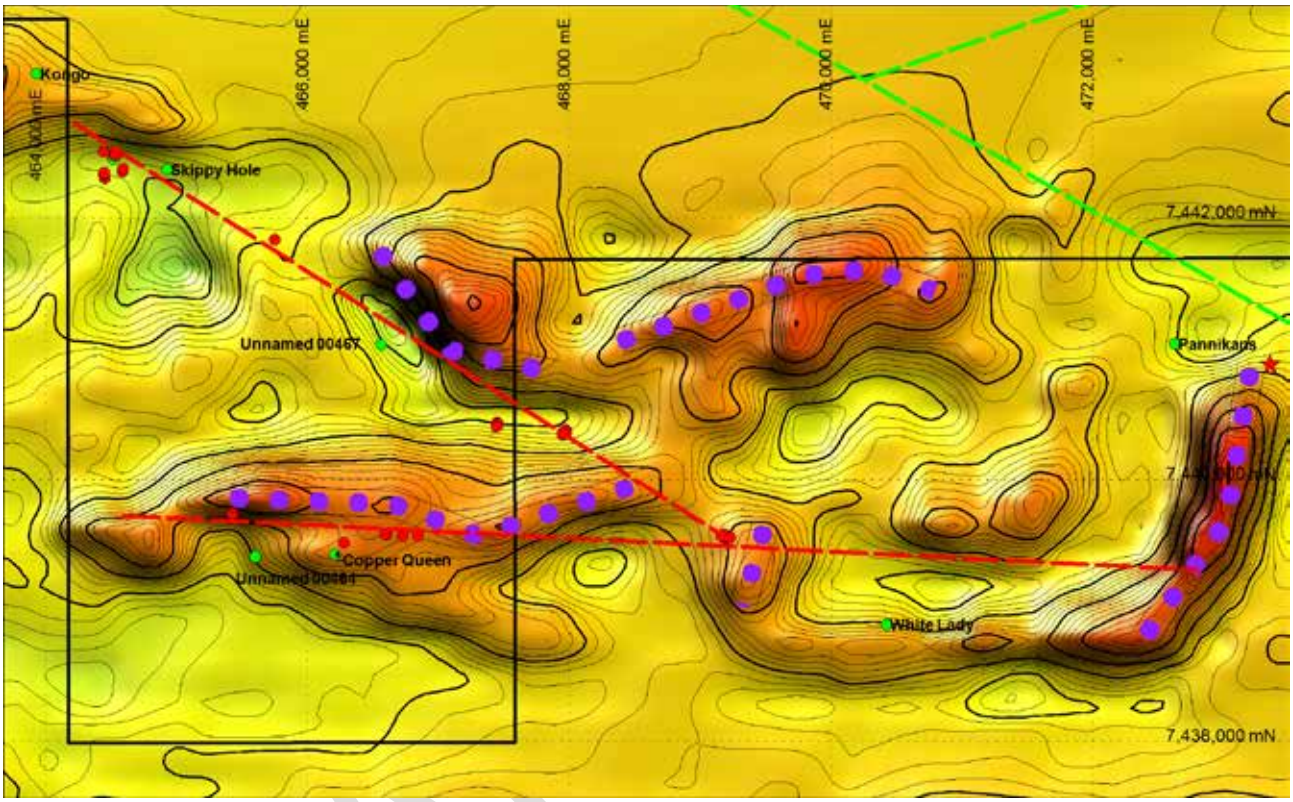

Figure 9: Shows the ASO-RTP transformation of magnetic data, and the location of RAB drill holes where copper >1000ppm (Shown in red). NB. In the majority of cases, peak assay results are not spatially correlated with the peak of the anomalies and/or the location occupies by the modelled magnetic bodies but sits along linear trends (red dashed lines), possibly brittle faults. The locations of untested targets are marked by the Purple Dotted Lines.

3. There may be something in the anomalies themselves that may provide some clues as to their mineral potential. For example, can we determine whether magnetite or Pyrrhotite is the dominant magnetic carrier? Does the amplitude of the anomaly tell us anything about the source depth or mineralogy? This may in turn tell us something about Redox and the likelihood of base metal enrichment. I think that the fact that the highest amplitude zone of the anomalous "skarn" is closest to the proposed source is significant. However, since it is off-tenement it does not warrant further discussion here. The other significant observation is that the anomaly modelled as the "Northern Anomaly" has a completely different magnetisation to the majority of the remanence. This can be elucidated by completing an alternate transformation of the magnetic data to reflect the earlier remanent magnetisation direction. To demonstrate this I have shown several different transformations of the data, and how they relate to the modelled body. In Fig 10, a comparison of the total magnetic intensity grid shown in A and B, a standard Reduction to Pole (C and D; which corrects to the magnetisation of the current magnetic Field) the Alice Springs

Orogeny Transformation (E and F; which corrects to the magnetisation present during the latest Alice Springs Orogeny at *ca* 300Ma (Dec 190, Inc: 75°). This comparison shows that neither the TMI, the RTP nor the ASO transformation have symmetrical anomalies nor is the modelled body coincident with the anomaly in any case. This means that the magnetisation caused by the body is not correctly mapped by any of these transformations. However, as shown previously, the majority of the snake-like anomalies are correctly mapped by the ASO_RTP transformation. So this particular anomaly is the exception.

In contrast, Fig 11 shows another two transformations, the first (A and B) is a transformation for an earlier part of the Alice Springs Orogeny which maps magnetisation with shallow SW magnetisations (Dec: 235° and Inc: +5°) and the other (C and D) is the Analytic Signal (Total Gradient) of 70m upward continued TMI. Note, in both cases the anomaly is symmetrical, and the modelled body is coincident with the peak of the anomaly. So it is therefore clear that the body has an earlier magnetisation than for many of the other anomalies in the area, it also has a larger amplitude anomaly. So this evidence would suggest that this anomaly is more likely to be precipitated during an earlier metamorphic/metasomatic event, or at least retain an earlier remanence. Secondly, it would appear to retain strong remanence, which might indicate pyrrhotite is more dominant (than magnetite) within the causative body. If these interpretations are indeed correct then this anomaly is more favourable than the others as a source of a primary skarn/ IOCG or indeed Magmatic Ni-Cu mineralisation. Furthermore, this target is completely untested by drilling, even though there is some secondary mineralisation observed just to the west.

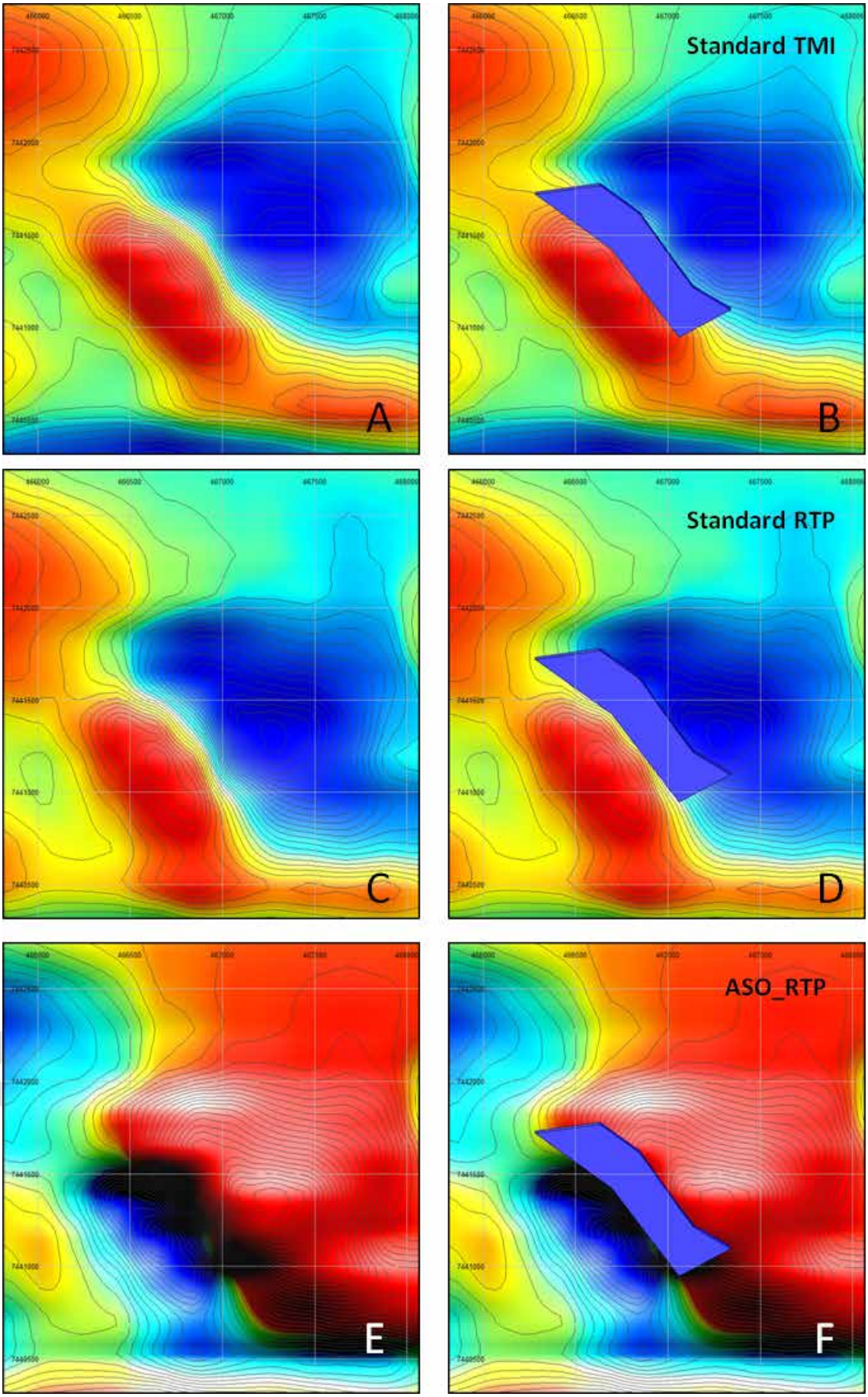

Figure 10: A comparison of three different magnetic grids/transformations, and their anomaly location relative to the modelled body. Total magnetic intensity grid shown in A and B, a standard Reduction to Pole (C and D; which corrects to the magnetisation of the current magnetic Field) the Alice Springs Orogeny Transformation (E and F; which corrects to the magnetisation present during the latest Alice Springs Orogeny at *ca* 300Ma (Dec 190, Inc: 75°).

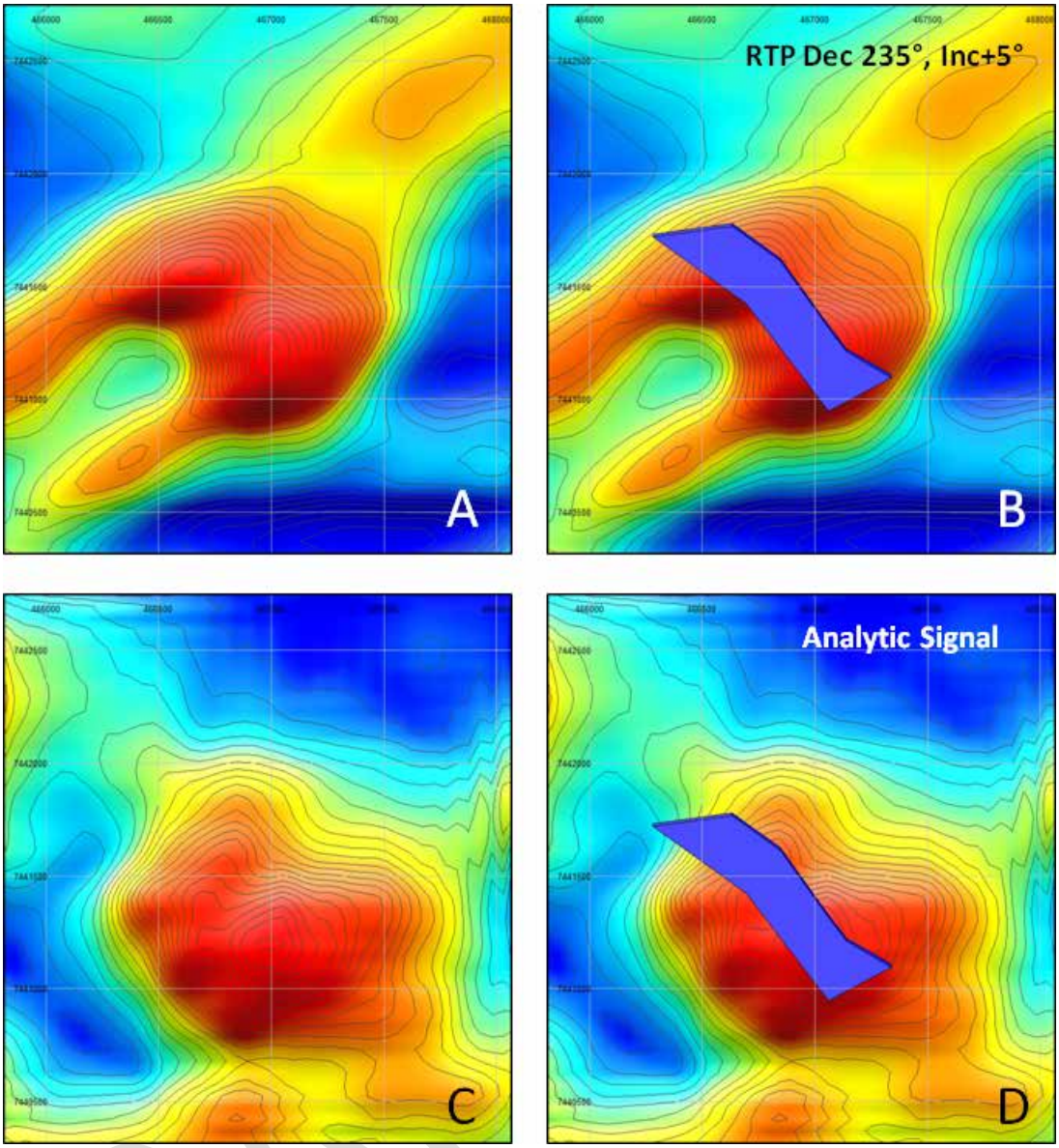

Figure 11: two transformations, the first (A and B) is a transformation for an earlier part of the Alice Springs Orogeny which maps magnetisation with shallow SW magnetisations (Dec: 235° and Inc: +5°) and the other (C and D) is the Analytic Signal (Total Gradient) of 70m upward continued TMI. Note, in both cases the anomaly is symmetrical (i.e., it has a comparable gradient on either side of the anomaly peak), and the modelled body is spatially coincident with the peak of the anomaly.

2.1.2 Northwest Anomaly

There is a discrete negative anomaly in the NW of the tenement which was also modelled Figure 12. Although this appears to be a fairly large anomaly in the TMI grid (Fig 13a), in the line data it is a sharp discreet anomaly. The model generated is a narrow lens which strikes NE (parallel to the mapped foliation in the area) and plunges toward the west. The interpreted body sits in the footwall of an interpreted fault, along a secondary structure? That is parallel to bedding? , as shown in Figure 13 (a-c).

It sits within the Iridina Gneiss, apparently within biotite gneiss unit and just NW of a contact with more calcareous gneiss (Fig 13b) and seems to be concordant with the structural fabric of the host lithology (Fig 13c). The Riddoch Amphibolite lies to the SW, in the hanging wall of an ~E-W striking

fault. Curiously, the biotite gneiss and calcareous gneiss appear to have a mild positive magnetic signature, but the amphibolite does not. In any case, the lithology associated with the anomaly is different to the all of the surrounding lithologies, but we could only speculate as to what it might be. Possibilities might include: a fault-bound lens of mafic material that postdates amphibolite facies metamorphism (e.g., Lloyd Mafic Suite); or some kind skarn alteration, either of which could show potential for mineralisation. The body modelled here is fairly small (100x500m), although large enough to mine given a good grade. It does appear to extend close to the surface and hence should be fairly easy to map in the field. There is a chance that this anomaly could be related to some kind of surface infrastructure, e.g., equipment used for mining of the nearby mica mines, but that can be tested during a field reconnaissance. The fact that this anomaly also sits along the lineament, as previously discussed in section 2.1.1., probably suggests it is a sliver of mafic intrusive, possibly intruded up the fault plane.

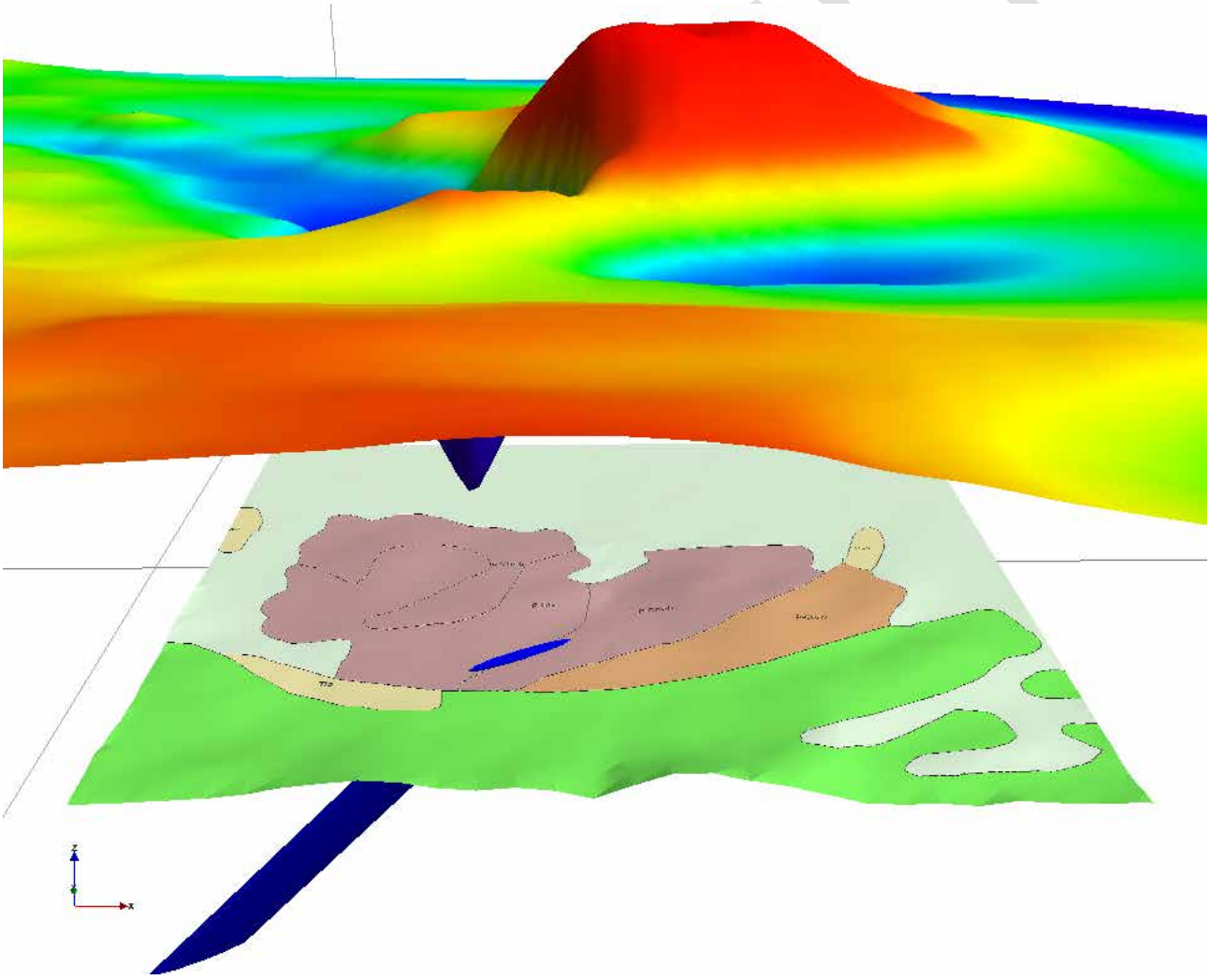

Figure 12: 3D view of the modelled body (dark blue) projected to the surface, and its position relative to the mapped geology and relationship to TMI grid sitting above.

Figure 13: A. The TMI grid and the anomaly in dark blue, and the modelled body outlined faintly in black; B. An excerpt from the 1:250k Geological map (Shaw and Wells, 1983), showing the position of faults, mica mines and different lithologies Ehi = Iridina Gniess, Ehn = Calcareous member of Iridina Gniess, Ehr = Riddoch Amphibolite. C. STRM topographic grid.

2.2 EL 29347

2.2.1 SW Targets

The Lineament (discussed in section 2.1) also runs through the SW corner of EL 29347 to the east, as shown in Fig 14. The portion covered by this tenement actually sits between two of the more distinct negative anomalies. However, there are a number of smaller 'pock-mark" negative anomalies sitting along the lineament between the larger anomalies. These appear to coincide with a number of mica quarries, with visible surface workings apparent in GoogleEarth™ imagery. There is also a feint lineation present in the GoogleEarth™ imagery that is coincident with the proposed lineament, which is coincident with the string of sharp negative magnetic anomalies; further evidence that it is indeed a real geologic structure. It would be reasonable to assume that the anomalies themselves are caused by Proterozoic ultramafic intrusive lithologies, because there are several discreet bodies mapped in the area (even though the mapped extent is inconsistent with the geophysical expression).

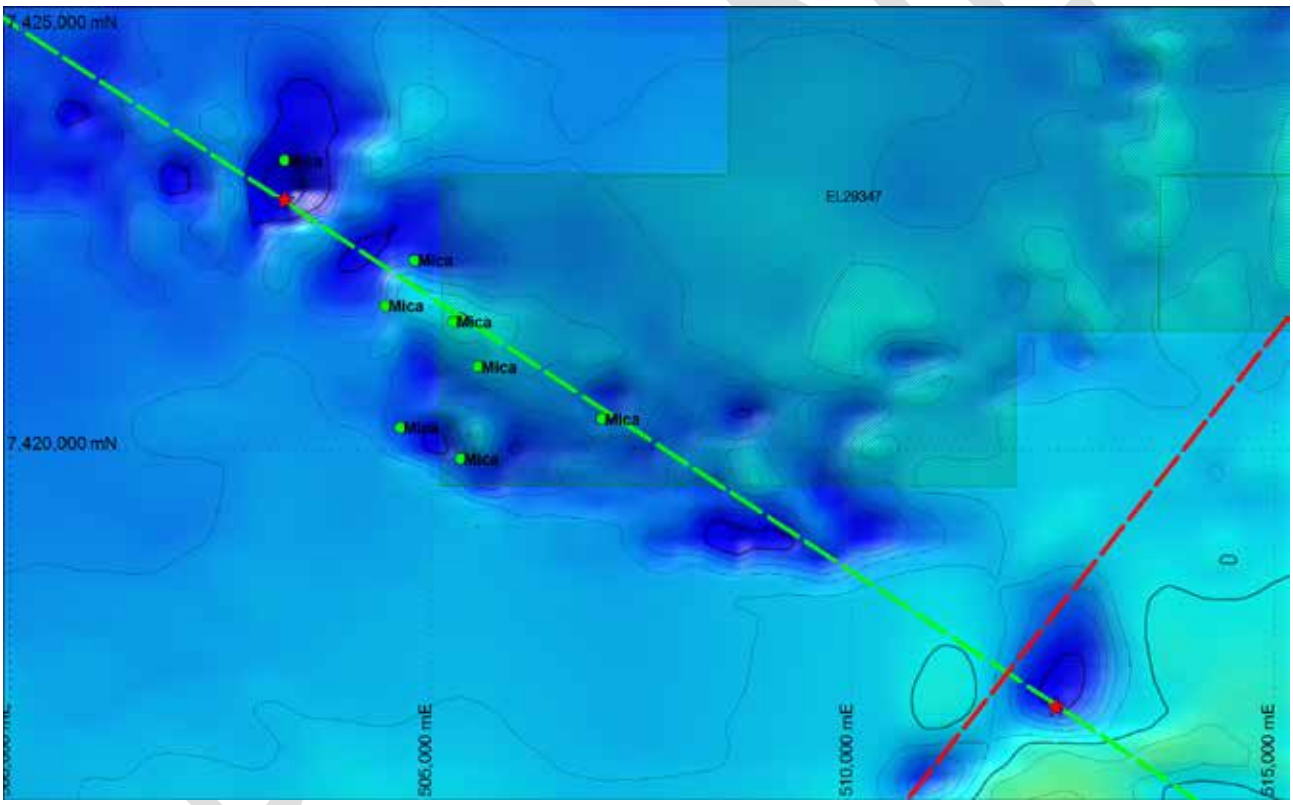

Figure 14: Total magnetic Intensity data over the southern portion of EL 29347, identifies a number of "pock-mark" negative anomalies, sitting in between two major negative anomalies (red stars), sitting along a major regional lineament (in green).

We modelled the two of these bodies which sit wholly within the tenement, and found that they are probably fairly shallow, with fairly limited depth extent and very small volume. Such bodies have been sampled elsewhere in the area, and were often found to be saucer-like sills often only a few metres thick e.g., Fig 15. In other instances they are modelled as lenticular bodies e.g., Fig 16.

In either case the bodies modelled here se do not have significant enough volumes to make them feasible targets for magmatic Ni-Cu-PGE style mineralisation.

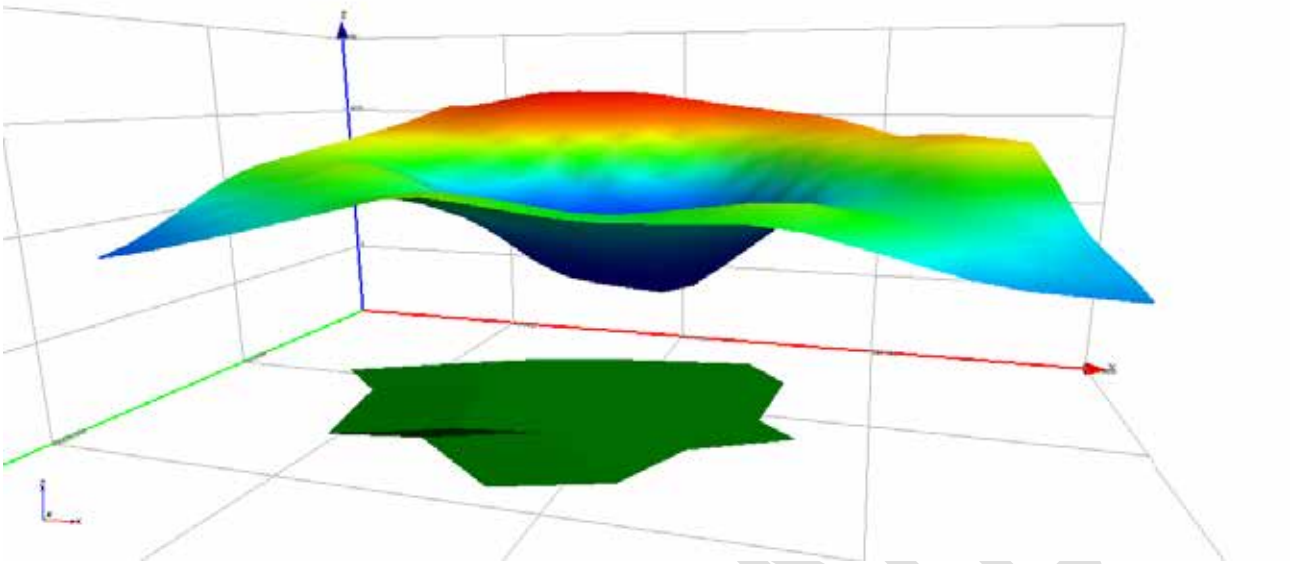

Figure 15: Target 2 on this tenement can be modelled as a thin saucer-like sill that is very shallow and has a very small volume.

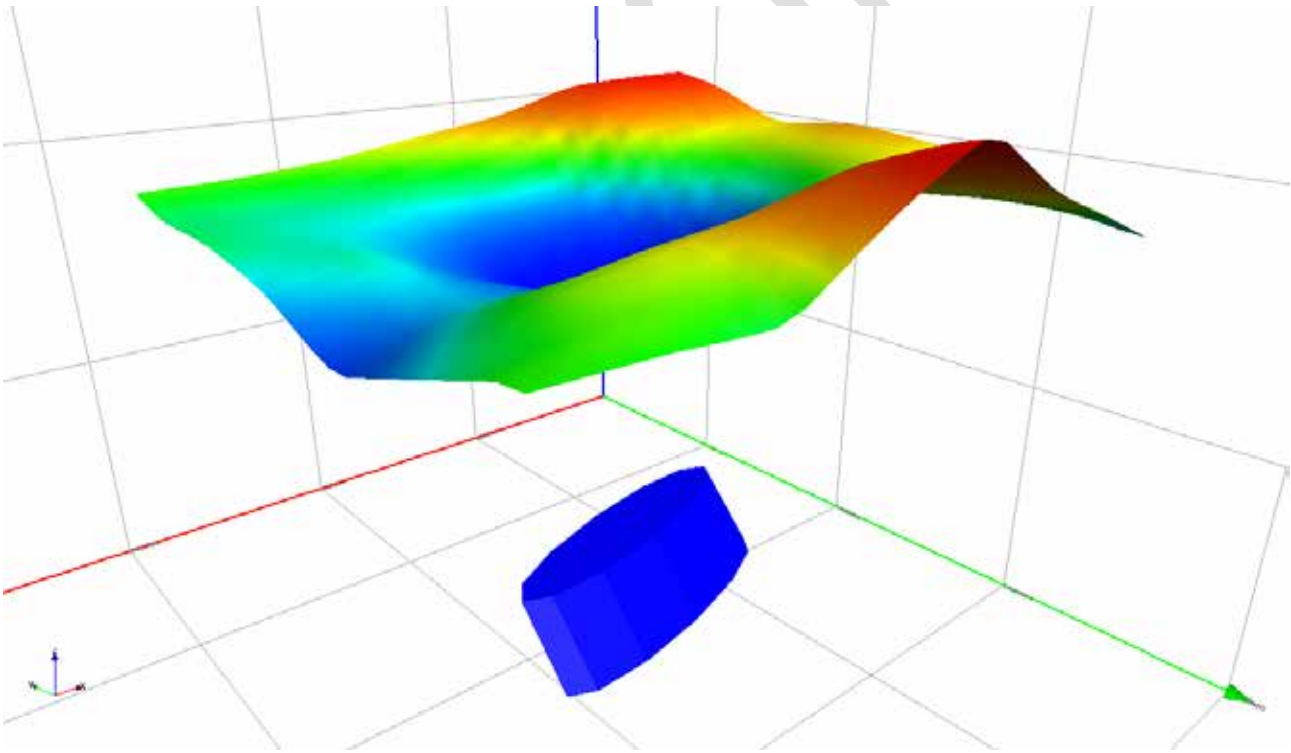

Figure 16: Target 1 was modelled as an elongated ellipsoidal prism. This body is deeper and thicker with much greater, but still in sufficient volume to make it a feasible target for Ni-Cu-PGE mineralisation.

I think this zone in general could be prospective for some form of hydrothermal or epithermal mineralisation. There does appear to be a mantle tapping structure present, it does appear to have channelled mafic magmas to the (present) surface and there does appear to be active metasomatism at some point, as evidenced by the mica-bearing pegmatites which have been mined throughout the area. Given there are no drill holes into this area, it should be considered a possibly prospective zone. However, I suspect that a secondary structure would be more

prospective, and obviously there would need to be further exploration of this area, using for example EM and ground geochemistry to further elucidate any potential.

2.2.2 Yambla Uranium Prospect

As a general rule, the spatial correlation between magnetisation and uranium is a negative one. In the instance of the Yambla Uranium Prospects, given the Uranium is thought to be hosted in retrograde shears (Gee, 2007), I suspect this assumption would hold true. However, given that there are several adjacent magnetic anomalies present in the vicinity of the prospect; I have completed some modelling to help elucidate the local architecture.

The main anomalies present, predominantly to the east of the prospect, are series of more or less aligned reasonably discrete positive anomalies (Fig 17a).

In this case it is important to review the actual data, because one of the main problems with magnetic data for this entire project is the lack of resolution. Luckily, over this particular area, there is high resolution data, with 200m spaced NE-SW oriented lines in addition to the standard 400m spaced N-S lines. The resolution of the later is ~25 times better, and the visual difference in resolution is astounding (as illustrated by Fig 17b).

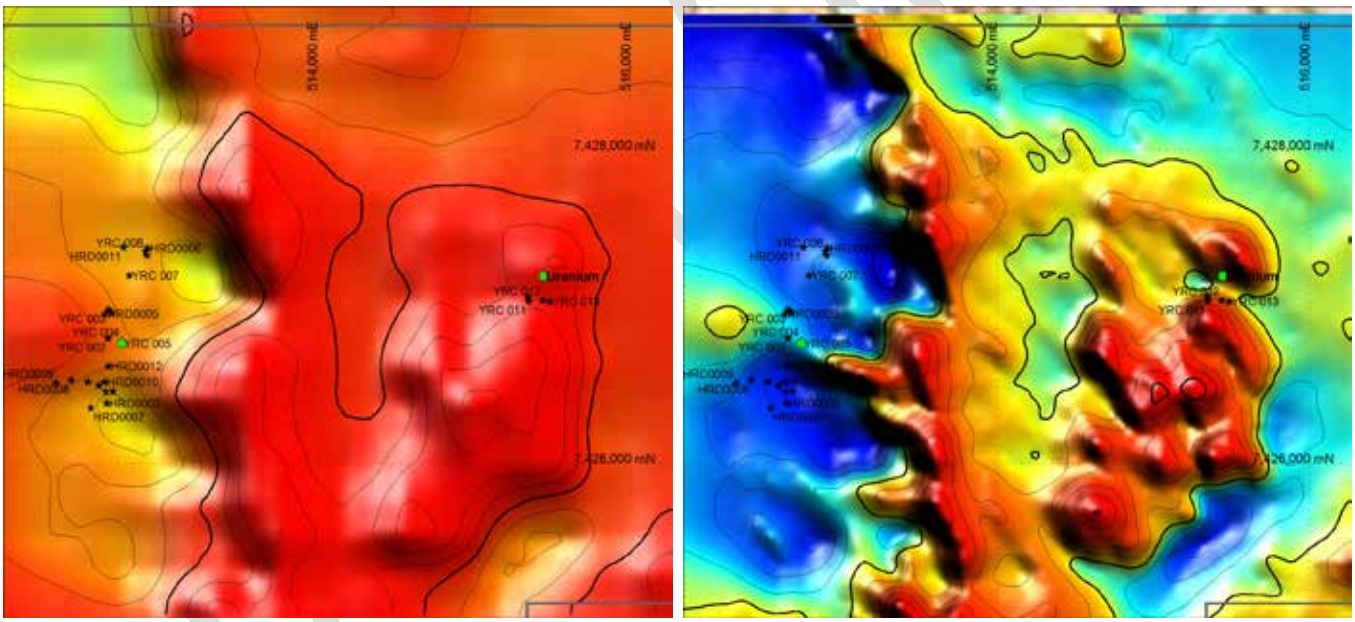

Figure 17: A comparison of the regional gridded TMI data (A), vs data gridded from the high resolution NE-SW-oriented 200m spaced data (B). NB. The increase in resolution is significant and provides much more detail.

Using the high resolution line data only, several discrete anomalies were modelled individually. The sub-surface architecture of the various resultant models is different, with some being of limited depth extent, and some plunging in different directions. However, we must consider that the anomalies interfere with each other, and furthermore there are always tradeoffs between dip magnetisation, depth and location, so we cannot be certain of much, other than the top of the bodies. In this case the tops of the bodies provide an interesting insight into the architecture of the system.

The yellow polygons, shown in Figure 18, represent the top of the modelled bodies. Their architecture in relation to the mapped geology suggests that they correspond with a stratiform geological layer. However, they appear to be cut and offset by a number of faults, and in one instance one of the corresponding bodies is in fact discordant with the overall strike of the magnetisation. Incidentally the discordant body is along strike from and intersects with a known Uranium prospect.

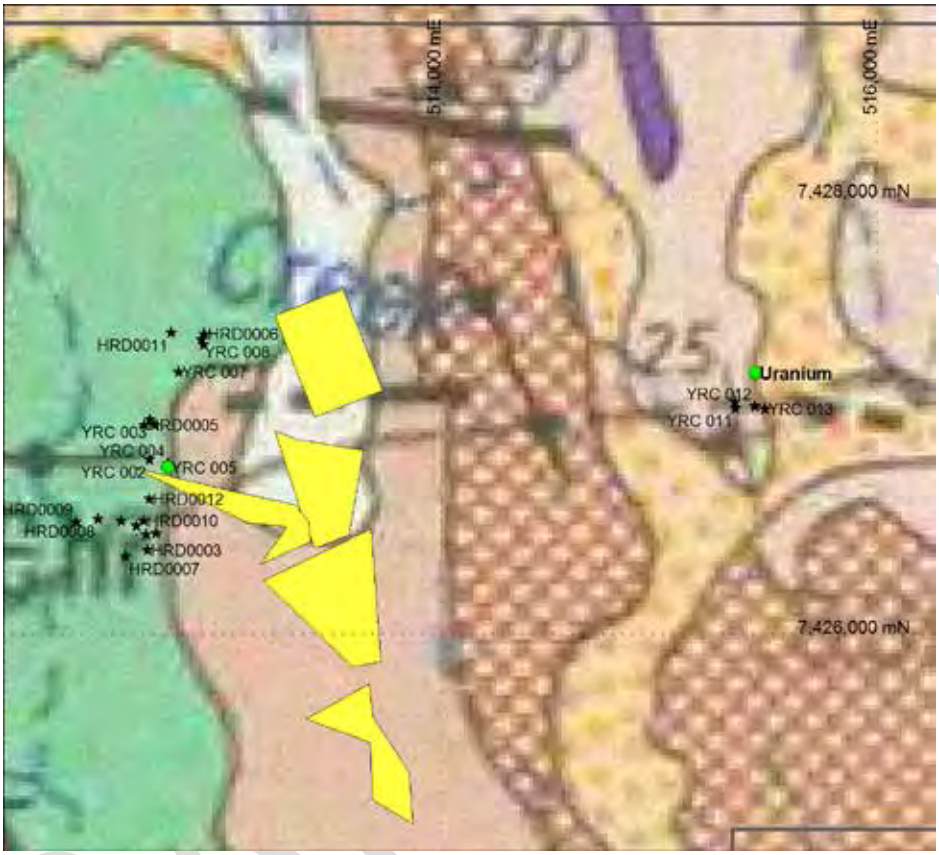

Figure 18: The top surface of the 5 modelled bodies, relative to the mapped geology (Shaw et al., 1985). Nb. The bodies are more-or-less stratiform but truncated, presumably by ENE-E faults.

In this particular case, it is useful to apply a 1st vertical derivative filter to help elucidate the surface structure of the area more accurately, as shown in Fig 19. In this case the 1VD magnetic image allows us to map not only the magnetic stratigraphy (marked in white dashed lines), but also the truncations of those horizons, presumably faults, as marked by black dashed lines.

Whilst, there does appear to be a spatial correlation between the uranium prospects and the interpreted faults, there is also a correlation between the uranium and a NE-oriented magnetised zone. This magnetised zone (marked with yellow dots, in Fig 19) does not appear to be sub-parallel to either the interpreted faults, or the stratigraphy. Hence we might interpret it as a transtensional dilation/ vein, related to the faulting. Such a dilation zone would make a favourable site for mineralisation, and more importantly provide a mechanism more favourable to the precipitation of economic grades of mineralisation, relative to a fault. Hence there is a possibility that this style of anomaly may provide a better target for mineralisation than the nearby fault-hosted uranium prospects. This and another similar magnetised zone to the south are both truncated at the

contact between their host stratigraphic unit and the amphibolite to the west, which supports the preposition that there is a primary rheological control on their development.

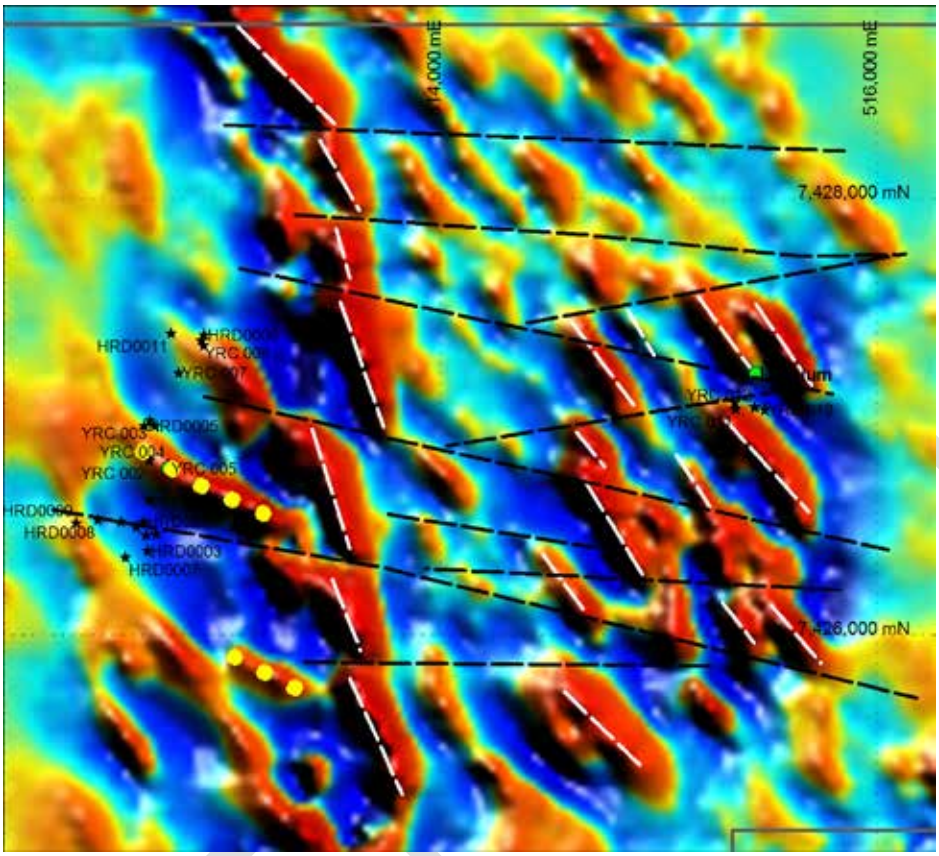

Figure 19: First vertical derivative filter applied to the high res gridded line data. Black Stars are drill holes, green dots Uranium prospects, black dashed lines are interpreted faults, white dashed lines are interpreted magnetised stratigraphy. The yellow dots mark zones that are discordant with the faults and stratigraphy, but coincident with Uranium mineralisation. These zones could be dilational, and prospective for Uranium mineralisation.

2.3 EL 29514

EL29514 contains two fairly large, discreet but complex anomalies which both preserve strong remanent magnetisation. As with the other anomalies modelled in this area, both these anomalies are mapped as Proterozoic ultramafic intrusions.

2.3.1 Western Anomaly

Anomaly 3, which sits in the west of the tenement, was modelled in part. It was found that the mapped extent of the intrusion is non-coincident with the modelled anomaly (Fig 20), i.e., the causative body is significantly smaller. Hence, we could reasonably assume that the body is not homogeneously magnetised. This heterogeneous nature of the magnetisation makes this anomaly a favourable target for magmatic Ni-Cu-PGE mineralisation, because it could mean there has been some fractionation, which is required to concentrate economic minerals. This could be easily tested with some fairly basic ground geochemistry over the intrusion. The magnetisation in the body (as modelled) is oriented toward 256 (WSW) with a sub-horizontal inclination of -3° (up). There could be a significant mathematical trade off between the orientation of the remanence and the plunge of the body in this case, because they are both oriented more-or-less E-W. Hence if the body were to have a steeper plunge, this could be accounted for to some degree by a steeper upward magnetisation. It is a moot point in this case because the body (as modelled) sits just 67m below the sensor (as shown in Fig 21), and furthermore crops out at surface (Fig 20b).

Figure 20: A. TMI anomaly over target 3 on EL29514; B. GoogleEarth™ imagery over the anomaly, and: C. the Mapped Geology over the anomaly (Shaw et al., 1985). NB. Although the mapped geology clearly correlates with the surface expression of the body, the magnetisation is not homogeneous within the intrusion.

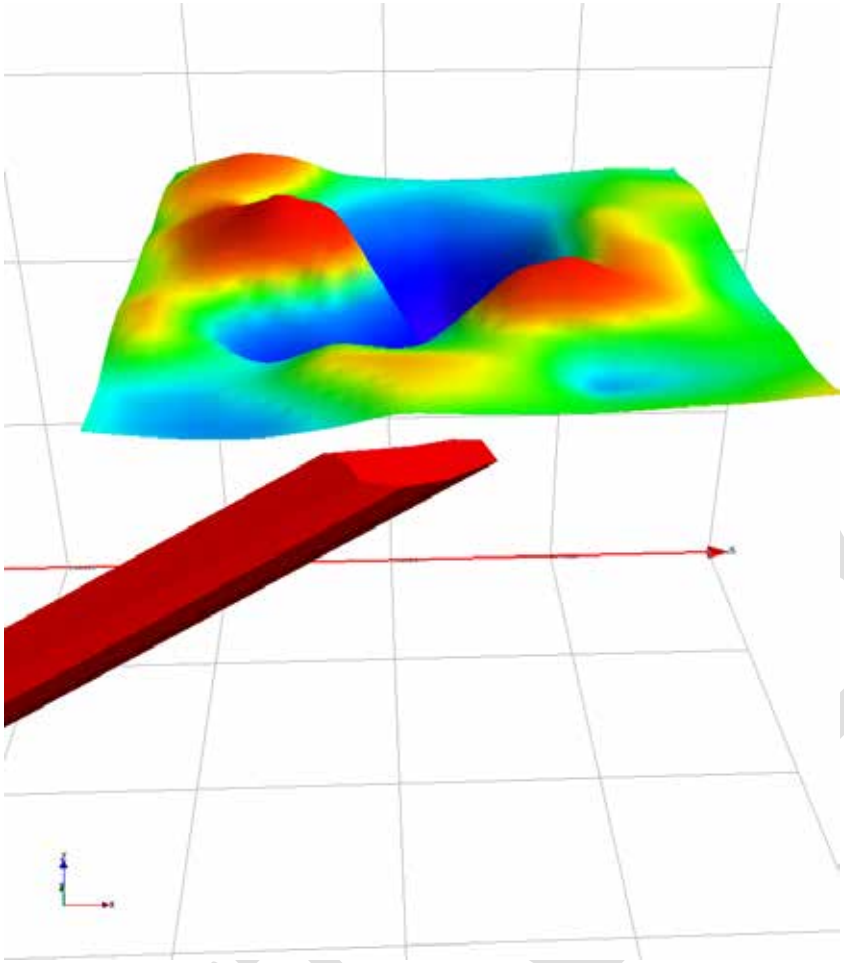

Figure 21: 3-D perspective view of the TMI anomaly over target 3 on EL29514 and a portion of the modelled anomaly, which has a shallow west plunging remanence direction.

2.3.2 Eastern Anomaly

Anomaly 2 (Fig 22, 23) sits in the east of the tenement and is of primary interest because it appears to preserve concentric zonation, with a negative anomaly coinciding with the core of the intrusion and a positive anomaly associated with the outer part of the intrusion (Fig 23). Such zoning is common in a number of different deposit types, but this particular style of bullseye zonation is most often associated with porphyry style deposits. The anomaly was modelled as three zones, an inner core which displays sub vertical remanent magnetisation (consistent with late Alice Springs Orogeny). Outside this there is a non-magnetic zone, and outside that there is a zone with positive magnetisation. As per usual, we cannot be sure of the exact architecture, because we do not know the magnetic properties of the rocks. However, if an Alice Springs Orogeny magnetisation is assumed for the core, and an induced magnetisation for the outer rim, then a fairly generic stock architecture model can be produced fits the data well (Fig 24).

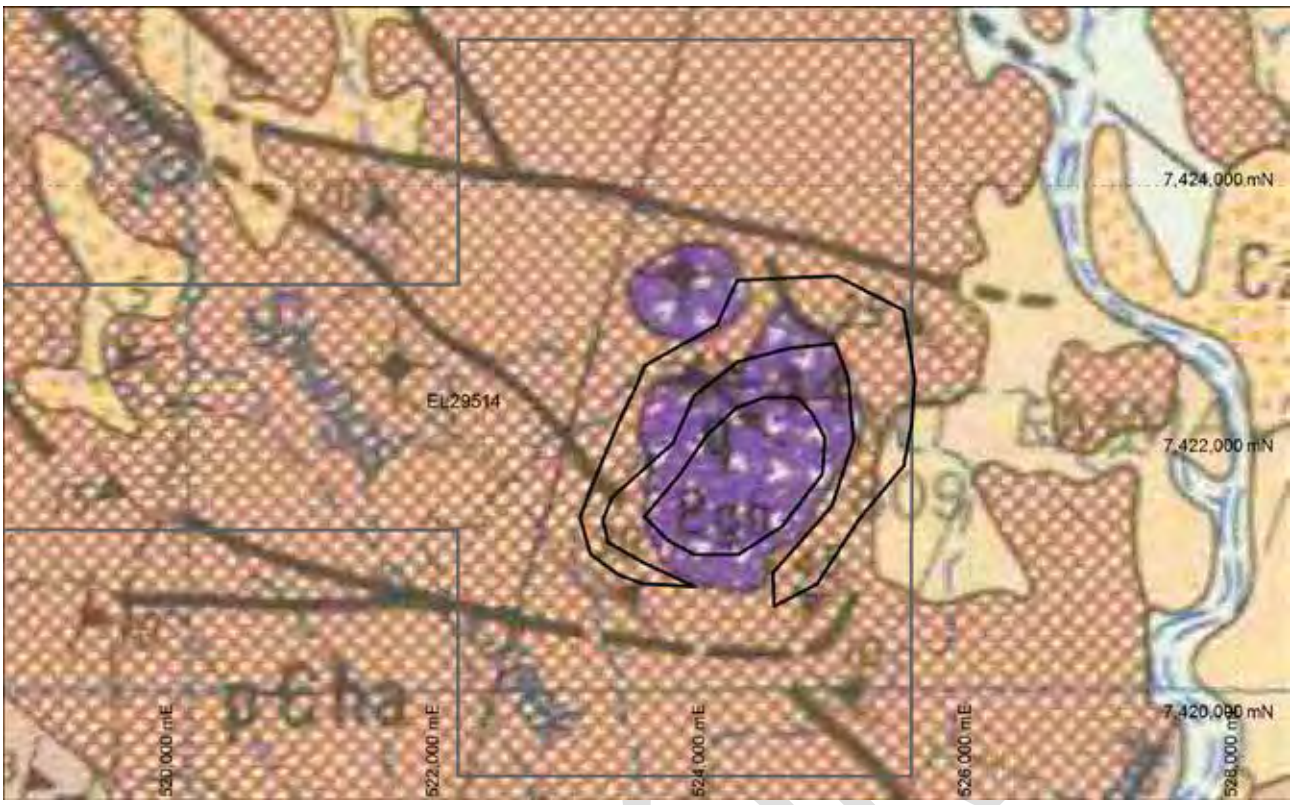

Figure 22: Map showing the modelled body and its position within EL29514, underlain by a segment of the Illogwa 1:250k mapsheet (Shaw et al., 1985).

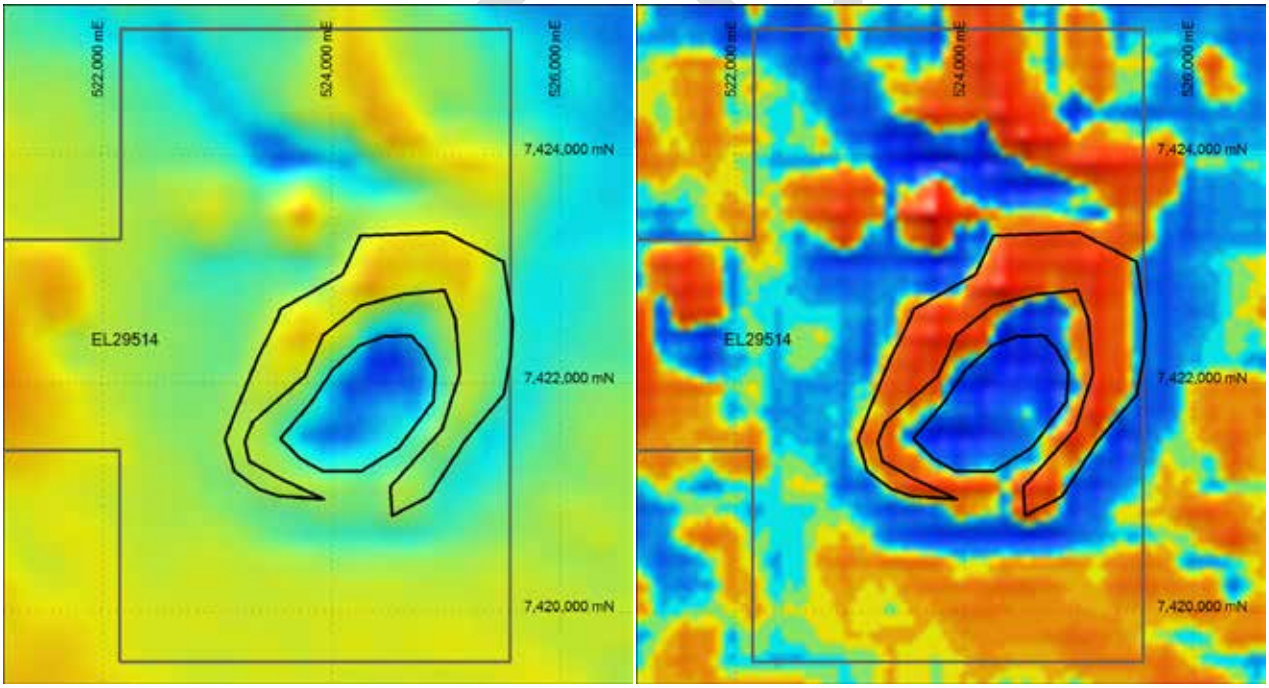

Figure 23: A. TMI data over the eastern part of EL29514, highlighting the position of the modelled intrusion; B. The same area but with the first vertical derivative of TMI grid. NB. The distinct concentric zonation of the anomaly.

The core is clearly mafic – ultramafic based on its dark outcrop appearance and negative magnetisation, and it is also quite prominent in terms of its topographic relief. It is likely to be a gabbro or gabbronorite. The zones outside of this core are recessive, and appear to be a light greeny brown in colour. So we can fairly assume the outer zones are of different lithology to the core. The pale colour might indicate that it has either a higher feldspar content (i.e., trending

toward anorthosite) or a higher pyroxene content (i.e., trending toward pyroxenite). I suspect the latter, because this intermediate zone has very low magnetisation (or null magnetisation) which is common in pyroxenites within the lower portions of layered intrusions (e.g., Alapieti and Lahtinen, 1986; Maier and Barnes, 1998). The outer magnetite zone could be caused by a residual layer (which is common toward the top of a layered intrusion) composed of, for example a Mt-rich anorthosite, or it could just be a rim of contact metamorphosed material (hornfels).

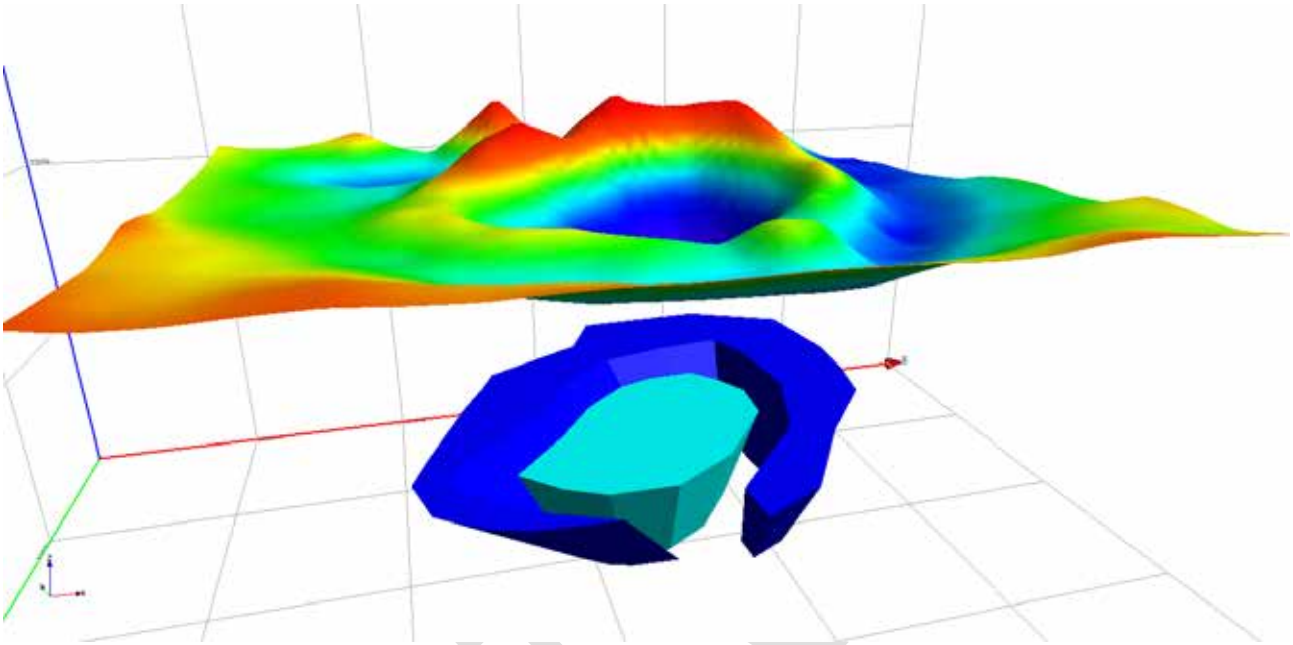

Figure 24: 3-D perspective view of the TMI anomaly over target 2 on EL29514 and the modelled body, as bowl-shaped intrusion consisting of two distinct magnetic zones, the inner zone with negative remanent magnetisation, and the outer with positive (possibly induced) magnetisation.

To summarise, this is a relatively large intrusion (>2km diameter), it displays some indicators of fractionation and /or magma mixing (i.e., petrophysical zonation), so I think it is a better than average candidate for a magmatic Ni-Cu-PGE deposit, and one of the two best candidates within Core's Arunta tenement package. The magnetic signature of the area to the north is also of interest, as the snake-like negative could be due to a feeder chonolith, which could be even more prospective than the actual stock intrusion. There is no drilling into this intrusion (as far as I can tell), and there is some potential for mineralisation, so I would rate this as a better target than most in the area. A suitable follow-up would be to conduct a site visit, and determine the mineralogy of the different (petrophysical) zones within the intrusion. If it is found that there has been fractionation, then a drill-hole should be designed to intersect the base-layers of the intrusion subsequent to some more detailed modelling. If it is possible to collect some oriented core/blocks, I would recommend testing the magnetic properties beforehand.

2.4 EL 29677

2.4.1 Northeast Anomaly

There are several interesting magnetic anomalies, as shown in Fig 25, which start in the NE of tenement EL29677 and spread across several tenements to the north and east. The highest amplitude of these was selected for modelling, because it appears to be a discrete anomaly with significant magnetisation. However, it does not appear to retain purely induced magnetisation as inferred from the lateral displacement between the high and low of the anomaly. Although the anomaly seems to be quite simple in the grid data, the anomaly is in fact difficult to model using the line data. This is mainly due to the fact that the lines have been flown NE-SW (Fig 26), which results in none of the lines adequately sampling the peak and trough of the dipole anomaly, e.g., as shown in Fig 27 a & b, which respectively sample only the peak and trough. The fact that the NTGS have not supplied altimeter data from the survey is also unhelpful (i.e., the vertical displacement of the sensor, from the ground is unknown). Never the less, a reasonably simple model was deduced.

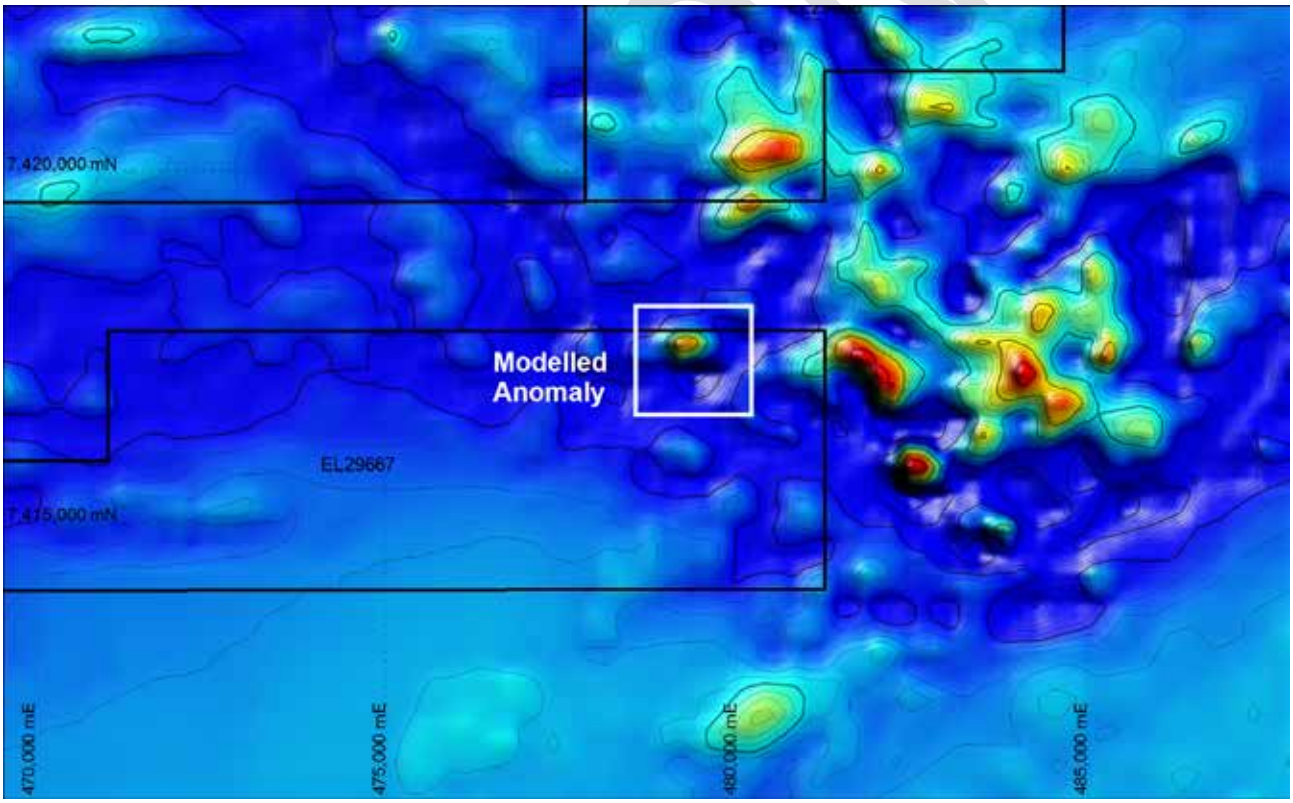

Figure 25: Map of TMI over the eastern portion of EL 29677, highlighting the modelled anomaly.

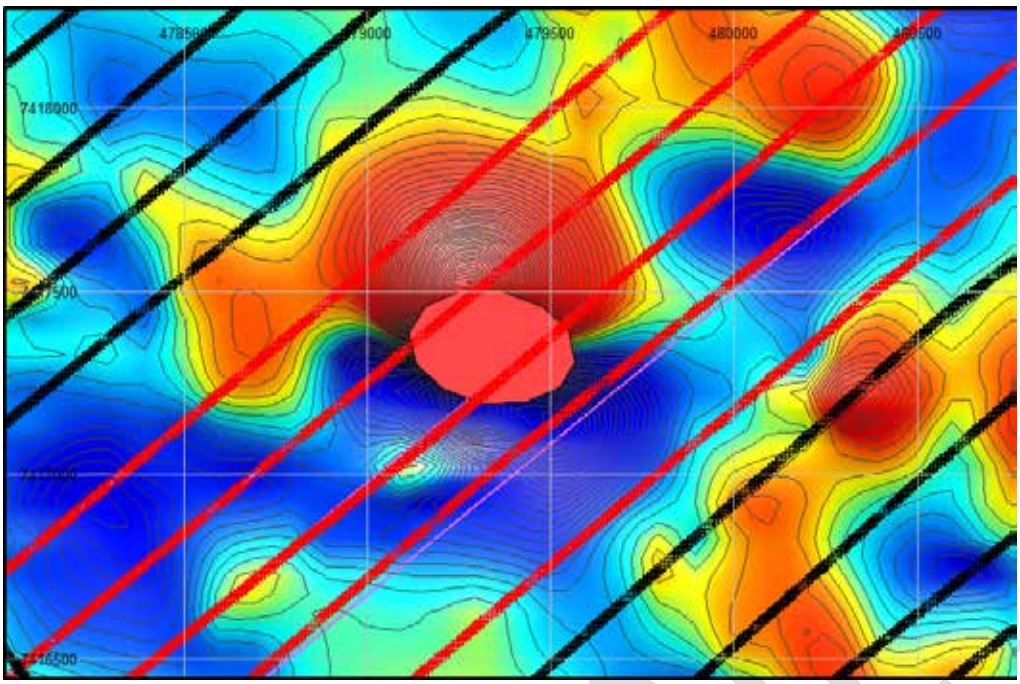

Figure 26: Map showing the TMI grid over the modelled body, and the orientation of the flight lines used for this survey. The oblique orientation of the flight lines results in none of the flight lines sampling both the high and low of the dipole anomaly (e.g., Fig 27).

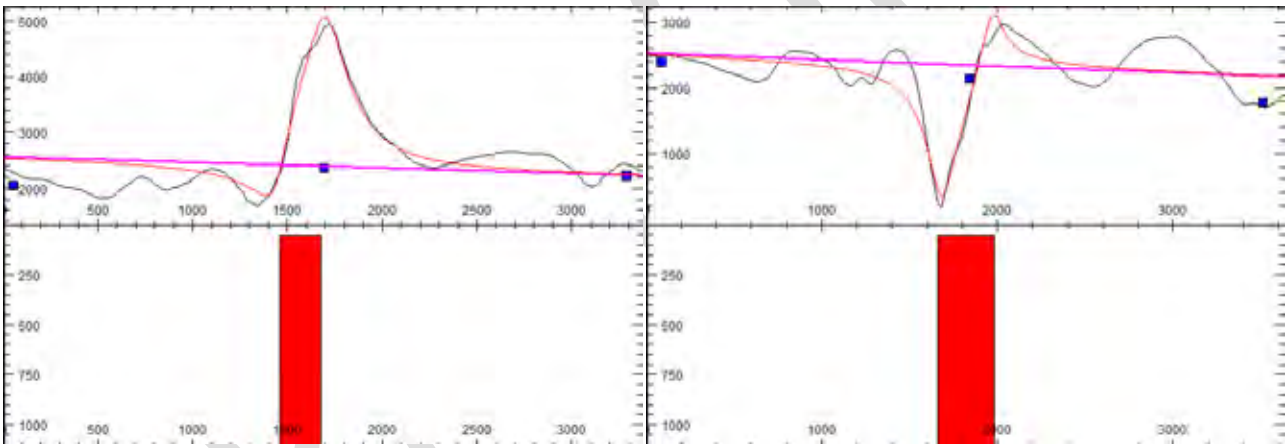

Figure 27: A. The second red line from the top (shown in Fig 26) primarily samples the peak on the high, whereas B. (the third red line from the top) primarily samples the low. This makes modelling compact sources difficult.

The resultant model (Fig 28) is an elliptical pipe that matches the measured data best when it is vertical in orientation, but it must be modelled with some component of remanent magnetisation to achieve a vertical orientation. The model shown can be modelled with both remanent and induced magnetisation. However in this case there is no need to evoke a remanence dominant magnetisation.

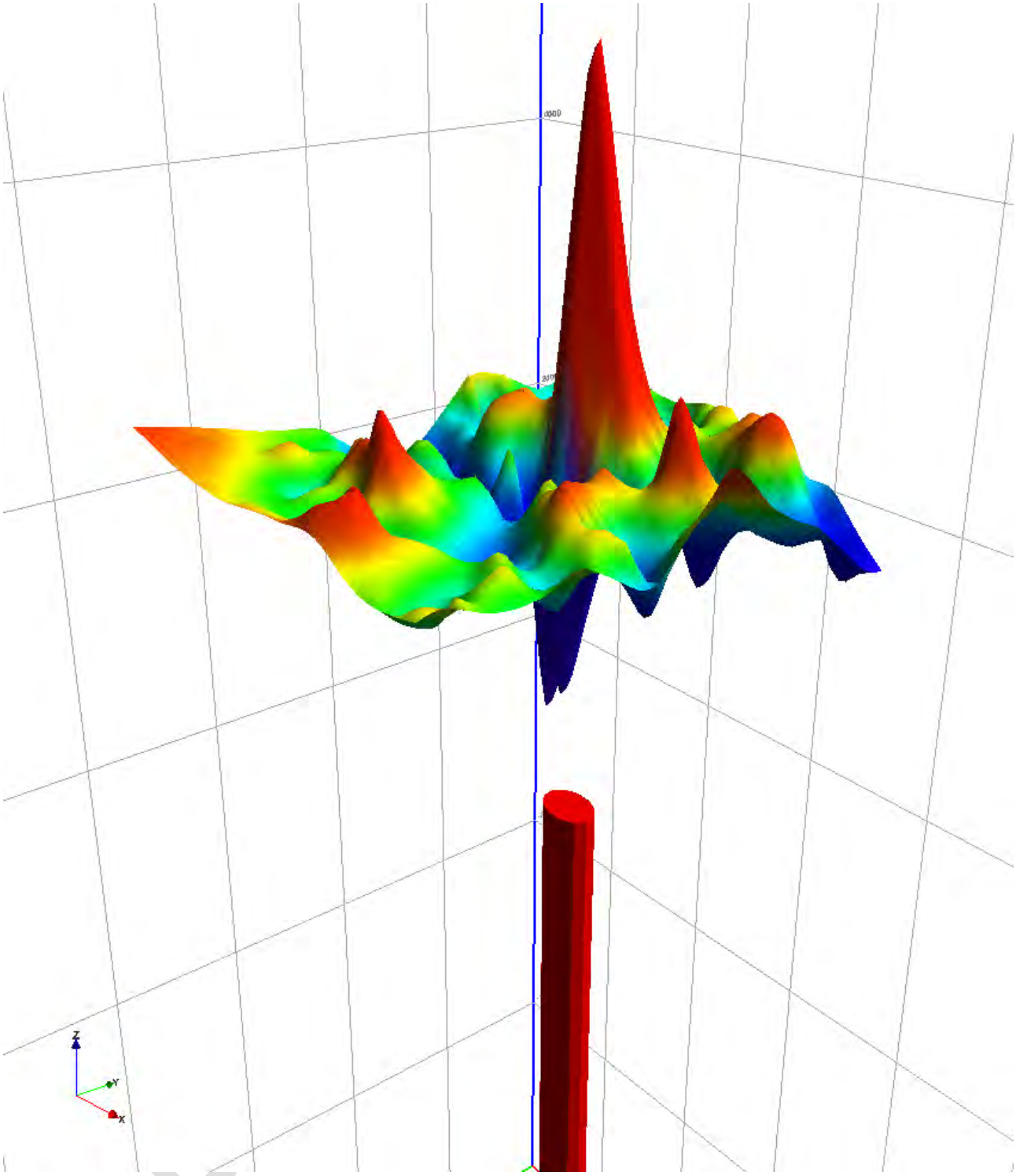

Figure 28: A 3-D representation of the TMI grid, above the modelled body, a vertical elliptic pipe.

This anomaly can be explained with remanence of 750 mA/m, that is about 2/3rd the strength of the induced component (0.25 SI), and oriented moderate down to the NNW. Hence, as modelled, the resultant magnetisation (the vector sum of the induced and remanent components) is oriented shallow up toward 352°. Alternatively a remanence dominant magnetisation oriented in the direction of the modelled resultant with strength of 867 mA/m would be equally plausible (e.g., Fig 29). Such magnetisations have been measured elsewhere in the Arunta and Amadeus (as summarised by Clark and Lackie, 2003). However, any number of scenarios are possible as long as the resultant is similar, and even then there would be a trade off between the dip/plunge of the

body and the magnetisation. So, in reality there are too many unconstrained variables to solve this problem *sensu stricto*.

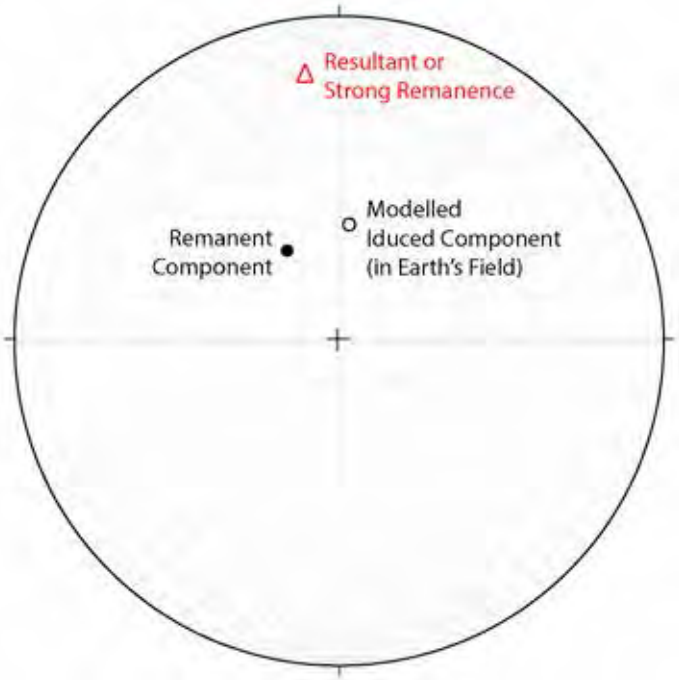

Figure 29: A stereonet illustrating the induced component and remanent component as modelled, and the fact that the resultant is an intermediate direction.

Whilst we cannot be certain of the exact magnetic properties, what we can state with some confidence is that the strength of the magnetisation as modelled is consistent with other locations that are thought to be due to Giles mafic intrusive rocks. This explanation of the modelled rock properties seems likely.

Alternatively, the anomaly morphology could also be considered typical of an IOCG-style magnetic anomaly. However, the fact that there appears to be strong magnetisation with at least some remanence suggests that the anomaly is not caused by coarse-grained magnetite alone, otherwise the anomaly would have a N-S-dipolar morphology. So if this were an IOCG there would need to be a significant amount of pyrrhotite to explain the fairly strong remanent component. In this case, the similarity between this anomaly and several anomalies to the east does not favour this hypothesis, since IOCGs do not typically occur in clusters.

The geology of the area around this cluster of anomalies is mapped as the Strangeways Metamorphics, and in particular as the Cadney Metamorphics (Fig 30), which includes some calc-silicate lithologies. Hence, it is possible (as discussed in Section 2.1) that the magnetic anomalism here is due to some kind of skarn which is sporadically formed, possibly by mafic rocks intruded into a carbonate-rich host. These skarns may or may not be associated with minerals of economic interest.

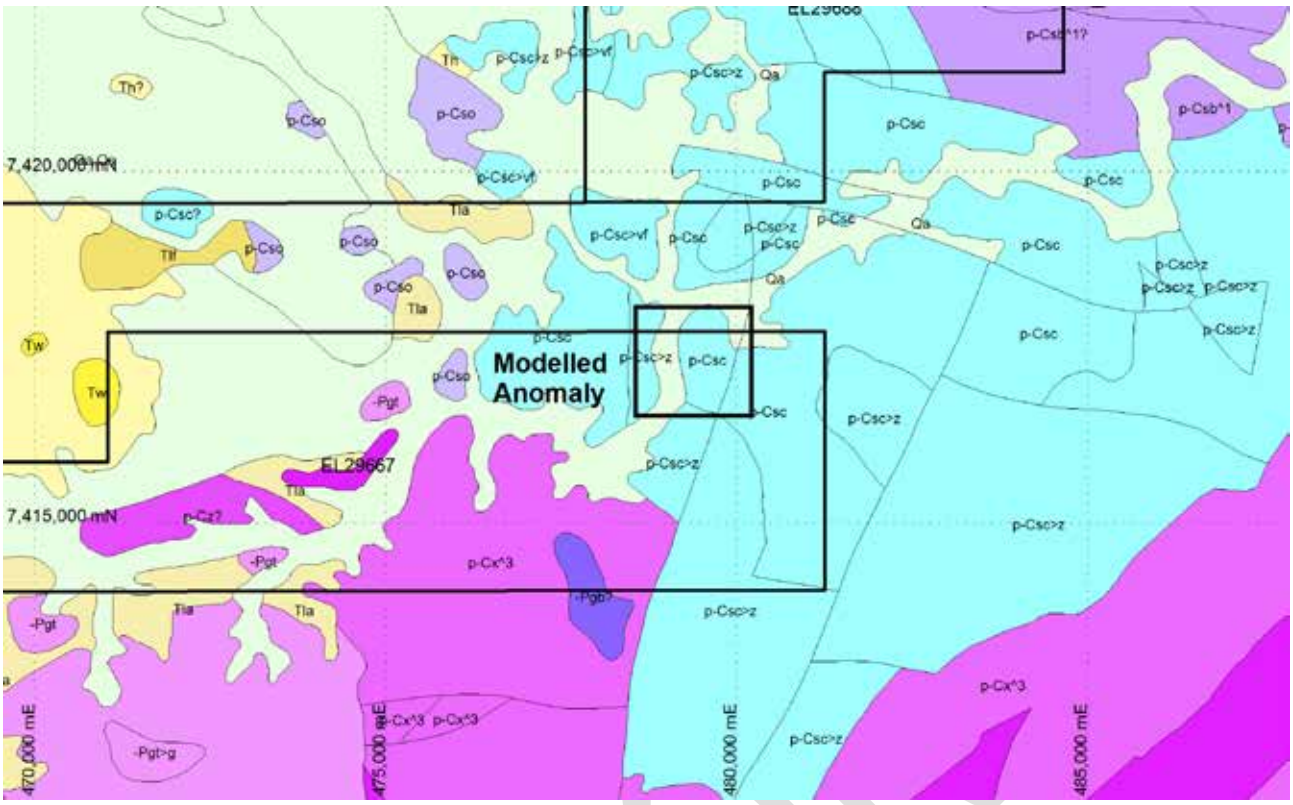

Figure 30: The mapped geology over the eastern portion of EL29677. The cluster of high amplitude magnetic anomalies coincided with the Strangeways Metamorphics, mapped in mint green.

2.4.2 Remainder of the tenement

There are several other anomalies within this tenement, particularly in the western block (Fig 31). However, these have significantly lower amplitudes, and generally longer wavelengths. Although these anomalies may be caused by similar lithologies, the causative bodies would appear to be deeper, and are possibly sitting below tertiary sedimentary rocks, and or are more deeply weathered. For this reason, I would favour the shallower, more highly magnetised sources located in the east of this area. However, that is not to say that I think it is a highly prospective target, just that it is more favourable than other targets in the west of the tenement. It would be advisable to further test the anomaly using supplementary geophysical and or geochemical techniques prior to drilling.

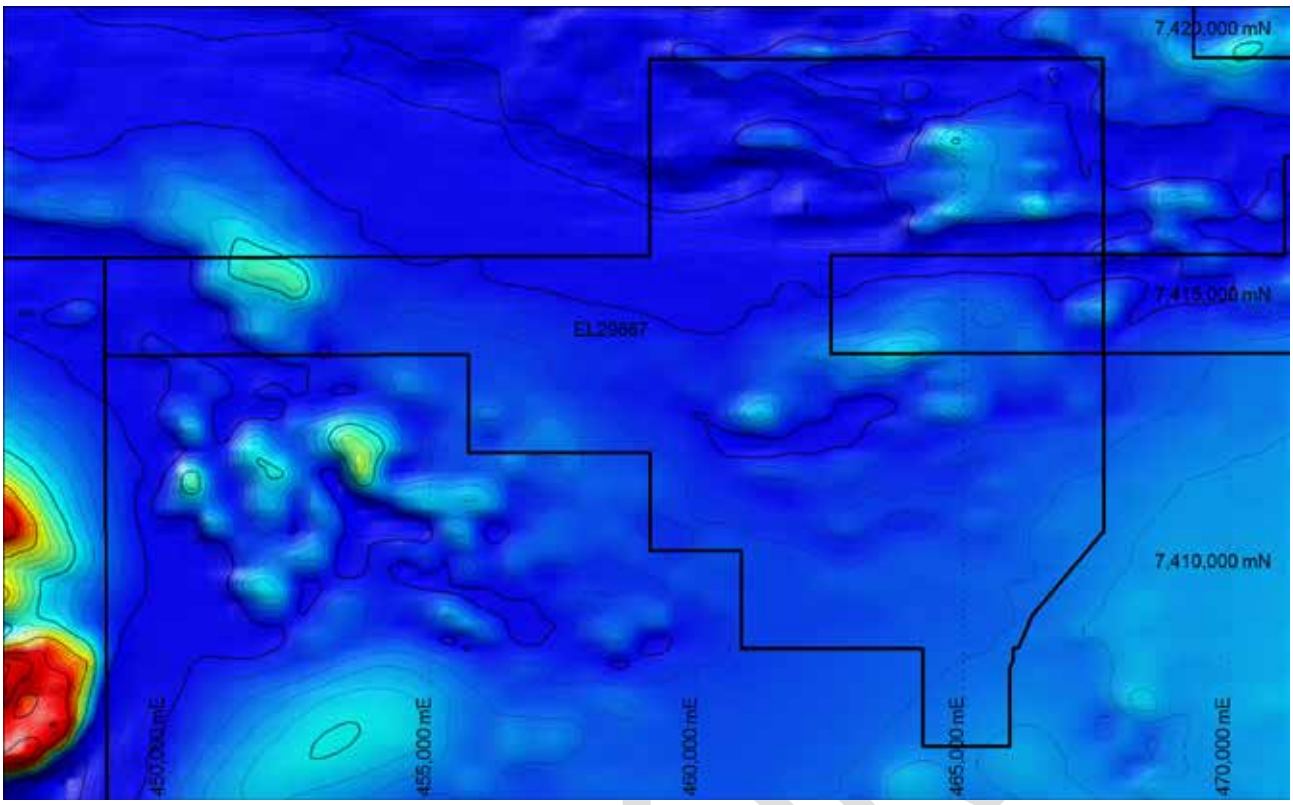

Figure 31: TMI grid over the western portion of tenement EL29677. The anomalies shown have significantly lower amplitudes, and longer wavelengths than the primary target, which is indicative of greater source depth.

2.5 EL 28546

Several further of the bullseye anomalies (as discussed in section 2.4) sit on tenement EL28546; however, many on them are either overlapping (other anomalies) or indistinct. Two of these anomalies, are modelled here, and are hereafter referred to as the SE and NW anomalies (Fig 32).

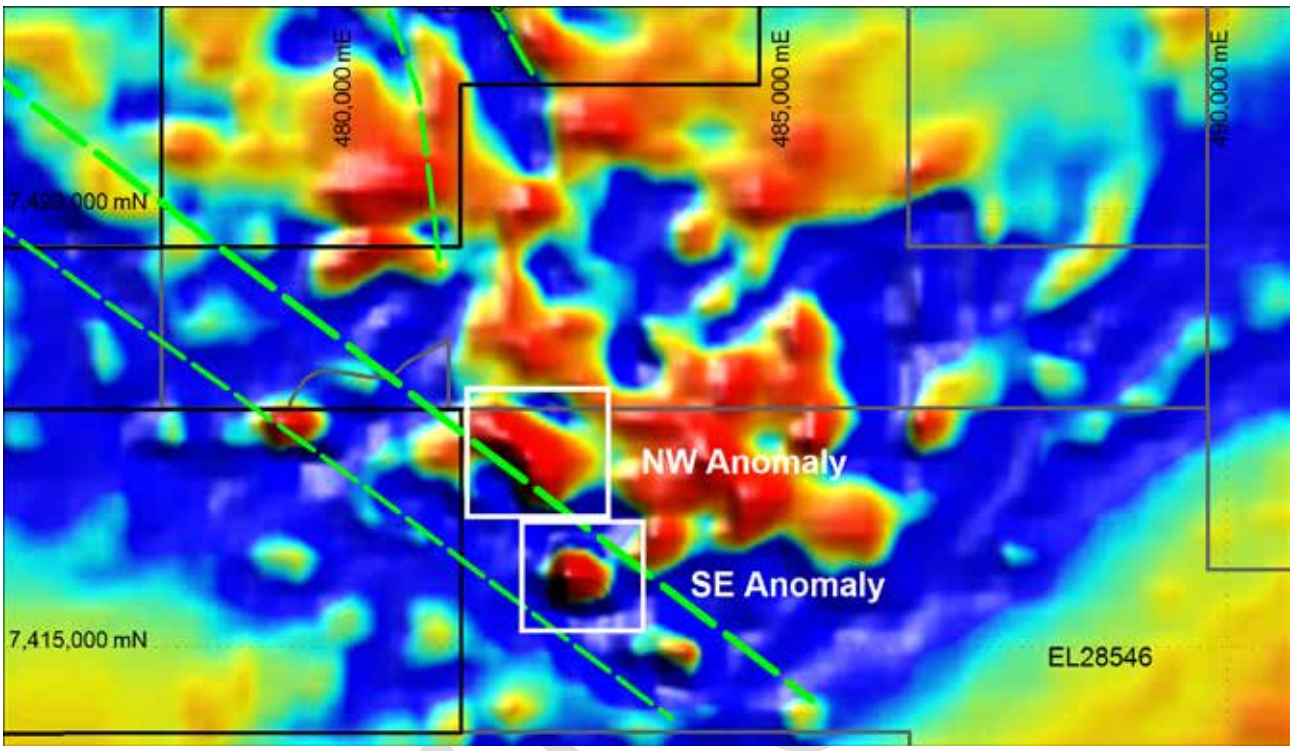

Figure 32: TMI data over tenement EL28546 and the location of the NW and SE anomalies and their context in relation to a proposed SE-NW Cu-lineament (marked in green).

2.5.1 Northwest Anomaly

The northwest anomaly is the larger of the two anomalies. It is intersected by 6-7 flight lines, and the peaks are of similar amplitude on 5 of those lines, so the source body is elongate. Although the body would seem to be banana-shaped based on the magnetic anomaly (Fig 33a-c), during modelling, it became apparent that the source architecture is more complex. It was necessary to use an inclined fold architecture to model the anomaly, as shown in Fig 34. Hence, the bullseye in the TMI data is really just an artefact of the gridding process which has taken two adjacent peaks and smoothed them into one. Unfortunately, this is all too common in gridded magnetic data, and emphasises the need to model using line data, not gridded data.

Because the Analytic Signal anomaly and the RTP matched so closely, it was inferred that the magnetisation of this body is primarily induced. Hence, only induced magnetisation was used to explain the anomaly in this case. There could be some remanence, but I doubt it would make significant difference to the modelling outcome, because the body is clearly very near-surface, or indeed at surface. The fact that one arm of the inclined fold model sits along a major lineament is of interest, because we could infer then that this body may represent a fault intersection, of the major lineament with a secondary structure, e.g., a Riedel P shear (Fig 35). As such, this target may have formed via hydrothermal alteration which has been channelled by the major structure into the secondary structure, providing a mechanism for de-volatilisation of a mineralised fluid, and

hence mineralisation. It is reasonably common for secondary structures to be mineralised, in preference to primary structures (as noted by many authors in the literature, e.g., Groves, et al., 2003; Austin and Blenkinsop, 2009).

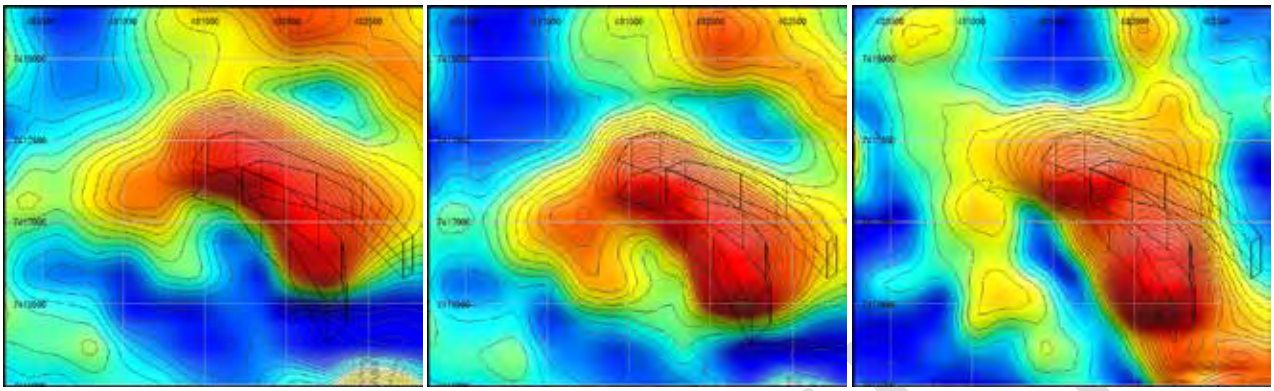

Figure 33: Shows the location of the modelled body relative to: A. the total magnetic intensity grid; B. the reduced to pole magnetic grid, and: C. the Analytic Signal of Upward continued TMI. NB. The RTP and Analytic Signal anomalies are more-or-less coincident, which implies that the magnetisation is oriented in the Earth's present field, i.e., it is predominantly induced, not remanent.

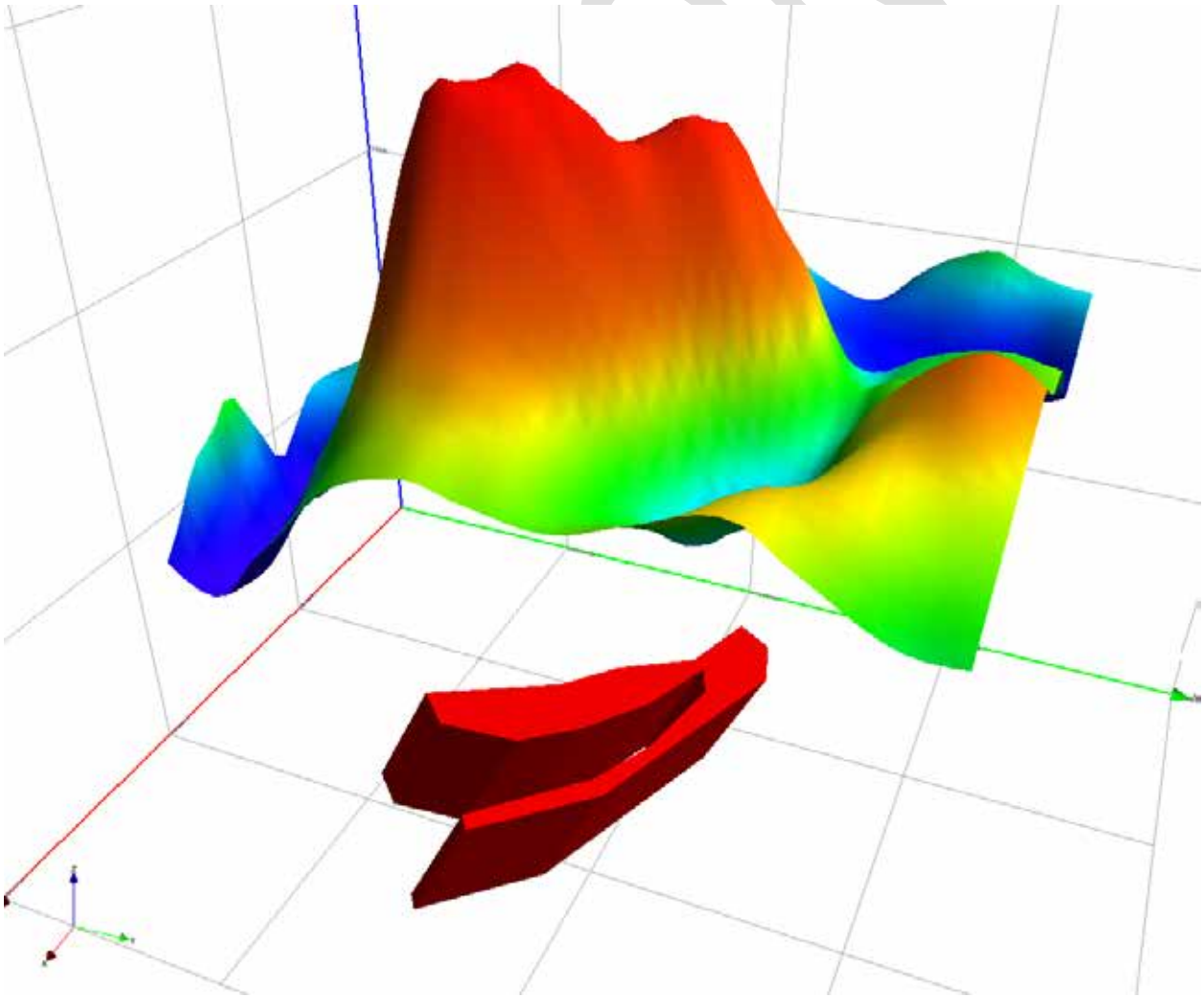

Figure 34: A 3-D representation of the TMI grid and the modelled body for the NW anomaly in tenement EL28546.

2.5.2 Southeast Anomaly

The SE anomaly is recorded on several of the NE oriented flight lines, but the peak is intersected primarily on only one line (3010731), with a peak amplitude of ~3500nT. Although the anomaly appears to be a simple bullseye in the gridded data, it is actually significantly more complex in the line data, and is composed of several overlapping shorter wavelength anomalies. So, while it is difficult to account for these shorter wavelength components in the absence of altitude data, what we can be certain of is that the sources are shallow.

When the SE anomaly was modelled with no constraints other than that it must have only induced magnetisation, the resultant body is a shallow (modelled as 31m below sensor), relatively thin, pikelet-shaped body, with fairly high susceptibility (0.3 SI) as shown in Fig 36.

When the body is modelled with remanence, it tends to be thicker, and the total magnetisation shallows toward horizontal (from the Earth's natural field). Other than that there is little difference, it is a pikelet-shaped body that is very shallow, with significant magnetisation.

This style of body (the pikelet) has been observed at other localities in the Arunta, and has previously been found to be due to a mafic sill at the Baldrick prospect, possibly of Lloyd age (*ca* 405 Ma). In this case there is no mafic-ultramafic bodies mapped, but that doesn't necessarily preclude the possibility. If the modelled equivalent susceptibility is more-or-less correct, then this body has a significant magnetite and or pyrrhotite content, but ultimately is probably a little on the small side to be considered a genuine Magmatic Ni-Cu-PGE or IOCG target. It could have some potential if an alternate model for mineralisation is applied. However, given the lack of constraint, it would be very speculative to do so.

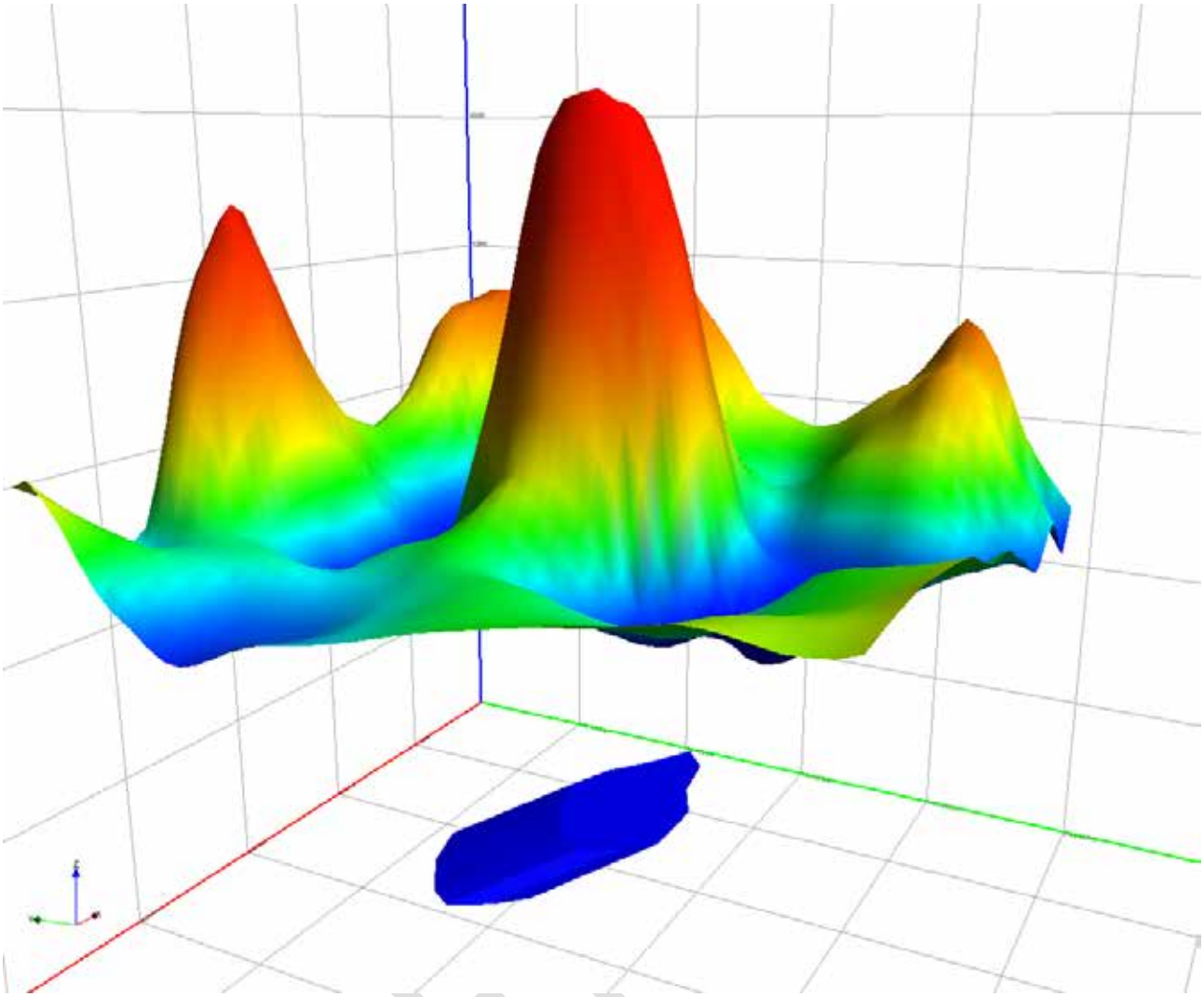

Figure 35: A 3-D representation of the TMI grid, above the modelled body, a pikelet-shaped sill.

2.5.3 Eastern Anomaly

Further along the same lineament, to the SE there is another interesting anomaly in the magnetic data. I consider it interesting for a number of reasons: 1. It is sitting along the Cu-Lineament; 2. it sits along a linear magnetised zone which runs NE-SW, and is probably related to primary lithological layering; 3. It sits adjacent to a the intersection of two relatively late (E-W and N-S) faults that appear to truncate the magnetised layers (as shown in Fig. 36).

This body was relatively simple to model, and the resultant body appears to be relatively shallow (probably at surface), and it has a triangular shape. The triangular shape is consistent with the analytic signal anomaly (the middle layer in Fig 37) and it has reasonably high susceptibility (0.17 SI) which is consistent with significant magnetite within the body. The body sits almost entirely within the NE quadrant of the fault intersection, which would be consistent with a fault-controlled breccia related to the faulting.

A number of similar faults cut these magnetised layers in a number of other places in this region, and in some cases the faults are associated with Uranium and REEs. This potential mineral

association, the structural location of the anomaly relative to a mineralised trend (primary structure) and to the intersection of two minor structures, and the relatively high modelled susceptibility are all consistent with IOCG mineralisation. I believe that this body has good potential for mineralisation. However, it is also possible that this anomaly is simply the result of the cutting of the magnetised layer by the two late faults. So that possibility should be tested.

To the south, both within this tenement and on EL28029 are several other instances where there are reasonably sharp magnetic anomalies located along faults, and although these may offer legitimate prospectivity for IOCG mineralisation, they are all significantly smaller and sit distal to the Cu- Lineament. Hence I believe they are targets that are only worthy of further work, after the main target has been tested.

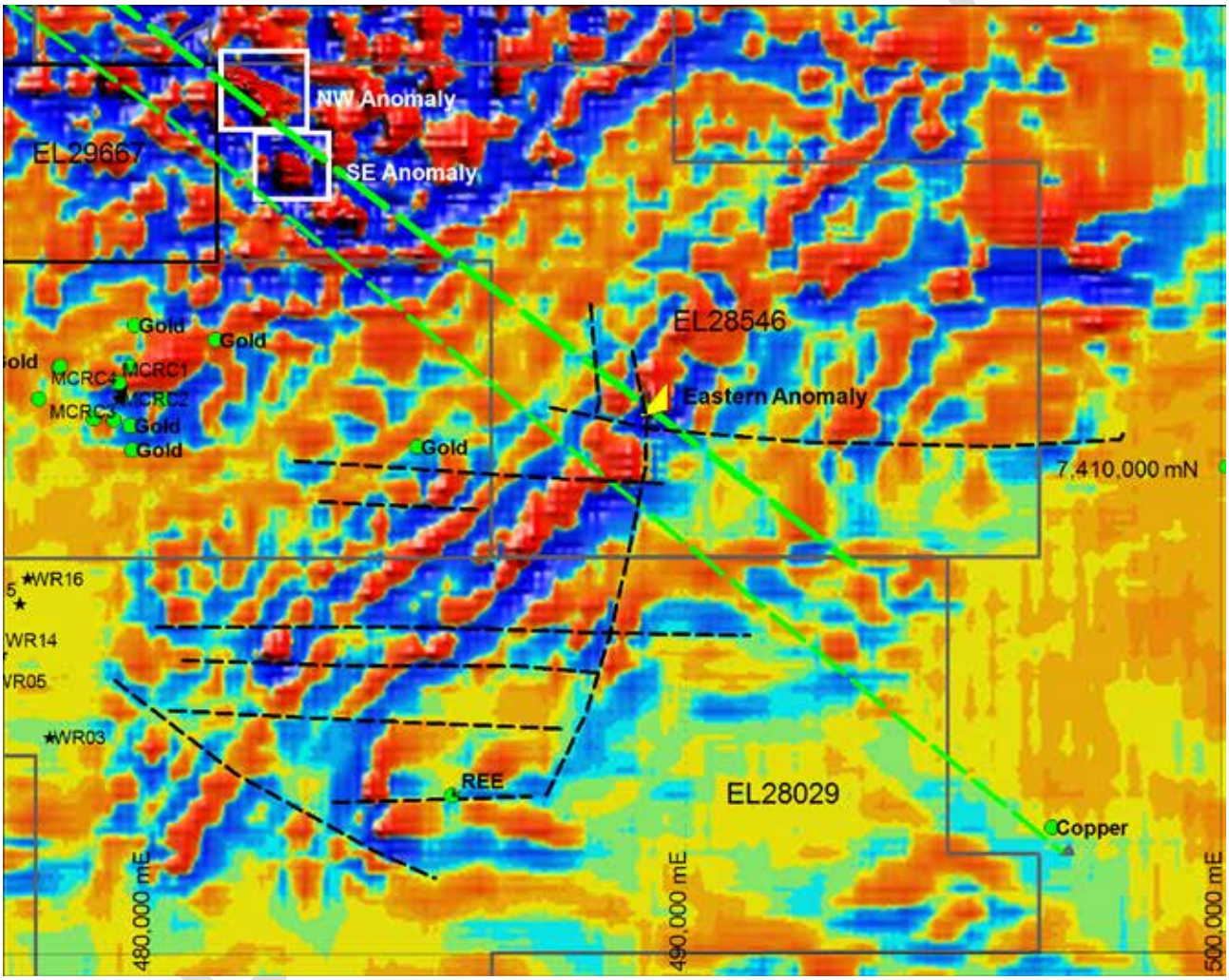

Figure 36: The first vertical derivative of TMI over El 28546 and EL 28029. Mineral prospects are marked by green dots, the Cu-Lineament marked by thick dashed green lines, secondary faults marked by thin black dashed lines, and the modelled body (Eastern Anomaly) is shown in yellow.

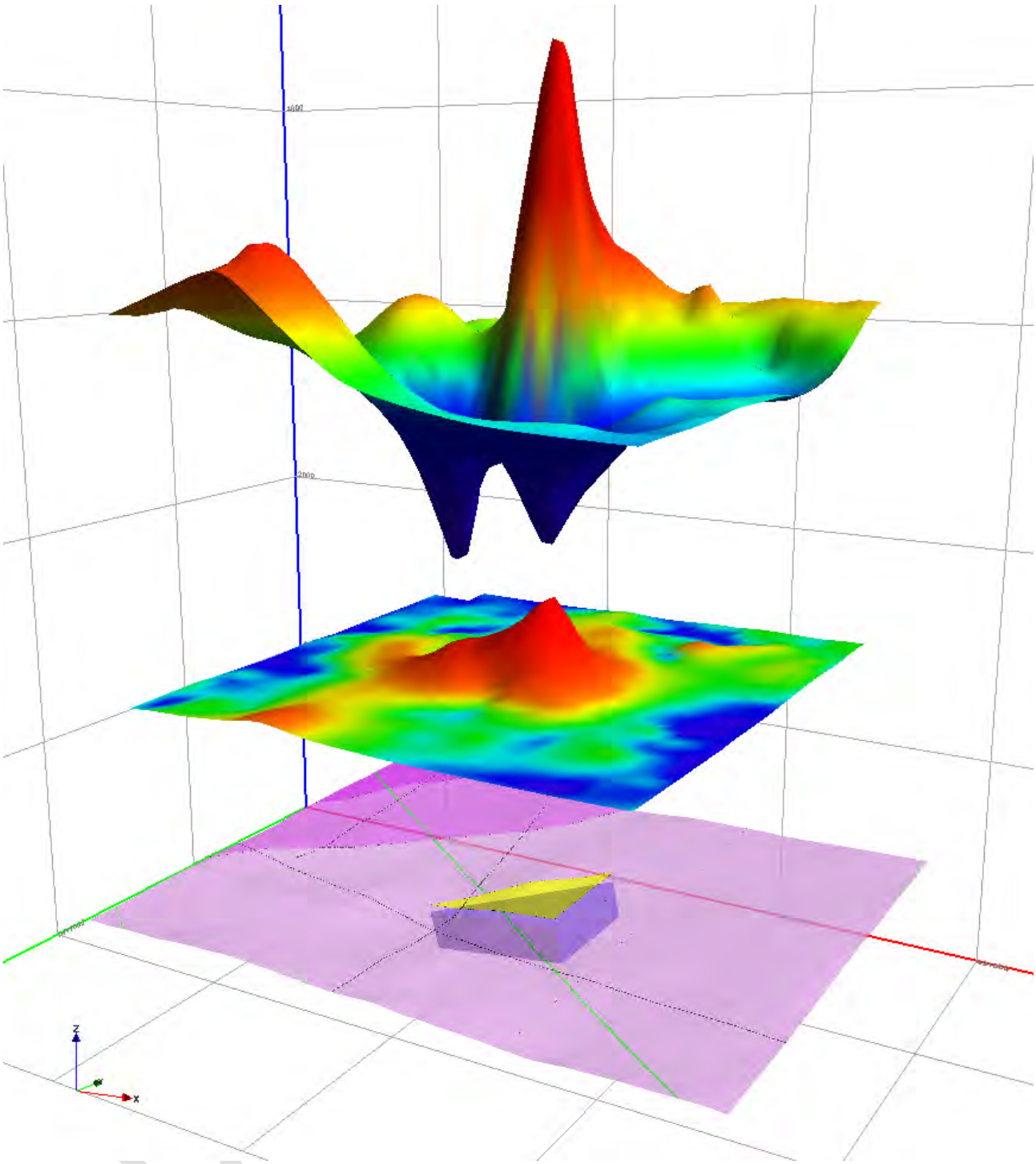

Figure 37: 3D visualisation of the TMI grid (top) over the Eastern Anomaly on tenement EL29546. The analytic signal grid (middle) predicts that the anomaly is caused by a more-or-less triangular prism. The Base layer shows the mapped geology and interpreted structural intersections discussed. The modelled body is shown in blue beneath the base geological layer.

2.6 EL 28029

Within tenement EL28029 there are several other instances of reasonably sharp bullseye magnetic anomalies located along faults, which are similar to the Eastern Anomaly on EL29546. Although these may offer legitimate prospectivity for IOCG mineralisation, they are all significantly smaller than the Eastern Anomaly, and sit distal to the Cu- Lineament. Hence I believe they are targets that are only worthy of further work, after the main target has been tested.

2.7 EL 29688

The main anomaly on this tenement is located more-or-less in the middle of the tenement (Fig 38) and sits along the NW-trending Cu-lineament. The anomaly is located close to drill hole HR 016, the results for which are contained in report CR1980-0125. I requested a copy of this report from the NTGS, but did not receive it (I suspect because it is not yet digitised).

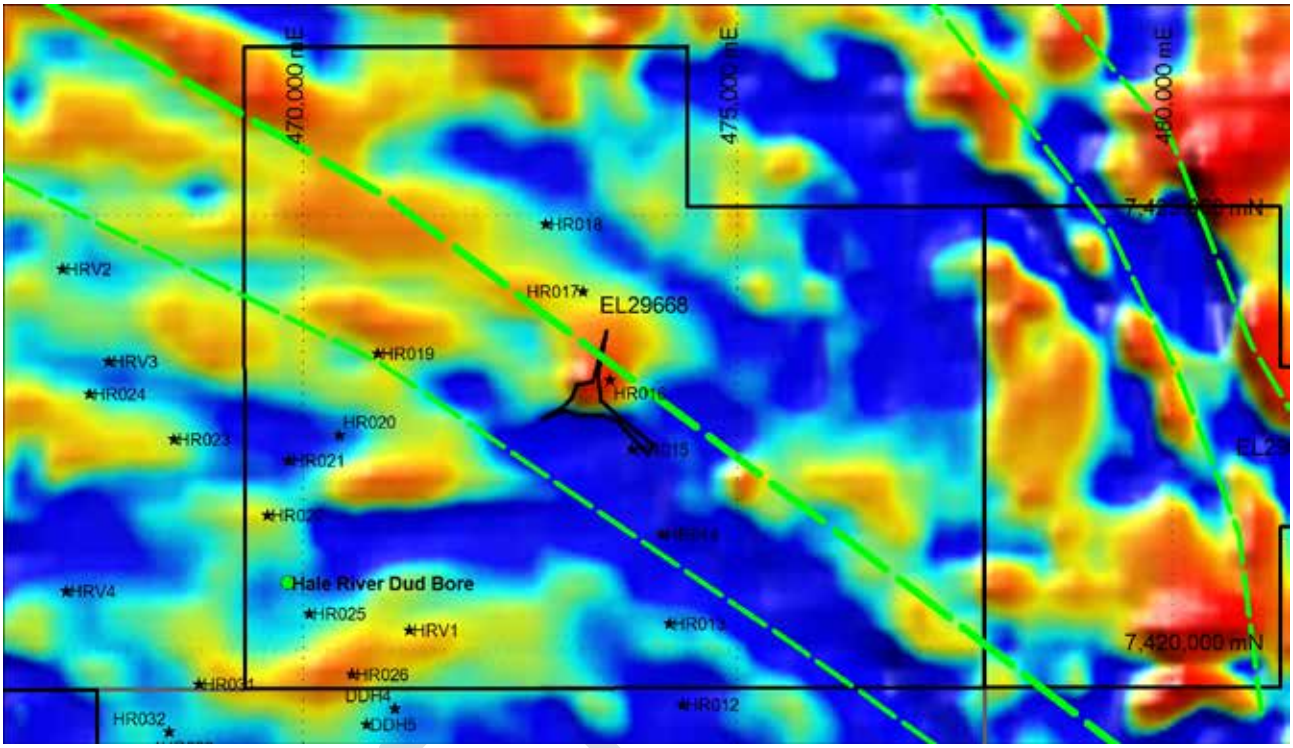

Figure 38: Shows interpreted lineaments associated with Cu shows (green dashed lines), previous drilling (black stars), and the location of the modelled Tri-Star body superimposed on TMI grid. NB. The prongs are parallel with structures in WNW and ENE orientations.

The seemingly simple bullseye anomaly is in fact much more complex in the line data. The resultant model generated is a three-pronged plunging prism (Fig 39). This body seems to be a better explanation of the data than a more simple pipe-like body (which was modelled separately, Fig 40), but it is difficult to be certain, considering the survey flight height is not known. From a geological perspective, the 3-pronged body is of greater interest, since it could represent magnetite and/or pyrrhotite deposited at a fault intersection during a hydrothermal event. One of the prongs of the modelled body appears to be sub-parallel to the NW-oriented Cu lineament, and the other two could conceivably represent a cross-cutting fault. A fault intersection is an ideal structural trap for IOCG or skarn mineralisation, and hence this body is a reasonably good Cu target in my opinion. It is reasonably large, has significant depth extent and volume, and also has a favourable architecture. I would consider this target: on par with the NW anomaly from EL28546. The one aspect that is not favourable is that the body appears to be 250 m below sensor, which means the depth is likely to be 150-200 m below surface.

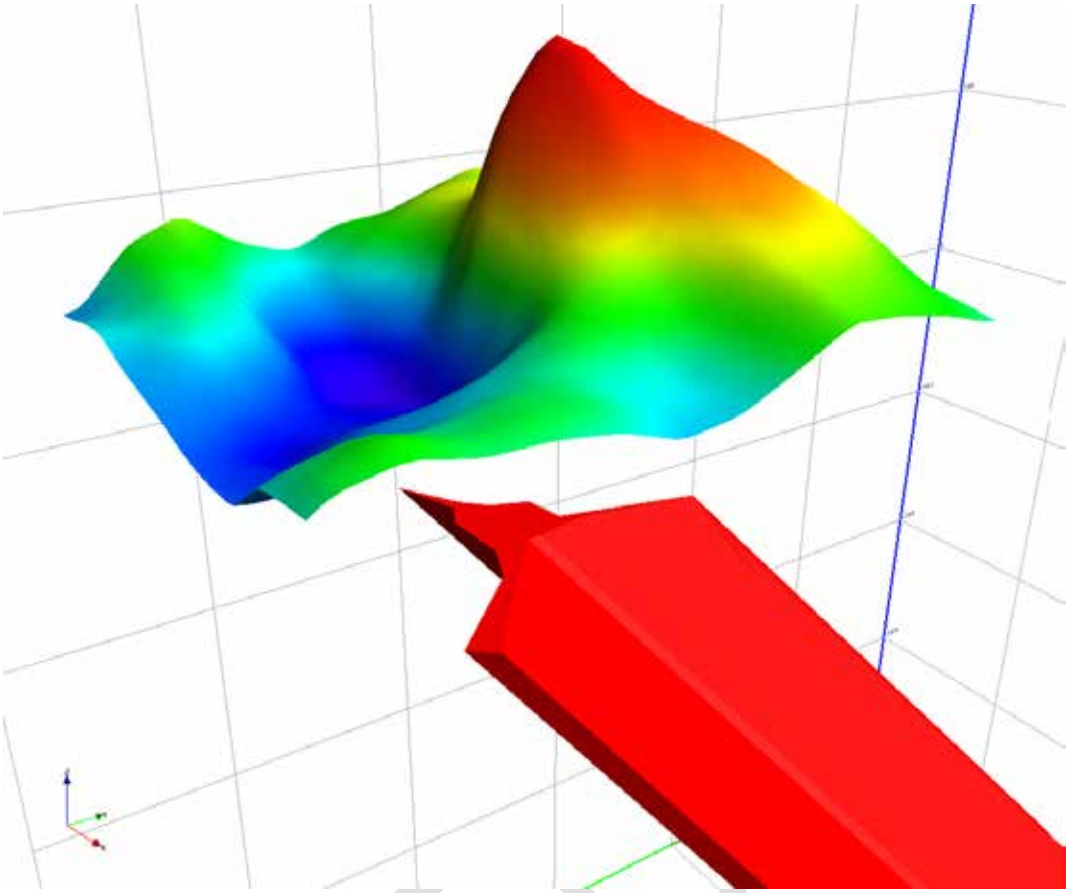

Figure 39: A 3-D representation of the TMI grid, above the modelled body, a Mercedes badge shaped prism.

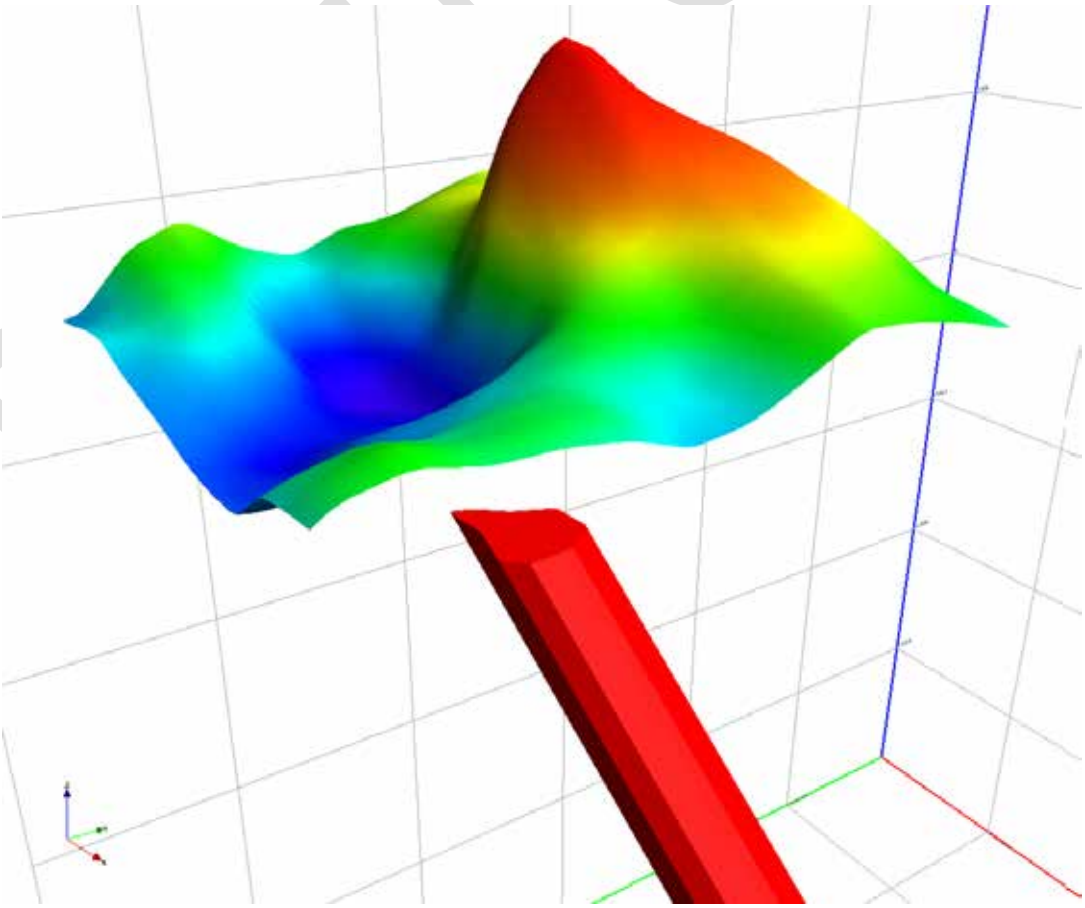

Figure 40: A 3-D representation of the TMI grid, above an alternate model, a relatively simple pipe.

2.8 EL 29687

EL 29687 contains at least two interesting anomalies in the magnetic data (Fig 41). Both appear to be located within the Cadney Metamorphics member of the Strangeways Metamorphics (Fig 42). The lithology reported to be predominantly calc-silicate (Shaw and wells, 1983), and so is potentially reactive, and there are a large number of copper prospects located within similar lithologies just off tenement to the NW. Furthermore, both anomalies straddle mapped 2nd and 3rd order faults, so there are several favourable indicators of skarn-style Cumineralisation for this tenement.

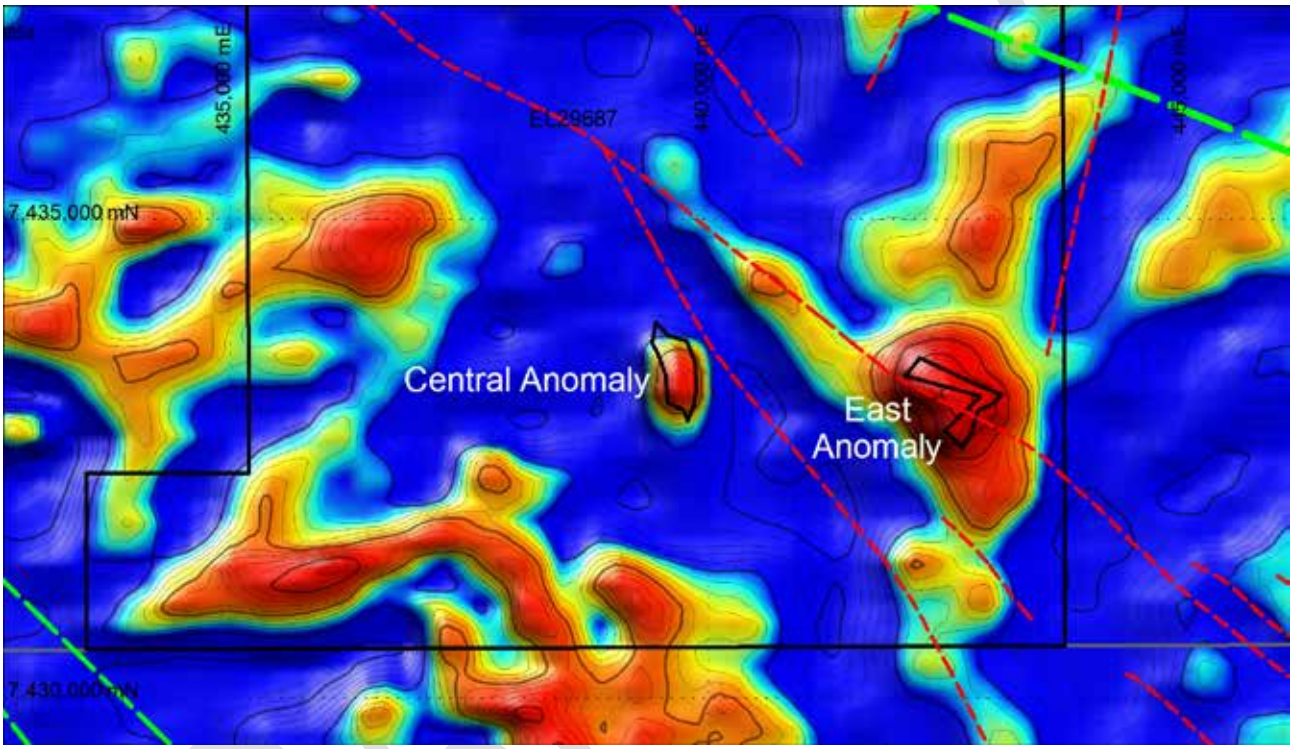

Figure 41: Map of the southernmost section of tenement EL 29687, detailing the position of mapped faults (red dashed), and the two modelled bodies (outlined in black) underlain by the TMI grid.

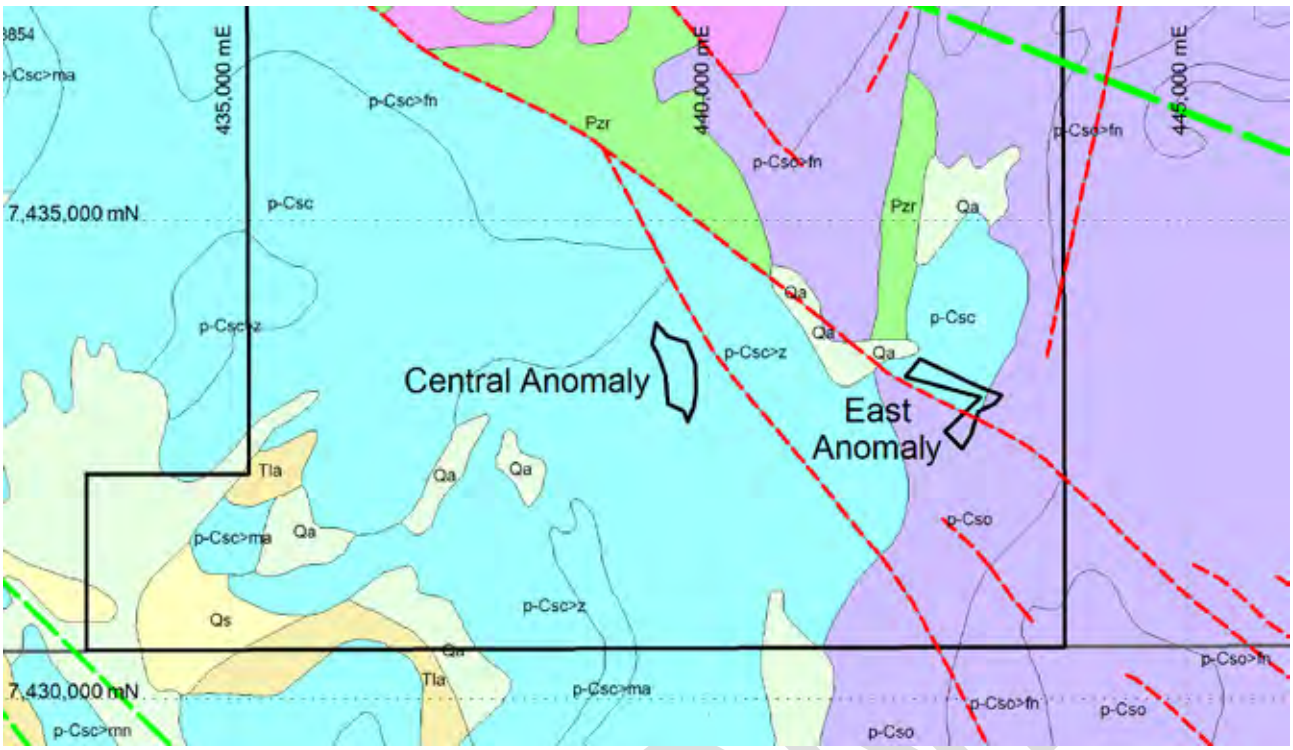

Figure 42: Map of the southernmost section of tenement EL 29687, detailing the position of mapped faults (red dashed), and the two modelled bodies (outlined in black) underlain by the digital 250k geology. P-Csc is the Cadney Metamorphics, p-Cso is the Ongeva Granulite, Pzr consists of retrograde schist, mylonite and breccia, clearly reflecting localised shearing.

2.8.1 East Anomaly

The eastern one of the two main anomalies is easily the largest, and it has a complex morphology, even in the gridded data (Fig 43). In this case The TMI image (Fig 43a) and the Analytic signal (Fig 43b) both suggest a chevron shaped source body. The modelling session resulted in an inclined chevron fold as shown in Fig 44 which appears to predominantly sit to the east of a major fault, in a zone of Cadney calc-silicate. The architecture of the modelled body suggests that it is either a segment of a fold, or that it is caused by magnetite precipitated in a fault intersection. Given that there clearly are a number of faults that appear to control the local architecture, and that the modelled susceptibility of the body is 0.6 SI (typical susceptibility of an IOCG deposit), I would favour the latter. Hence I think this is a very good target for an IOCG style deposit. Based on the modelling (which does have its limitations) there is clearly significant magnetite in any case.

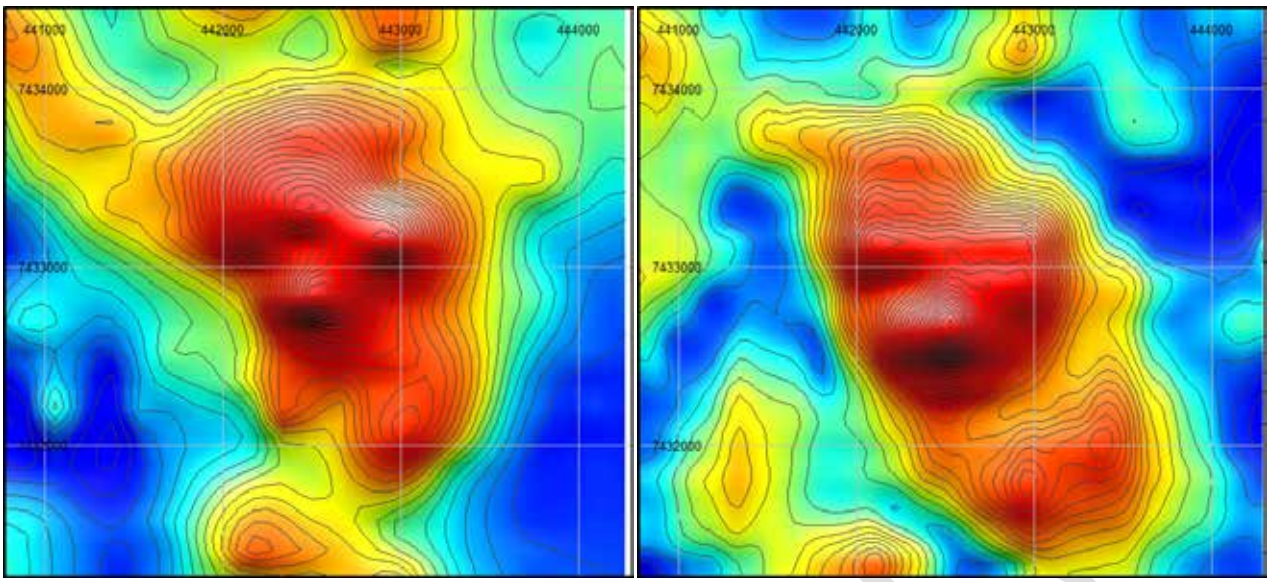

Figure 43: A. TMI grid over the east anomaly; B. Analytic Signal of 20 m upward continued TMI. NB. Both preserve a chevron-shaped peak.

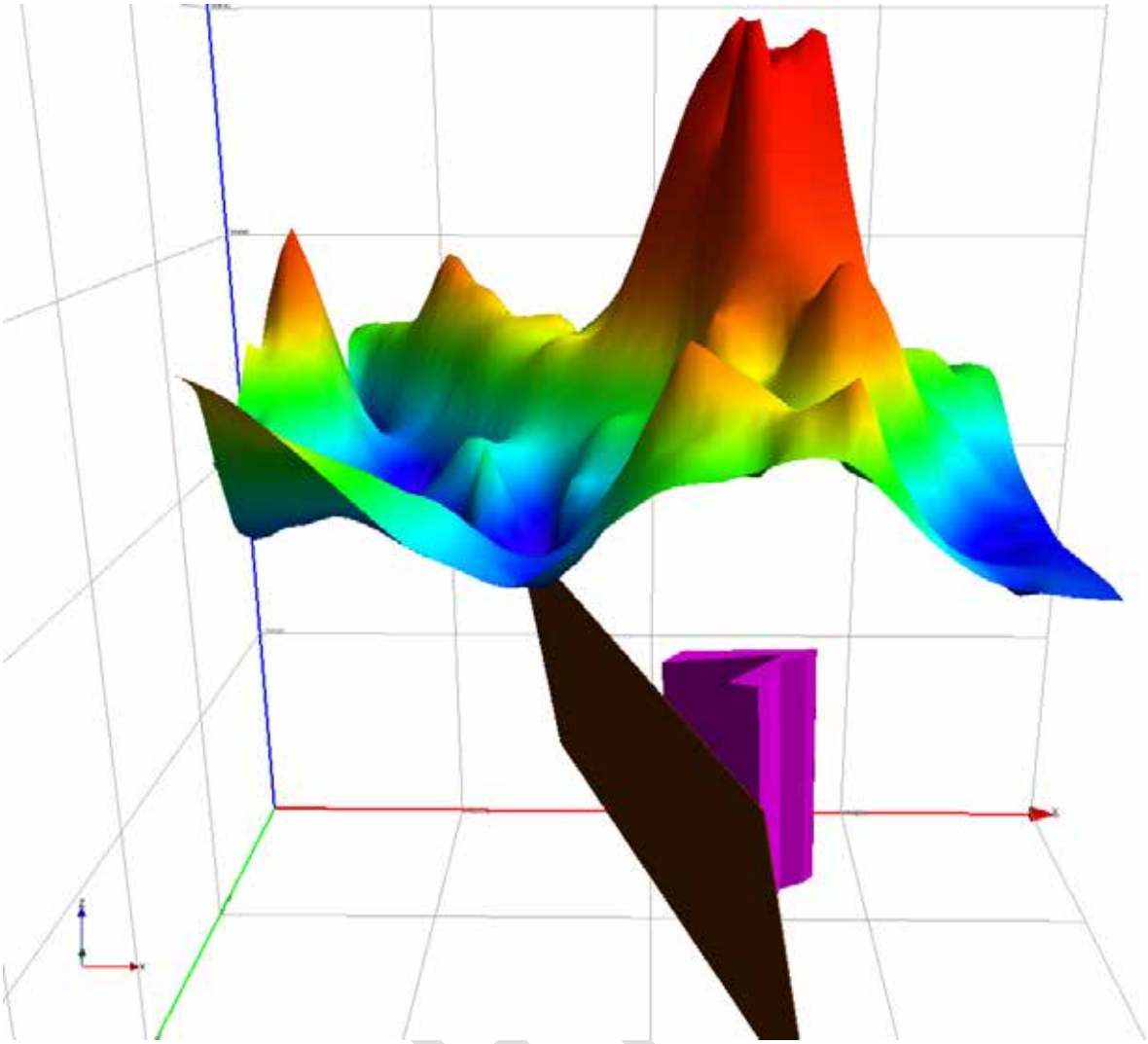

Figure 44: A 3-D representation of the TMI grid coincident with the east anomaly, above the modelled chevron source. Fault (brown) is shown for context.

2.8.2 Central Anomaly

The central anomaly is a fairly simple bullseye target which is consistent with many IOCG anomalies in the Gawler, Tennant Creek and Cloncurry districts. However, this is more an artefact of poor resolution data than anything else. The anomaly is really only intersected by one flight line so our modelling is not well constrained. The flight lines are N-S oriented and 400m (+/-) apart, so the body is probably only half that width, and it is modelled as 200 m below sensor, so it probably sits at somewhere between 100 and 150 m depth. The body was modelled both using only induced magnetisation (Fig 45a), and also allowing remanent magnetisation (Fig 45b). There will be a certain amount of trade-off between the plunge of the body and the magnetisation direction and hence we can observe that the body that incorporates remanence is slightly steeper in plunge, other than that the modelled bodies are very similar. This would lead me to suspect that both are a fairly close reflection of the actual architecture of the body. Whilst the anomaly and pipe-like architecture of this body are comparable with several IOCG deposits, its magnetisation is a little on

the weak side for it to contain significant magnetite. So overall I think the central target is far weaker than the highly prospective eastern target.

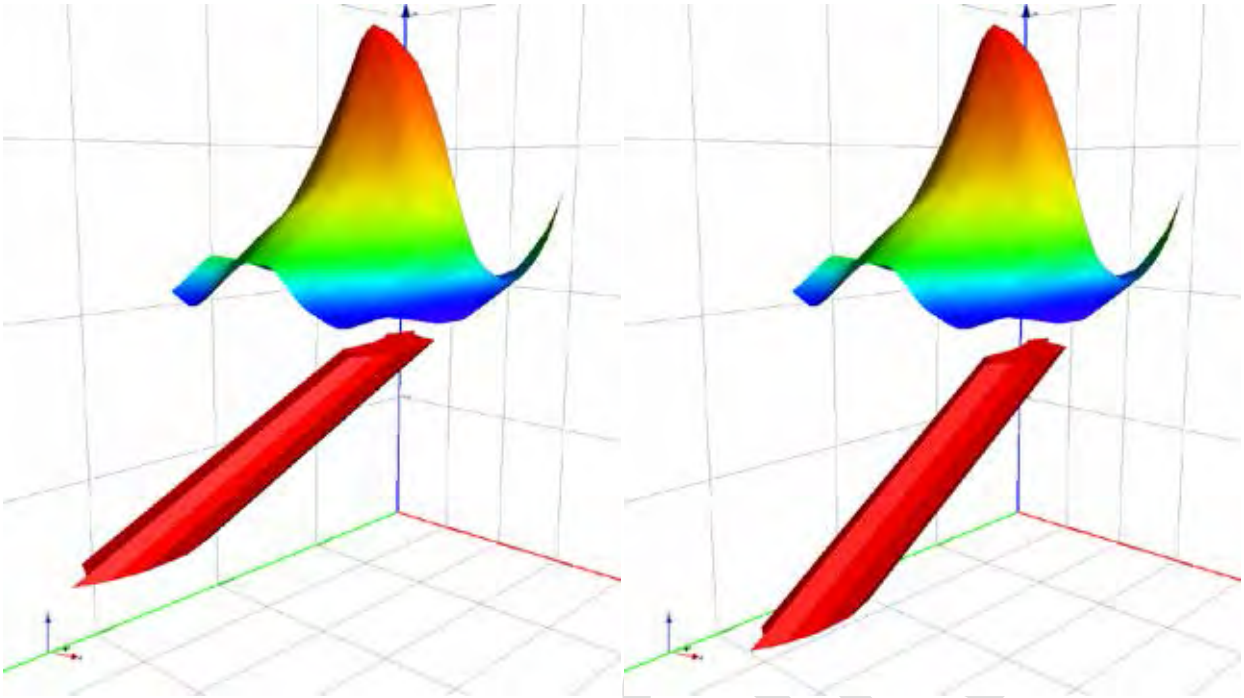

Figure 45: A. 3-D representation of the TMI grid above a pipe-like body where only induced magnetisation is used; B. An alternate model where magnetisation direction is allowed to vary (i.e., allowing remanence). NB. The induced body is a little shallower, but other than that the bodies are very similar.

2.9 EL 28853

EL 28853 contains a number of relatively distinct magnetic anomalies (Fig 46). The largest of these in terms of area and amplitude is located in the NE corner of the tenement. This anomaly appears to occupy a rather interesting structural position at the intersection of two faults, in what could be some kind of pull-apart or flower structure (i.e., the zone has experienced either transpression or transtension, forming an array of sub-parallel faults). Either scenario is favourable for hydrothermal mineralisation (e.g., IOCG) depending on the specific strain and temperature/pressure conditions during mineralisation. These faults appear to be coincident with copper shows just off tenement to the east, which is obviously also a favourable indicator of mineralisation.

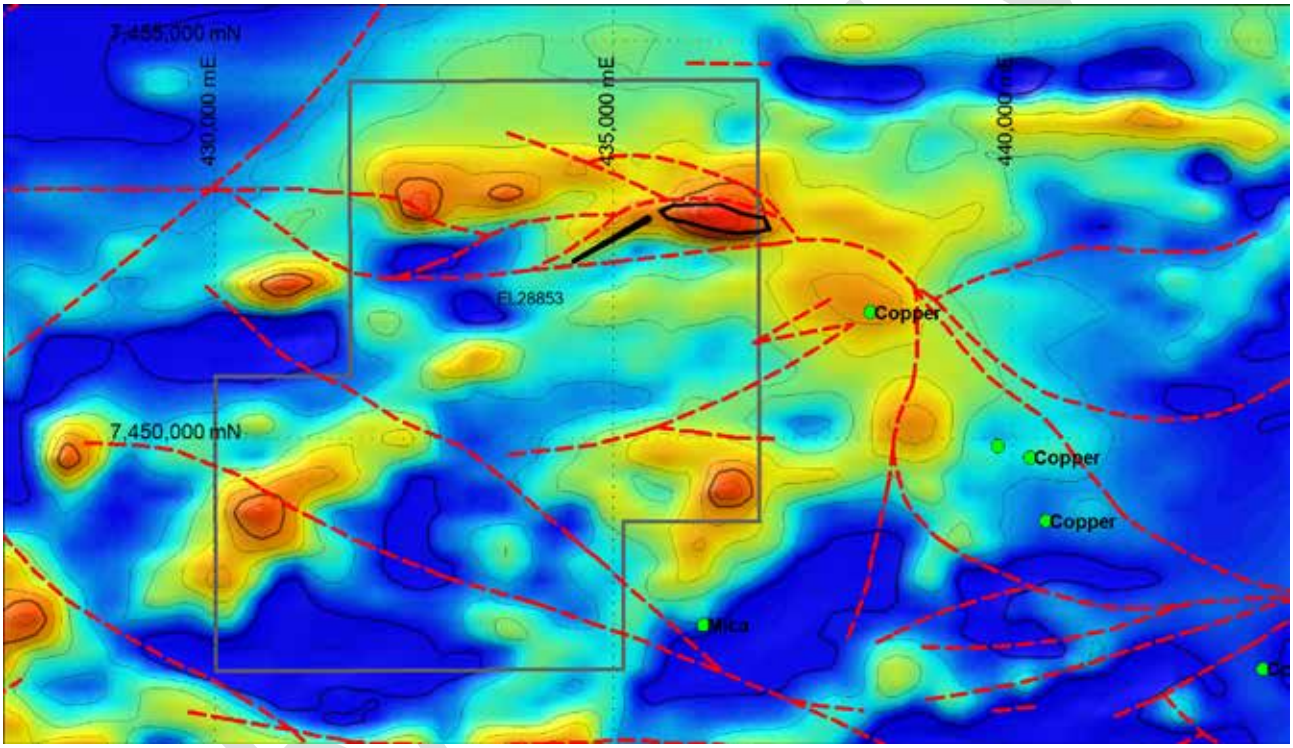

Figure 46: Shows the extent of EL 28853, mapped faults (dashed red), Cu occurrences (green dots) and the location of the modelled bodies above an image of the TMI grid.

The fault zone appears to sit at a lithological boundary between muscovite-biotite gneiss, to the north and amphibolite to the south (Fig 47). Numerous studies from Cloncurry (e.g., Butera, 2004) demonstrate that there is a correlation between IOCG mineralisation and mafic rocks, and mafic rocks are observed in hanging wall of several deposits (e.g., Monakoff (Austin et al., 2013b). The muscovite-biotite gneiss is a favourable host rock because it may become permeable under specific strain conditions.

The modelling results (Fig 48) are startlingly consistent with the mapped geology of the area, in particular the fault architecture. To model this particular anomaly, two bodies were used, and the resulting bodies have very different properties. One is a thin ENE-oriented tabular body with a reasonably high susceptibility (0.2 SI), that sits perfectly parallel to one of the interpreted faults.

The other body is a lens shaped body that is reasonably thick, with a lower susceptibility (0.07 SI) that sits oblique to the other body and the interpreted faults. If we consider these results together they are more interesting again, because this style of architecture suggest that the lens shaped body could be a mineralised fault jog. The thinner tabular zone could feasibly contain magnetite alteration, whereas the jog has lower susceptibility, which might indicate a high ratio of Fe(±Cu) sulphide to Fe-oxide. This kind of structural control and redox zonation is fairly common in IOCG deposits (e.g., Monakoff: Austin, 2013b).

Alternatively, the anomaly could be caused by a breccia zone related to the mapped fault intersection. This anomaly mimics the anomaly to the SE, which has an associated copper show. However, the anomaly modelled to the SE is shallower and or more magnetised. In either case, all the signs are positive, and I feel that there is good potential for mineralisation here.

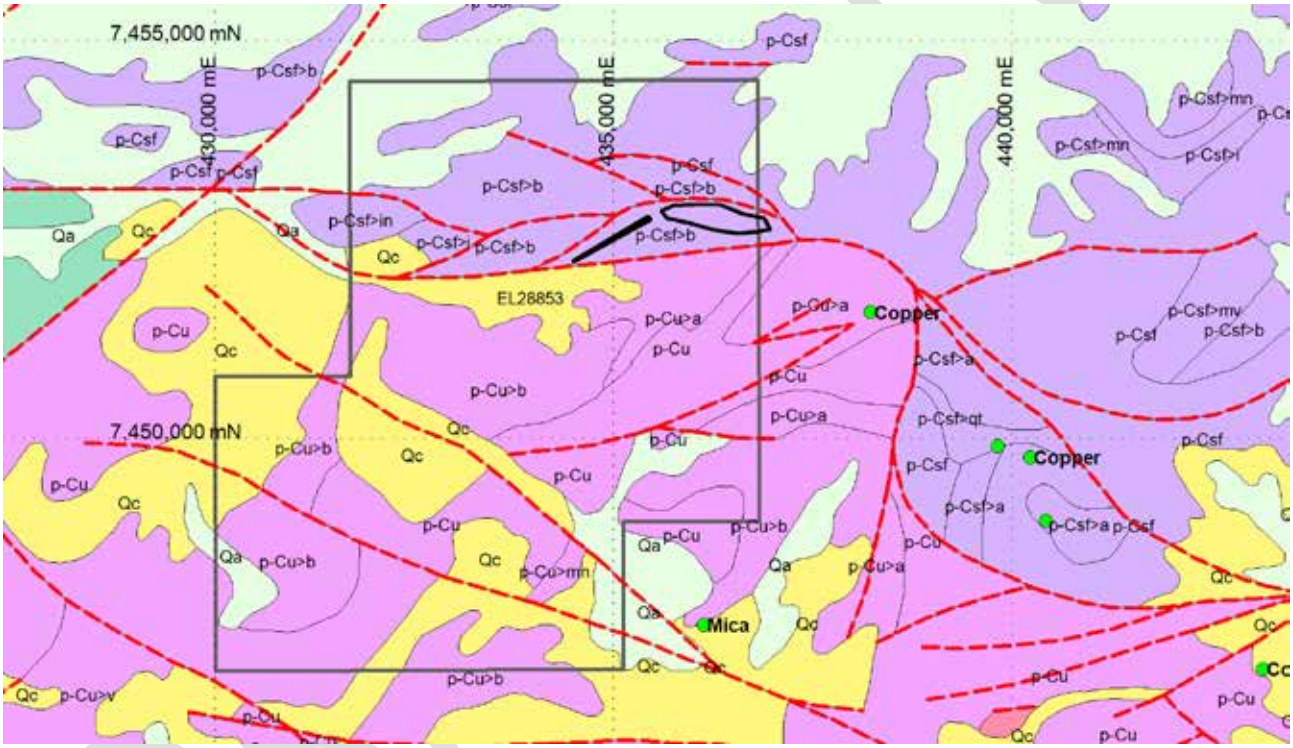

Figure 47: Shows the extent of EL 28853, mapped faults (dashed red) and Cu-occurrences (green dots), above the mapped geology of the area. The purple corresponds to a muscovite-biotite gneiss unit, whereas the pink unit correspond to a more amphibolite-rich unit, both of which are part of the Strangeways Metamorphics

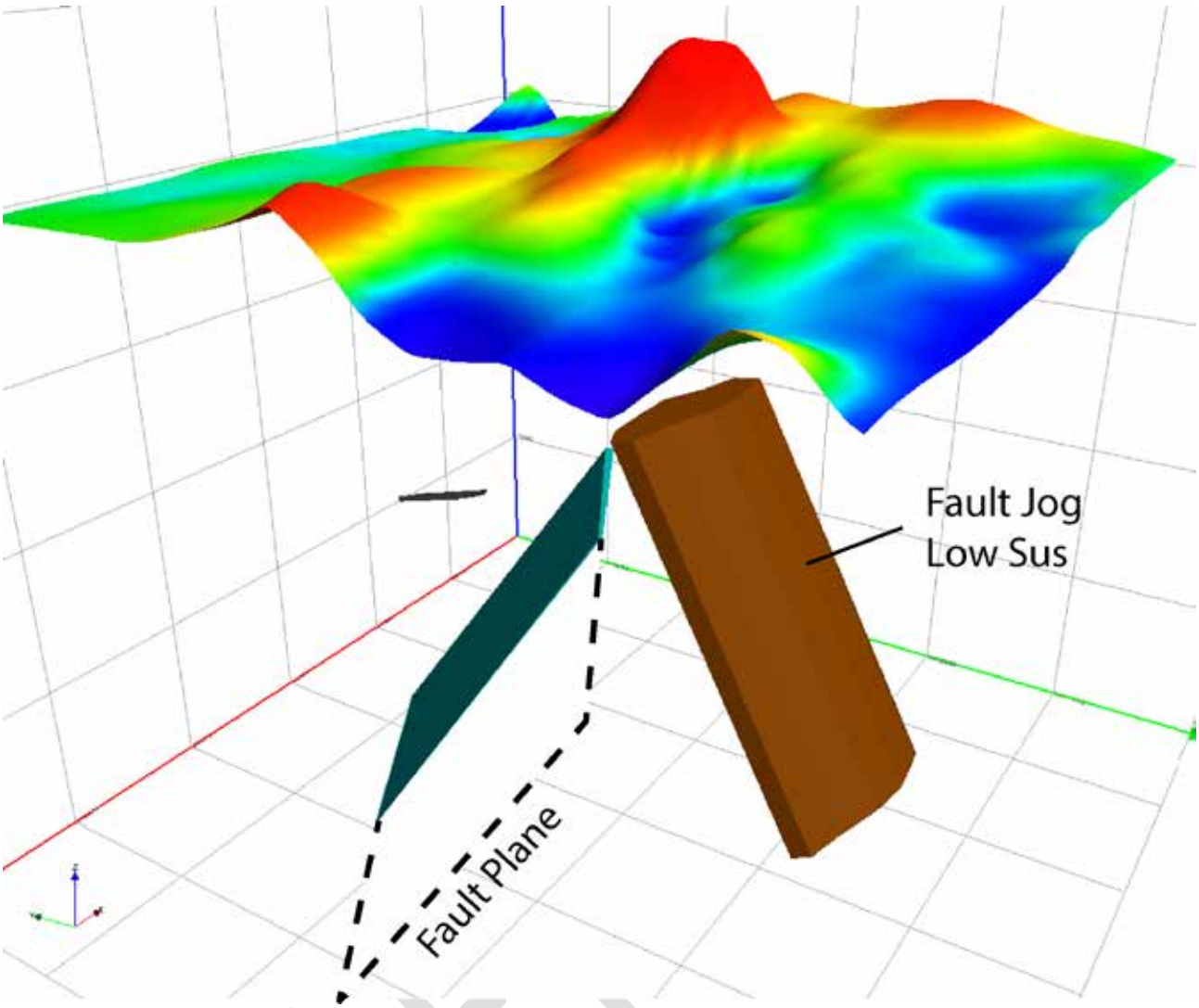

Figure 48: A 3-D representation of the TMI grid above the modelled bodies. The results are suggestive of a fault-jog model for mineralisation.

2.10 EL 29512

2.10.1 Eastern Block Anomaly

EL 29512 hosts one fairly complex magnetic anomaly (Fig 49a) which appears to be associated with a mafic intrusion as mapped by Shaw et al, (1985: Fig 49b). From the spatial relationship of the mapped intrusion, to the magnetic anomaly, and the analytic signal of the magnetics (Fig 50a) it is fairly clear that there is significant petrophysical heterogeneity within the intrusion. The southern part of the intrusion coincides with high amplitude positive and negative anomalies, the central zone is non- or weakly magnetic, and the northern zone is moderately magnetic. There appears to be a dominant ESE-trending structural grain to the lithologies, and this grain appears to be cut by several N to NW–striking faults. There is also significant topographic relief (Fig 50b), with a portion of intrusion occupying a ~900m mountain. This together with the fact that there is only 400m spaced line data, and no survey height data make modelling this anomaly very difficult.

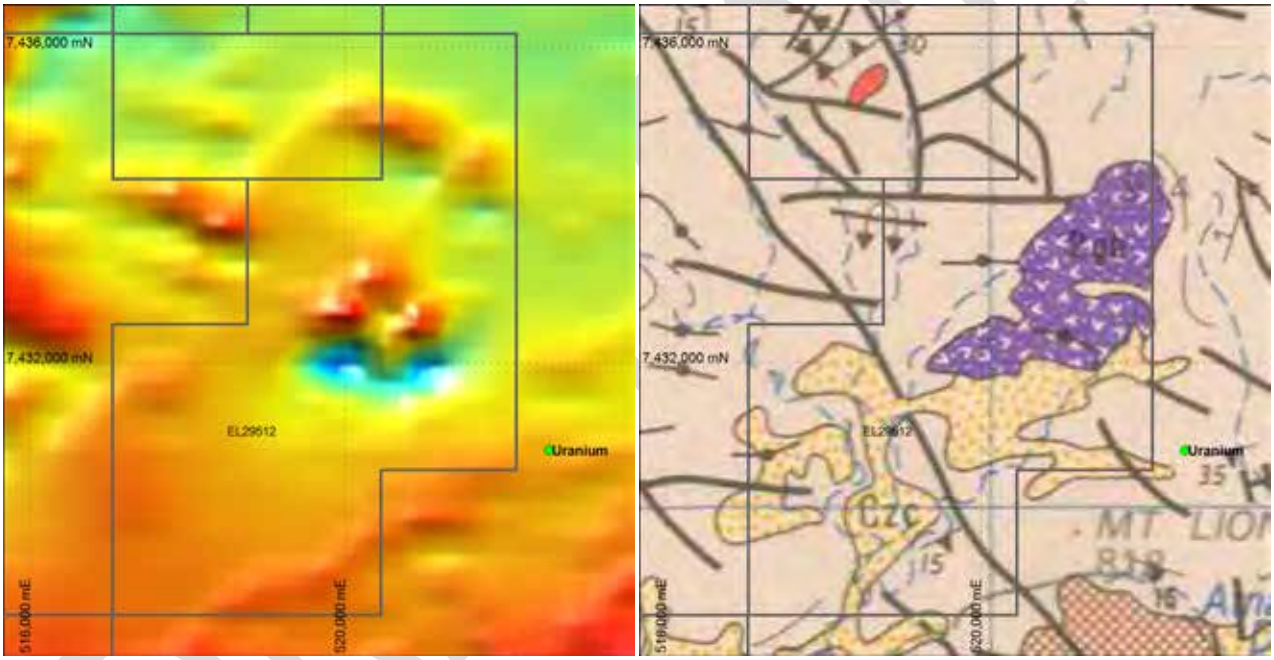

Figure 49: A. Total magnetic intensity grid over EL 29512, highlighting a complex anomaly with positive and negative components; B. The complex anomaly is coincident with a large mafic intrusion (as mapped by Shaw et al., 1985)

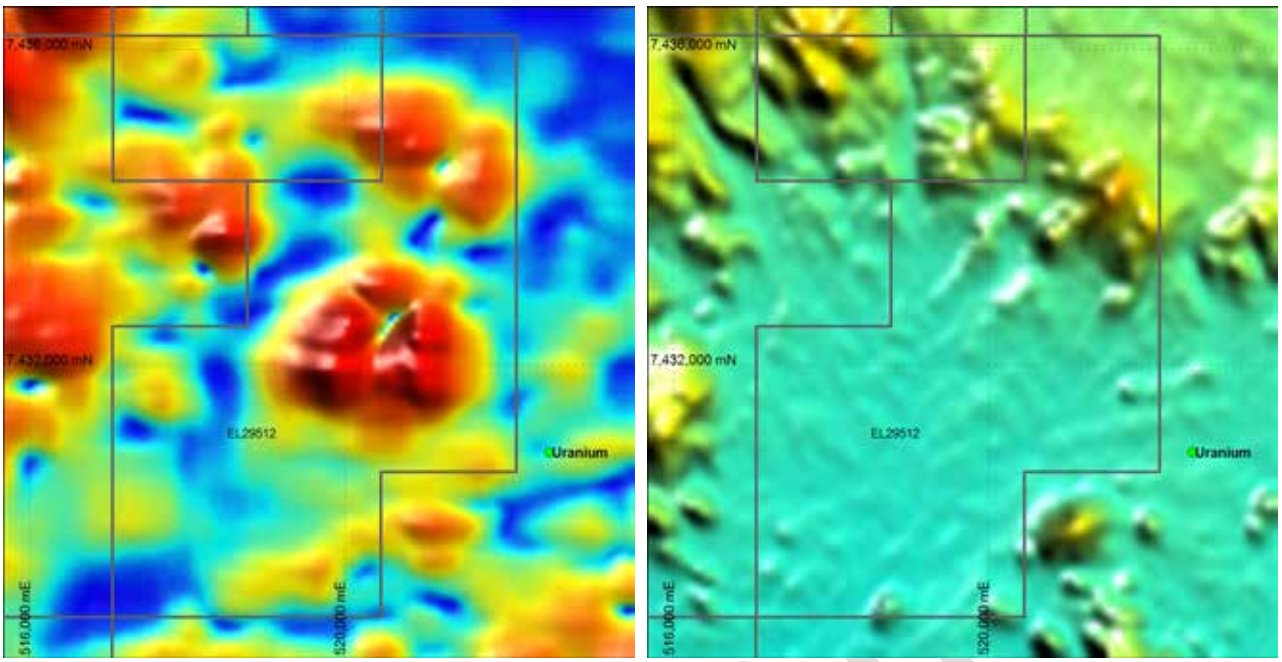

Figure 50: A. The analytic signal of TMI grid, which highlights the sources of magnetisation whether positive or negative, shows that magnetisation is strong in the southern part of the intrusion, weak in the middle, and moderate in the north; B. SRTM topographic data over the tenement highlights significant relief associated with the northern part of the intrusion.

Since there is no flight height data available I have not been able to utilise the data for accurate 3-D modelling. However, it was necessary to at least approximate the flying height for this modelling session, due to the extreme relief. So I have used the SRTM topographic data to make an approximated flying height by smoothing the SRTM topographic data and adding 80m to the elevation. Whilst, this is a good approximation, it is flawed in many ways. The main problem is that planes tend to climb and descend on very different trajectories, so if a survey is completed by flying adjacent north and south survey lines, such as is generally the case, then the height above ground will be highly variable around sharp topographic highs, not a smooth surface like the approximated surface I have used here. Nether-the-less an approximation is better than nothing in this case.

It was not possible to generate a sensible result using inversion due to the complexity of the source bodies, and the poor quality data. However a sensible model was developed by forward modelling, utilising GoogleEarth™ and SRTM data to make inferences about the structure present. GoogleEarth™ data was enhanced to help differentiate different lithologies within the intrusion based on their visual appearance. For example, there is a clear contrast in colour between the north and south of the intrusion (Fig 51). It was possible to infer a steep south-dipping layering using the SRTM data, and a number of faults could be observed in both GoogleEarth™ and SRTM which run N- to NW. These inferences were used to underpin the architecture of a forward model.

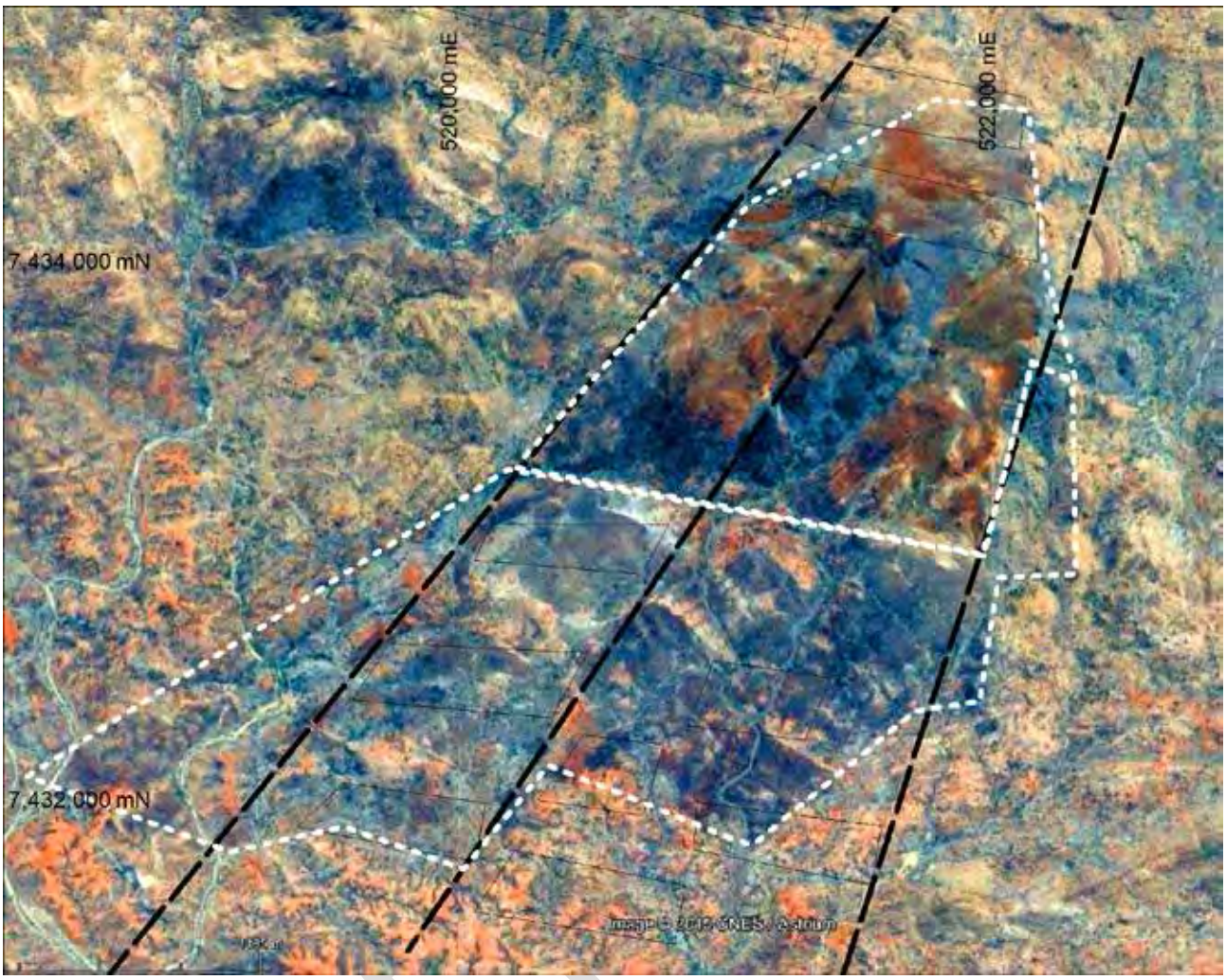

Figure 51: An enhanced GoogleEarth™ image over the intrusion highlights the broad architecture of the intrusion.

In addition, an RTP (reduced to pole) transformation of the TMI data was used to determine that the southernmost part of the intrusion displays strong remanence. This was inferred from the fact that a strong negative anomaly was still present in the RTP (as shown in Fig 52). NB. Normally for an induced body the RTP transform will convert a dipole anomaly (generally caused by a predominantly induced magnetisation) to a symmetrical positive anomaly.

The resultant model matches the data fairly well (to within 6% rms) over eight individual lines, using an estimated flight height. In the model, all the bodies are sub-tabular, dip to the south, and are offset by a number of faults. Their properties are variable, with the southernmost layers (left side of Fig 52) displaying strong downward oriented remanence, and the layers immediately north having reasonably strong induced magnetisation. The central zone is correlated with the high relief part of the intrusion, which is browny-red in colour (as opposed to bluey-black). This zone is essentially non- or weakly magnetic. The northernmost modelled zone (right side of Fig 52) is moderately magnetic, with either induced or positive remanent magnetisation. This part of the intrusion in particular appears to continue to the west, however it is offset in numerous places.

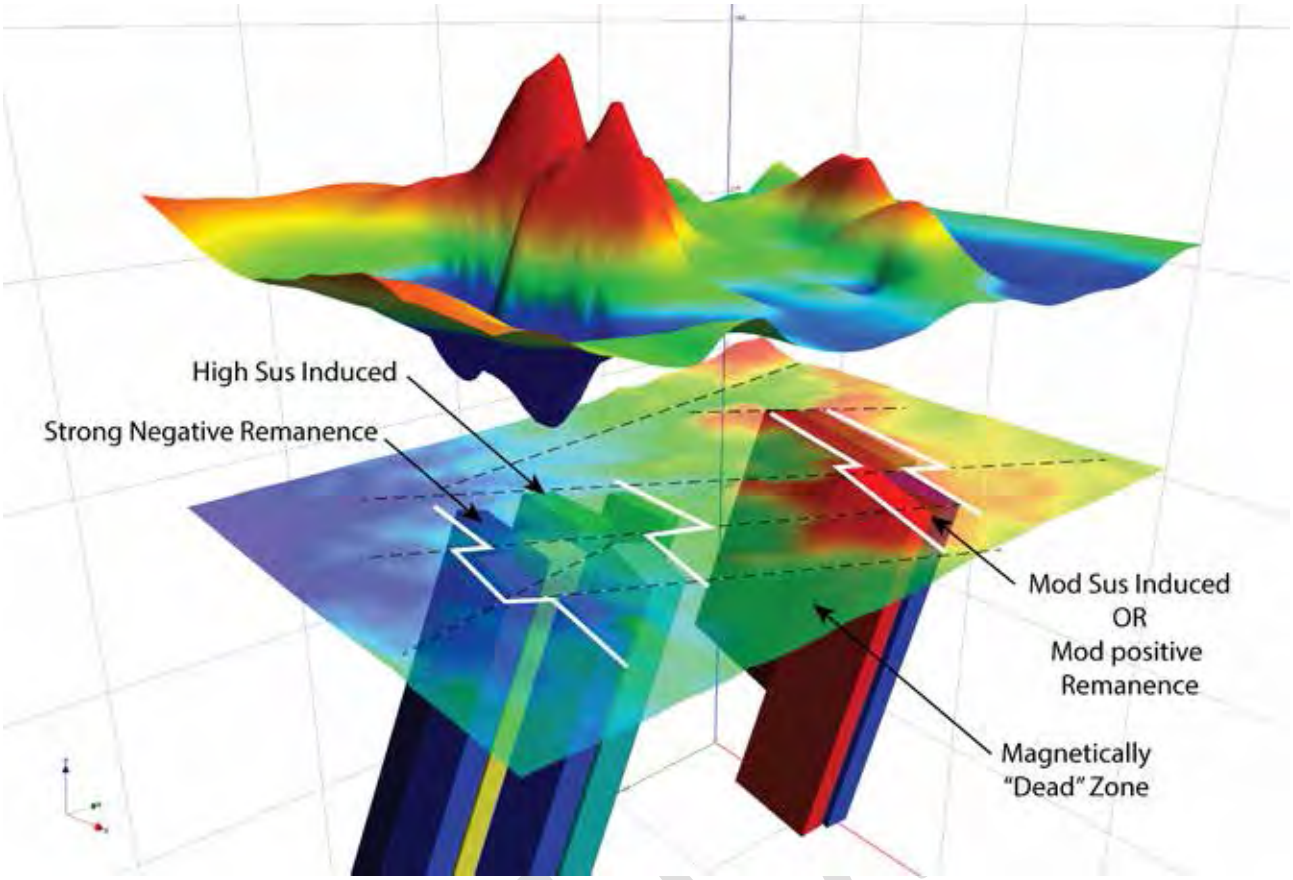

Figure 52: A 3-D representation of the TMI grid above a series of sub-parallel modelled bodies. The three different zones, alternating strong induced and strong remanent magnetisation (left), non-magnetic (central) and weakly magnetic (right) are consistent with layering in magmatic layered intrusions. Hence the northernmost zone (right) could be prospective for Ni-Cu-PPE mineralisation.

Geologically, this modelling result is very interesting, because the results are consistent with a layered intrusion. The southern zone could be interpreted as the upper layers which consist of interlayered Mt-rich horizons (residual melt) with strongly remanent horizons. The central zone is essentially non-magnetic, and this could be correlated with the cumulate phase, which in this case, based on the brown colour, could be an orthopyroxenite. The weaker magnetisation in the northern zone could reflect magnetisation in pyrrhotite, which could furthermore be associated with other sulphides and possibly with Ni-Cu-Au, and or PGEs. This interpretation is highly speculative, and is dependent on the original mapping (Shaw et al., 1985) being accurate. An alternative interpretation is that these are somewhat separate bodies of mafic rocks, intruded as sub-parallel sills. In any case, collection of samples on the ground should provide a good insight into the geochemistry of this particular intrusion.

2.10.2 Northern Block anomalies

The northern block of tenement EL29512 contains a string of three prominent anomalies, sitting along a NW-SE oriented lineament (Fig 53). Based on the 1:250 k mapping (Shaw et al., 1985) and on the surface expression (as mapped by GoogleEarth™) it is reasonably clear that all the anomalies sit just to the east of a major NW-oriented structure, which is manifested by visible quartz veining over a wide zone (approximately 0.5 – 1 km). There are also two secondary structures, which intersect the major NW-striking fault, these are oriented approximately E-W, and sit just north of the NW anomaly (Fig 54). The anomalies all sit along a major structure, possibly on secondary intersecting faults, and their position in relation to the fault intersection is favourable for certain styles of hydrothermal mineralisation, e.g., IOCG. Hence, these targets were further explored, using magnetic modelling.

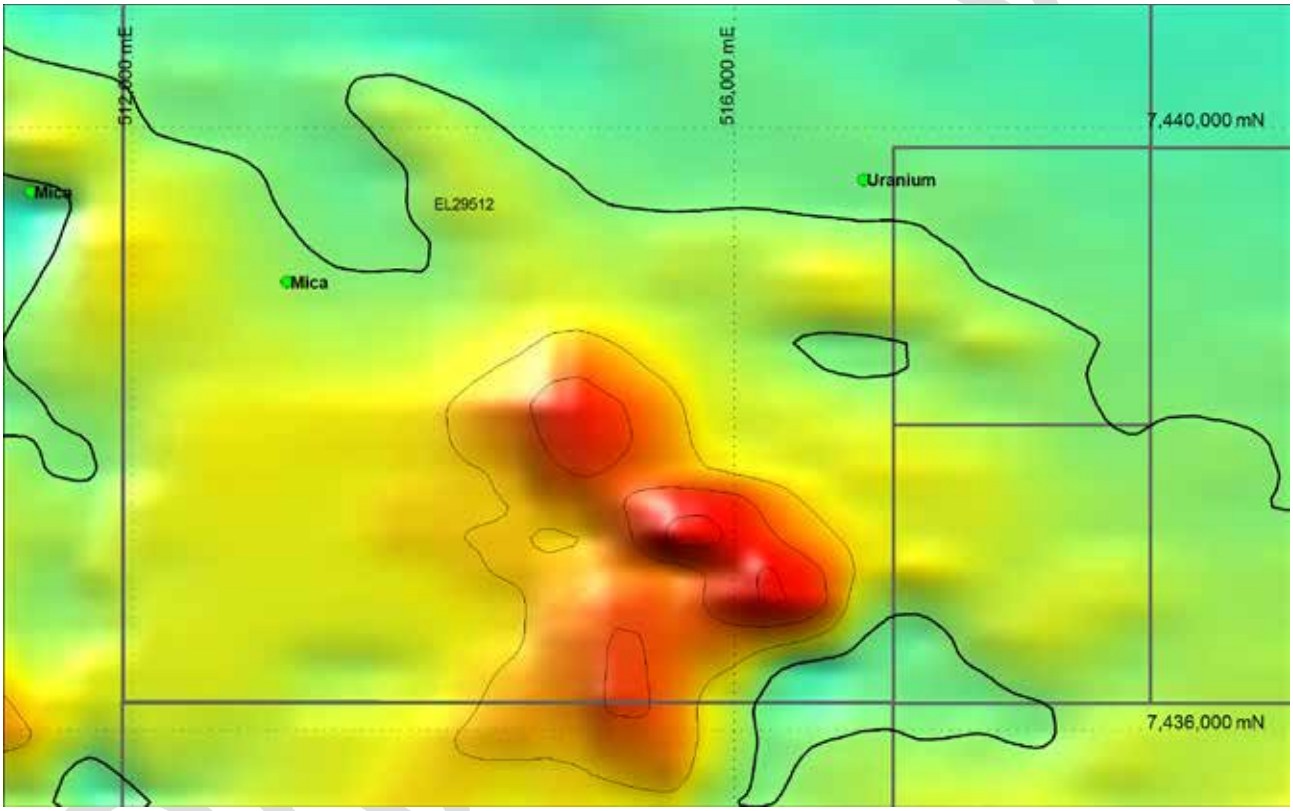

Figure 53: Total magnetic intensity grid over the southern portion of the northern block of EL29512 highlighting a string of three magnetic anomalies aligned NW-SE.

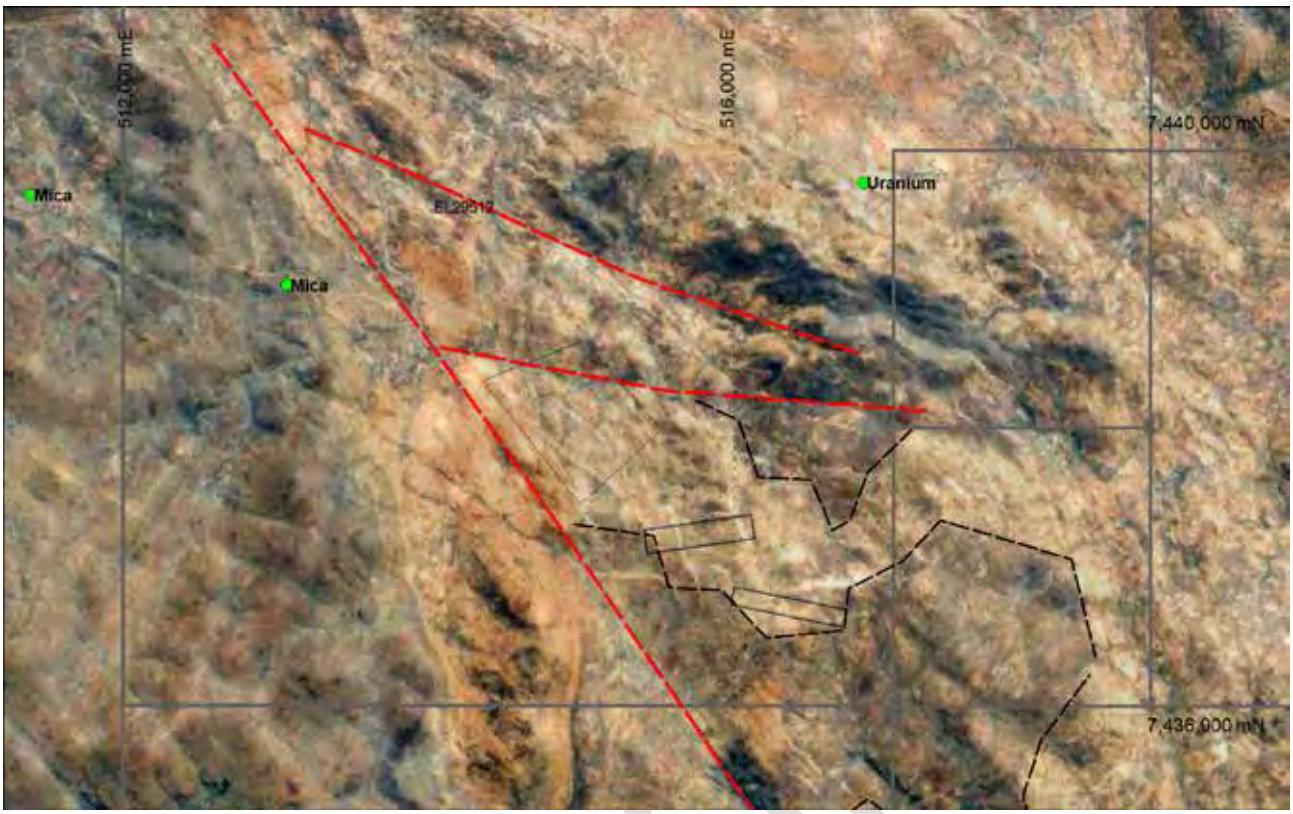

Figure 54: An enhanced GoogleEarth™ image over the intrusion highlights the broad architecture of the area. A number of primary and secondary structures are shown in dashed red, lithological boundaries marked in dashed black, and the modelled bodies are highlighted in thin solid black lines.

The SE and central of these anomalies are reasonably sharp indicating they are near surface, whereas the NW anomaly is more rounded, indicating it is much deeper. It was possible to model the two sharper anomalies with simple tabular bodies, using only induced magnetisation. The resultant bodies are sub-vertical and strike E-W to ESE. The orientation is consistent with the secondary faulting, so it could possibly represent hydrothermal alteration related to the major structure, but localised by the secondary faulting. Conversely, the strike is also consistent with the regional layering as observed in the intrusion to the SE, and so these bodies are potentially just fragments of magnetised layers within the regional lithological package, which have been dislocated due to faulting and or brecciation. The fact that these bodies are modelled with susceptibilities of 0.057 SI and 0.042 SI certainly favours the later, because any significant amount of magnetite would have a susceptibility of >0.1 SI. There are, however, numerous styles of mineralisation that are not associated with significant magnetite.

The NW anomaly can also be modelled using only induced magnetisation, but the resultant model needs to have a dip of approximately 30° south. This is not entirely unrealistic, but I suspect it is improbable in this terrain. So the body was remodelled, this time allowing remanent magnetisation. The new resultant model has a similar top surface, a large, thick, more or less tabular (diamond-shaped) body (shown in dark blue on Fig 55), and with total magnetisation oriented approximately 65° up to the SE. As modelled the body has a Koenigsberger ratio of 0.9, with more or less equal proportions of induced and remanent magnetisation. Assuming this is more or less correct, the remanent vector component is shallow down to the south. Of course it is impossible to be certain, so it does not warrant further discussion. It is of interest, however, that the body does not require a large Koenigsberger ratio to be modelled using a conventional

architecture. This point would suggest that the magnetisation could well be due to fine grained magnetite, rather than pyrrhotite. Hence, I suspect that the magnetisation is probably due to a weakly magnetic lithology, rather than any type of hydrothermal mineralisation.

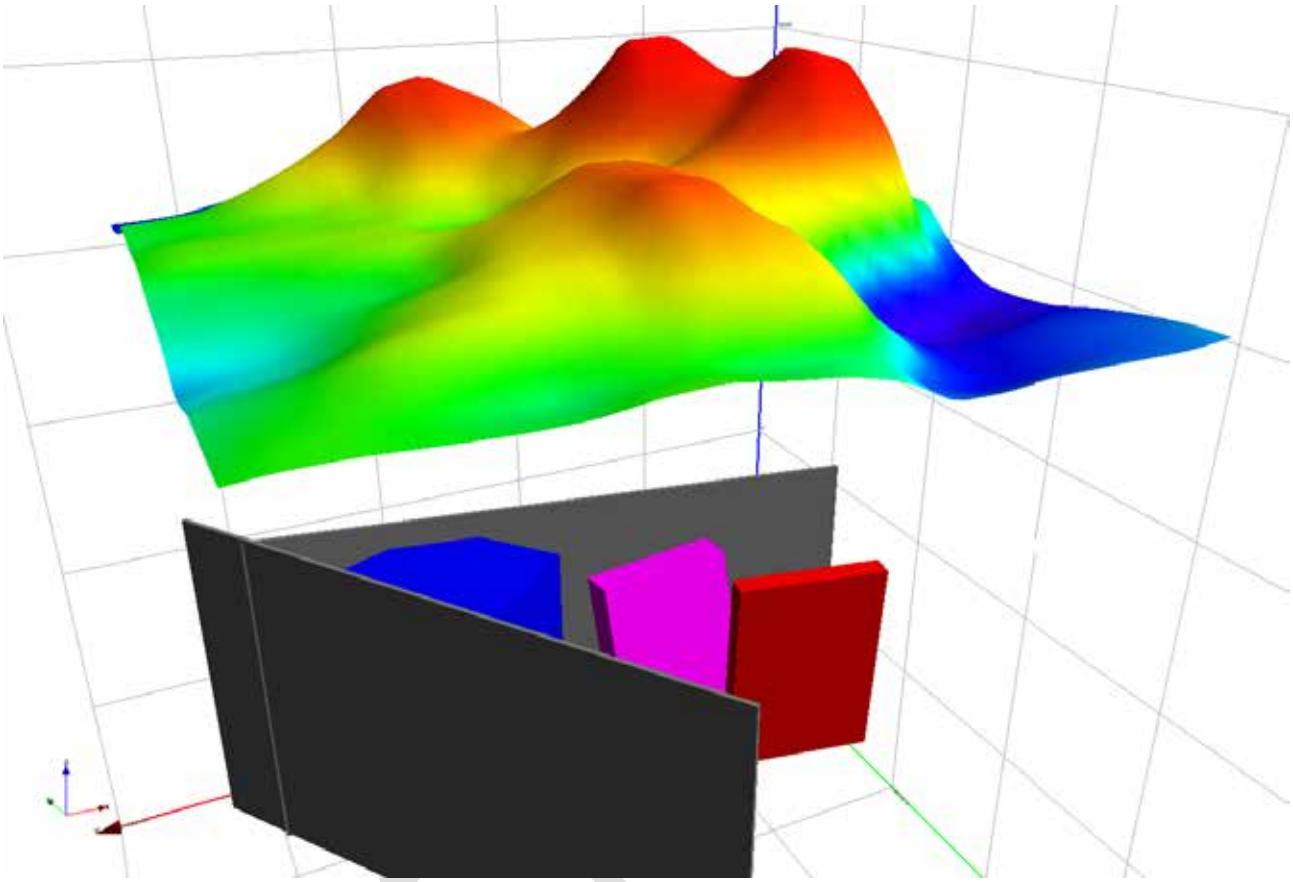

Figure 55: A 3-D representation of the TMI grid above a series of tabular bodies that explain the anomaly. The grey thin bodies mark the location of the interpreted faults in 3-D.

3 Conclusions

One of the main difficulties in working in an area such as this is that there has been limited systematic exploration carried out this far. Much of what is known about mineral prospects can be attributed to early prospectors, and in reality the data is little more than a point marking where somebody dug a hole. Similarly, the mapped geology can only be considered a guess much of the time, because the area is geologically complex, and there are inherent difficulties discriminating between lithologies in high grade metamorphic terrains, because many of the rocks tend to look the same. The mapping by the NTGS seems to predate the magnetic data, and in most cases the mapped geology appears to be at odds with the magnetic data. For example, the interpreted faults bear no resemblance to what I have interpreted from the 1st vertical derivative. The area covered by this report is vast, it is poorly known, and since no data or literature summary was made available by the client for this project, every aspect of what has been carried out in this study is "from scratch". It was not possible to complete a detailed review of prior exploration for the entire area due to time constraints, and furthermore, this kind of fundamental exploration work is not within the scope of the project.

Beyond this rather obvious limitation, there are further issues with the primary dataset utilised for this report. In general the NTGS data is poorly levelled, and in this area no flight altitude data was incorporated in the line data files. This has made the modelling more difficult than necessary, and also has meant that the potential errors associated with the modelling are larger than necessary. Unfortunately, there is nothing that can be done about this, other than to apply pressure to the NTGS to improve the quality and utility of their public datasets. In many cases the data used was only of poor resolution (400m line spacing). This too imposes significant limitations on the accuracy of the results.

While there is a paucity of data that can be used to really constrain the interpretations made in this report, and while the accuracy of the results are in some cases questionable, I am still excited by a number of these anomalies. In particular, those which have a favourable structural context (fault intersections and jogs), favourable host lithology and magnetic properties (e.g., Carbonate lithology and strong remanence), which are also proximal to known Cu occurrences. There are indeed several such targets, across a number of different tenements. There are also a number of anomalies that occupy favourable structural positions (fault intersections, jogs) that are proximal to known Au, Cu, REEs and or U, and that have significant magnetisation (and by inference magnetite present). These are prospective for IOCG mineralisation. In relation to potential for Magmatic Ni-Cu-PGE mineralisation, the bodies need to be fairly large, show signs of fractionation (e.g., petrophysical zonation) and be near surface if they are to have any chance of being economic. Hence, it is my feeling that only two targets are worthy of follow up at this stage. Both are relatively large, and display evidence of zoning (which is inferred to reflect fractionation).

I have ranked the best of the targets empirically, based on their size, proximity to known mineral occurrences and their structural style (Figure 56).

Tenement	Target Name	PotentialMineralisation style	Estimated depth	Ranking
EL29689	Southern Skarn	Cu Skarn	near surface	1
EL28853	NE Anomaly	Fault Jog IOCG, ISCG (* S= sulfide)	50-100 m	2
EL29512	Eastern Block	Magmatic Ni-Cu-PGE	at Surface	3
EL29687	East Anomaly	Cu Skarn, IOCG	~50m	4
EL28546	NW Anomaly	Cu Skarn, IOCG	near surface	5
EL28546	Eastern Anomaly	IOCG-REE-U	at Surface	6
EL29514	Eastern Anomaly	Magmatic Ni-Cu-PGE	at surface	7
EL29347	Yamlba WNW body	Hydrothermal Uranium	near surface	8
EL29688	Central Anomaly	Structurally controlled Cu/ Skarn/IOCG	~150 m	9

Figure 56: Table showing the best ranked anomalies reported on herein

I believe these targets are worthy of further work, e.g., field mapping, ground geochemistry and/or detailed geophysics, which should further differentiate the potential of these tenements. However, I would also note that there does need to be further work before any of these "targets" could be considered genuine prospects, because the data on which these interpretations are made is poor, and there are few additional constraints.

4 References

Alapieti, T. T. and Lahtinen, J. J., 1986. Stratigraphy, petrology, and platinum-group element mineralization of the early Proterozoic Penikat layered intrusion, northern Finland. Economic Geology 81, 1126-1136.

Austin, J. R., and Blenkinsop, T. G., 2009, Local to regional scale structural controls on mineralization and the importance of a major lineament in the eastern Mount Isa Inlier, Australia: Review and analysis with autocorrelation and weights of evidence: Ore Geology Reviews, 35, 298–316, doi: 10.1016/j.oregeorev.2009.03.004.

Austin, J. R., Schmidt, P. W. and Foss, C. A., 2013a. Magnetic Modeling of Iron Oxide Copper-Gold Mineralization constrained by 3-D Multi-scale Integration of Petrophysical and Geochemical data: Cloncurry District, Australia. Interpretation 1, T63-T84.

Austin, J. R., Schmidt, P. W. and Lilly, R., 2013b. Anisotropy of Magnetic Susceptibility (AMS) and Paleomagnetism applied to the differentiation of structural and metallogenic controls on Iron Oxide Copper-Gold (IOCG) mineralisation: a case study from Monakoff, NW Queensland. Extended Abstracts, 23rd ASEG Conference and Exhibition, Melbourne.

Butera, K.M., 2004. The role of mafic rocks in the genesis of IOCG and base metal deposits, Mount Isa Eastern Succession, NWQueensland, Australia. In: Barnicoat, A.C., Korsch, R.J. (Eds.), Predictive Mineral Discovery Cooperative Research Centre—Extended Abstracts, June 2004 Conference. Geoscience Australia, Canberra, pp. 21–22.Chang, Z . & Meinert, L.D., 2008. Zonation in Skarns – Complexities and Controlling Factors. Extended Abstract, PACRIM Congress 2008.

Clark, D. A. and Lackie, M. A., 2003. Palaeomagnetism of the Early Permian Mount Leyshon Intrusive Complex and Tuckers Igneous Complex, North Queensland, Australia. Geophys. J. Int. 153 (3): 523-547. doi:10.1046/j.1365-246X.2003.01907.x

Gee, G., 2007. EL 9890 Yambla, Annual Report and Final Report. Deep Yellow Ltd.

Groves, D. I., Goldfarb, R. J., Robert, F. and Hart, C. J. R., 2003. Gold deposits in metamorphic belts; overview of current understanding, outstanding problems, future research, and exploration significance. Economic Geology 98(1):1-29

Maier, W.D. and Barnes, S.-J., 1998. Concentrations of rare earth elements in silicate rocks of the Lower, Critical and Main Zones of the Bushveld Complex, Chemical Geology, 150, Issues 1–2, 85-103, ISSN 0009-2541, http://dx.doi.org/10.1016/S0009-2541(98)00054-0.

Needham, R.S. & Stuart-Smith, P.G., 1987, Coronation Hill U-Au mine, South Alligator Valley, Northern Territory: an epigenetic sandstone-type deposit hosted by debris-flow conglomerate. BMR Journal of Australian Geology & Geophysics, 10, 121-131.

Potter, J.R., 2003. Partial Relinquishment Report for EL 10078 (Mt Riddoch). Tanami Exploration NL.

Seat, Z., Beresford, S.W., Grguric, B.A., Waugh, R.S., Hronsky, J.M.A., Gee, M.A., Groves, D.I. & Mathison, C.I., 2007. Architecture and emplacement of the Nebo-Babel gabbronorite-hosted magmatic Ni-Cu-PGE sulfide deposit, West Musgrave, Western Australia. Mineralium Deposita, 42(6), 551-581.

Shaw, D.R. , Senior, B.R. , Offe, L.A. , Stirzaker, J.F. , Walton, D.G. , Apps, H.E. , Freeman, M.J. 1985. Illogwa Creek, Northern Territory, 1:250 000 geological series map. Sheet SF/53-15, 2nd edition. Bureau of Mineral Resources, Australia & Geological Survey of NT 1v.

Shaw, D.R. & Wells, A.T., 1983. Alice Springs, Northern Territory, 1:250 000 geological series map : sheet SF/53-14. Bureau of Mineral Resources, Australia & Geological Survey of NT.

CONTACT US

t 1300 363 400
+61 3 9545 2176
e enquiries@csiro.au
w www.csiro.au

AT CSIRO WE SHAPE THE FUTURE

We do this by using science to solve real issues. Our research makes a difference to industry, people and the planet.

As Australia's national science agency we've been pushing the edge of what's possible for over 85 years. Today we have more than 5,000 talented people working out of 50-plus centres in Australia and internationally. Our people work closely with industry and communities to leave a lasting legacy. Collectively, our innovation and excellence places us in the top ten applied research agencies in the world.

WE ASK, WE SEEK AND WE SOLVE

FOR FURTHER INFORMATION

Mineral Resources Flagship
Jim Austin
t +61 2 9490 8876
e james.austin@csiro.au
w www.csiro.au